Young's modulus for enamel has presented several inconsistencies in the literature.

Spears (1997) used a 3-Dimensional finite element analysis model on enamel and found reason for the inconsistencies in the literature with regards to the Young's modulus. He postulated that this decrease may be in part explained by the change in mineral content found as the enamel traverses from the surface to the dentine. Another possibility claimed, is the direction of applied force. Predicted values of Young's modulus are presented to range from 19-91 GPa perpendicular to the orientation of the crystals, to 93-113 GPa parallel to the orientation of the crystals.

Craig et al., (1960) obtained a value for Young's modulus of 77.9 ± 4.8 GPa. Craig and Peyton (1960) determined the elastic modulus of cusp enamel and reported a range varying from 9.1 x 106 to 13.6 x 106 psi with an average of 12.2 x 106psi ± 0.9 x 106 psi. While Gilmore et al., (1970) obtained a value for Young's modulus of 73 Gpa. Prior to this Stanford et al., (1960) obtained a value for Young's modulus as low as 9.65 ± 3.45 Gpa (Table 2.5).

Table 2. 5. The Physical Properties of Cementum and Enamel.

AUTHOR	TEST	CEMENTUM		ENAMEL	
	(Indenter)	Elasticity (UNITS)	Hardness (UNITS)	Elasticity (UNITS)	Hardness (UNITS)
Hodge & McKay (1933)	Brinell Hardness		85 BHNs		
Craig & Peyton (1961)	Indentation			11.3(±0.7) - 12.2(±0.9) Psi X 10^{-6}	
Rautiola & Craig (1961)	Knoop Hardness Test		40(KHN)		

AUTHOR	TEST	CEMENTUM		ENAMEL	
		Elasticity (UNITS)	Hardness (UNITS)	Elasticity (UNITS)	Hardness (UNITS)
Willems (1993)	Nano-indentation (NI)			90.6 GPa	3.39 GPa
Poolthong (1998) Trial	Nano-indentation	10.8 GPa	0.4 GPa		
Poolthong (1996)	NI Cervical 1/3	11.5 ± 0.5 - 13.4 ± 0.3 GPa	1.4 ± 0.05 - 1.6 ± 0.10 GPa		
Poolthong (1996)	NI Apical 1/3rd	9.2 ± 0.3 - 9.4 ± 0.2 GPa	0.8 ± 0.06 - 0.9 ± 0.12 GPa		
Clark et al (1997)	NI Apical 1/3rd	12.3 ± 2.03 GPa	0.36± 0.08 GPa.		
Poolthong (1998)	Nano-indentation Middle 1/3rd (20µm Spherical)	11.95 ± 1.24 GPa	0.63 ± 0.06 GPa	79.09 ± 3.13 GPa	3.39 ± 0.07 GPa
Oliver & Pharr (1992)				72 GPa	8 GPa
Poolthong (1998)	Nano-indentation Apical 1/3rd	8.55 ± 0.84 GPa	0.57 ± 0.48 GPa		

AUTHOR	TEST	CEMENTUM		ENAMEL	
		Elasticity (UNITS)	Hardness (UNITS)	Elasticity (UNITS)	Hardness (UNITS)
Craig (1993)	KHN			84.1 GPa	3.1 GPa, 343-430 KHN's
Kodaka et al (1992) , Ryge et al (1961)	Vickers Hardness				242-462 Kg/mm^2
Poolthong (1998)	Nano-indentation (Berkovich) {X-section}			72.71 ± 2.01 GPa	4.17 ± 0.11 GPa
Poolthong (1998)	Nano-indentation (Berkovich) {Longitudinal-section}			77.73 ± 1.39 GPa	4.90 ± 0.21 GPa
Poolthong (1998)	Nano-indentation {X-section} (20µm Spherical)			81.71 ± 4.30 GPa	3.39 ± 0.07 GPa
Poolthong (1998)	Nano-indentation {Longitudinal-section} (20µm Spherical)			69.12 ± 2.69 GPa	

Willems (1993) reported enamel elasticity as 90.59 GPa, which he obtained using a nano-indentation tip. He used loads of 0.2N applied to a pyramidal diamond indenter, having a triangular base.

Poolthong (1998) reported the elasticity of enamel as being 69.12 ± 2.69 GPa in longitudinal section. While in cross-section it was found to be significantly higher at 81.71 ± 4.30 GPa. He used a 20μm spherical indenter with a loading force of 150mN. The Berkovich indenter was used under the same force levels of 150mN reported a significantly larger at 77.37 ± 1.39 GPa in longitudinal section, whereas in cross-section he reports a lower value at 72.71 ± 2.09 GPa.

2.8 Scanning Electron Microscopy

2.8.1 Surface Scanning

The scanning electron microscope and electron microprobe are two powerful instruments which permit the observation and characterization of heterogeneous organic and inorganic materials. In these instruments, the area to be examined is irradiated with a finely focused electron beam, which may be static or swept across the surface of the specimen (Goldstein et al 1981). The types of signals produced when the electron beam impinges on a specimen surface include secondary electrons, backscattered electrons, Auger electrons, characteristic x-rays, and photons of various energies (Goldstein et al 1981). These signals are obtained from specific emission volumes within the sample and can be used to examine many characteristics of the sample (composition, surface topography, crystallography, etc.). In the scanning electron microscope (SEM), the signals of greatest interest are the secondary and backscattered electrons, since these vary as a result of differences in surface topography as the electron beam is swept across the specimen. The secondary electron emission is confined to a volume near the beam impact area, permitting images to be obtained at relatively high resolution (Goldstein et al 1981).

In the electron probe microanalyzer (EPMA), frequently referred to as the electron microprobe, the primary radiation of interest is the characteristic x-rays which are emitted as a result of the electron bombardment. The analysis of the characteristic x-radiation can yield both qualitative and quantitative compositional information from regions of a specimen as small as a few micrometers in diameter (Goldstein et al 1981).

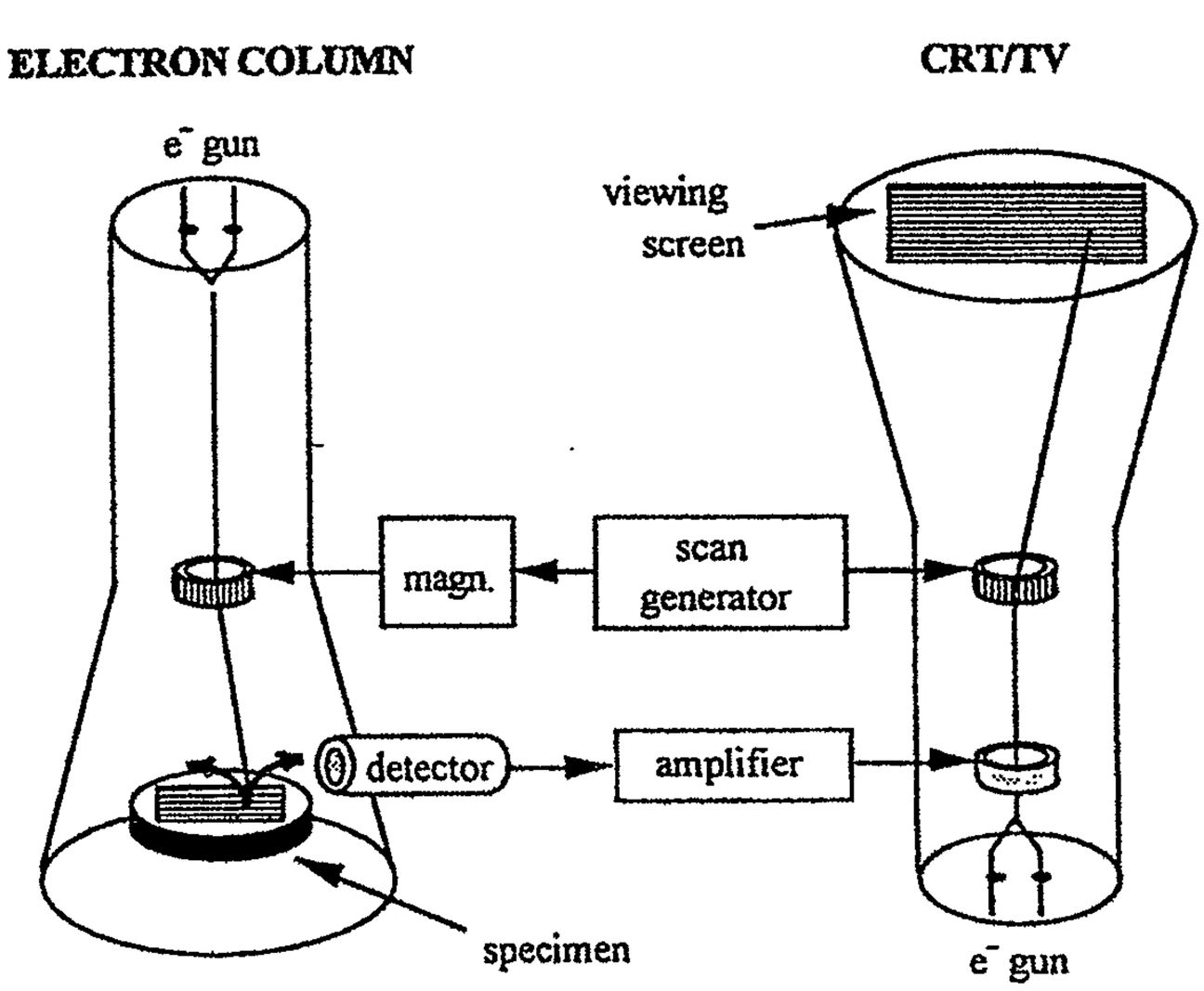

Figure 2. 8. Diagram showing the principles of a scanning electron microscope (Australian Key Centre for Microscopy and Microanalysis Laboratory Manual 1998).

The scanning electron microscope (SEM) is made up of two electron beam devices linked together as shown in Figure 2.8. In the "electron column" an electron beam is focussed on to the surface of the specimen and scanned across a small rectangular area. The electron beam interacts with the atoms in the sample and generates a range of signals. The electron column is linked to a cathode ray tube (TV tube) firstly by using the same scan generator to drive both beams (i.e. by synchronizing the scans) and secondly by using one of the signals generated at the specimen to control the brightness of the spot on the TV screen.

When the electrons pass into the sample there are 2 main interactions:

1. Elastic scattering where there is angular scattering but no loss of energy. This "billiard ball" type of scattering leads to the production of backscattered electrons (BE) when electrons undergo multiple scattering or a single large angle scattering event and come back out of the sample as shown in Figure 2.9.
2. Inelastic scattering, or energy loss events where there is a loss of energy but only very small angular scattering. There are many different types of energy loss events and for most of the interactions there is only a small loss of energy.

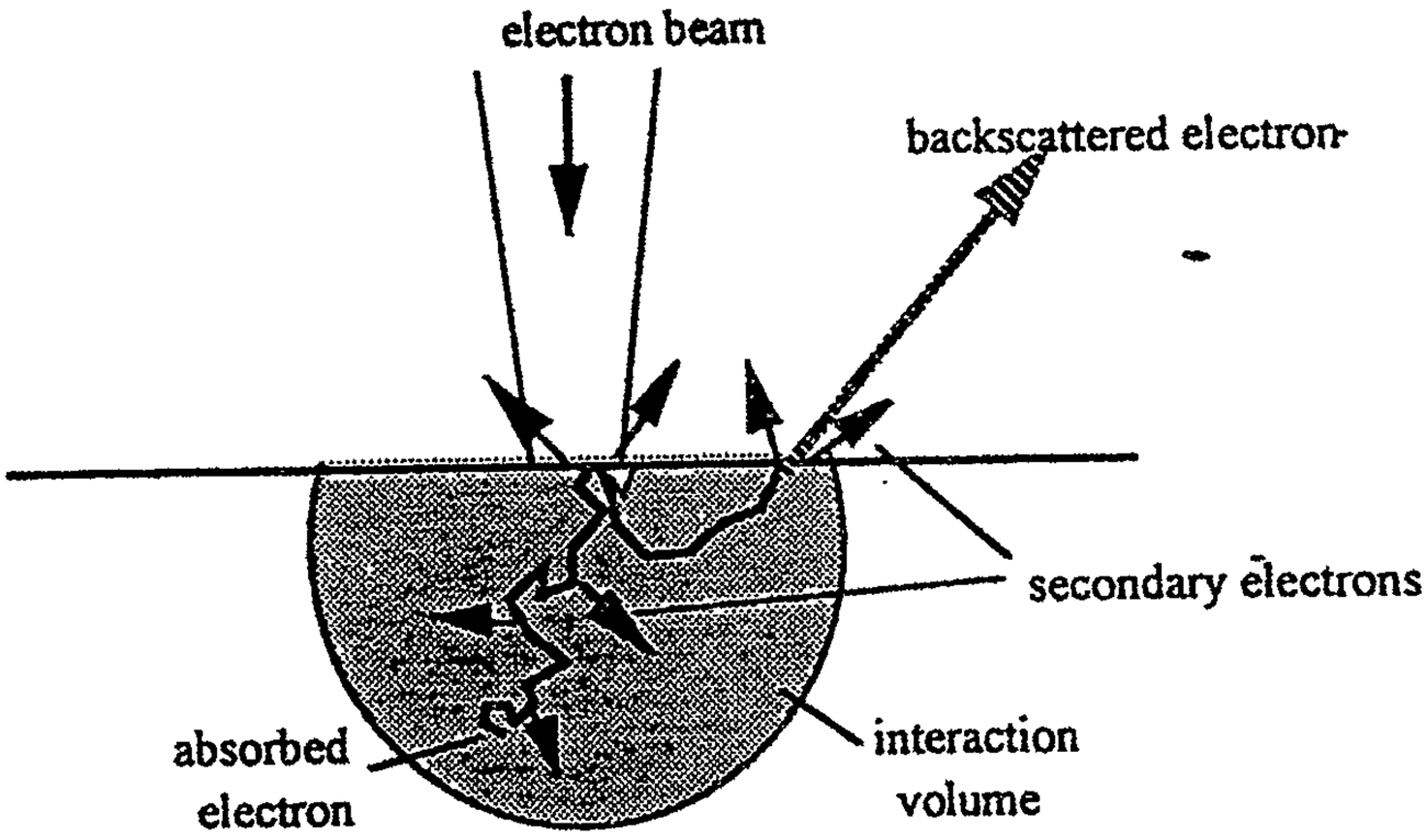

Figure 2. 9. The production of secondary and backscattered electrons (Australian Key Centre for Microscopy and Microanalysis Laboratory Manual 1998).

If a beam electron stays in the sample, eventually it will lose all its energy and be absorbed by the sample as shown in Figure 2.9; it is these electrons that contribute to the absorbed specimen current signal. A secondary electron (SE) is produced when a beam electron interacts with an atom and causes one of the loosely bound outer shell electrons to be ejected from the atom. These ejected electrons are usually low in energy, and can only escape from the sample if they are generated very close to the surface. X-rays, Auger electrons and cathodoluminescence are other examples of signals arising from energy loss events (Australian Key Centre for Microscopy and Microanalysis Laboratory Manual 1998).

2.8.1.1 Principles of X-ray microscopy

Many techniques have been developed to measure variations in mineral concentration in calcified tissues (Kinney et al 1994). At the microstructural level, these techniques include optical microscopy (OM) (Silverstone 1970), X-ray micro-radiography (MR) (Elliott et al 1981, Featherstone et al 1983), and backscattered scanning electron microscopy (BSEM) (Boyde and Jones 1983, Marshall et al 1989, Nelson 1990, Kinney et al 1994). All of these techniques have drawbacks. Both OM and MR require thin sections, while BSEM requires polished surfaces. Thin sections and polished surfaces are difficult to prepare, and artifacts are introduced by the preparation (Ten Cate et al 1991). OM correlates changes in birefringence to changes in mineral concentration, a quantitative relationship between mineral density. Microradiography, though extremely sensitive to changes in mineral concentration, provides a through-thickness measure of the X-ray attenuation coefficient. The possibility of overlapping structures and non-planar surfaces makes quantitative measurements of the mineral density prone to error. Finally, the lack of good standards makes BSEM difficult to quantify and to relate to compositional changes (Kinney et al 1994).

2.8.2 Energy dispersive analysis (Edax)

Chemical analysis in the scanning electron microscope and electron microprobe is performed by measuring the energy and intensity distribution of the x-ray signal generated by a focused electron beam. There are two methods available;

1. Wavelength-Dispersive Spectrometer, and
2. Energy-Dispersive X-Ray Spectrometer.

The X-ray signal from the sample passes through a thin Beryllium window into a cooled, reverse-bias Lithium-drifted Silicon detector. Absorption of each individual x-ray photon leads to the ejection of a photoelectron which gives up most of its energy to the

formation of electron-hole pairs. They in turn are swept away by the applied bias to form a charge pulse which is then converted to a voltage pulse by a charge-sensitive preamplifier. The signal is further amplified and shaped by a main amplifier and finally passed to a multichannel analyzer (MCA), where the pulses are sorted by voltage. The voltage distribution can be displayed on a cathode ray tube or an X-Y recorder. The contents of the MCA memory in most recent instruments either reside directly in a computer or can be transmitted to a computer for' further processing such as peak identification or quantification (Goldstein et al 1981).

Introduction of the electron probe has made it possible to analyze very small samples in a nondestructive way and to relate the distribution of various elements to the histologic structure of the tissue (Hals and Selvig 1977).

Röckert 1958 examined the cementum of monkeys by quantitative X-ray microscopy and found Calcium to vary within a wide range 0.1 to 0.83 mg Ca/mm^3. This variation lead to the conclusion that cementum was not completely mineralized or homogeneously mineralized.

Cohen *et* at. (1992), using energy-dispersive X-ray analysis, have found such large variations in Calcium and Phosphorus content from surface to surface of individual teeth (also between the teeth) that these authors concluded that exposure to the oral environment has little effect on either calcium or phosphorus content or the ratios between them.

Tohda (1996) prepared ground sections to be microradiographed and used for electron-probe and electron microscopic studies. Microradiographically the cervical acellular cementum which had not been exposed to the oral environment showed a rather homogeneous mineralization. However, a certain incremental pattern reflecting variations in mineral density was discerned. Two of the root surfaces which had been exposed to the oral environment appeared similar to the non-erupted specimens, but the remaining 4 exhibited a distinct surface layer of higher radiopacity.

Renz et al 1997 used Electron dispersive X-ray analysis in a scanning electron microscope (EDX linescans in SEM) to record the Ca Kα and the P Kα signal over the whole cementum width. They showed a slight intensity variation.

2.9 Storage and Preparation

Experimental teeth have been stored in a variety of solutions (Rautiola and Craig 1961, Clark 1997, Poolthong 1996, 1998). These are chosen so as to preserve and disinfect the teeth. The solutions generally tend to be of the aqueous variety until embedding in resin. It has been reported that initial water loss from the cut dentine occurs within five minutes and *85%* of the total weight loss occurs within 30 minutes (Jameson et al. 1994). Water loss from dentine has also been reported to affect its mechanical properties and may predispose the tooth to fracture (Jameson et al. 1993). There is no similar study on enamel owing to small size and dimensions of enamel, however, a spherical indenter was used and the elastic modulus was found to increase due to dehydration (Staines et al. 1981). The effect of prolonged storage on the physical properties of cementum has not yet been studied. Rautiola and Craig (1961) looked at storage in tap water, neutral formalin, or direct embedding into plastic was reported to have no apparent effect on microhardness of dentine and cementum. However the time period of storage was not mentioned. Their effects however could have been nullified as a result of their method requiring the resin embedding prior to microhardness testing.

Waters (1980) suggested common methods of storage of extracted teeth include distilled water, tap water or a physiological salt solution. However he warned that mineral dissolution is possible and a change in water content can occur if the storage sets up an unfavorable osmotic gradient.

It is possible that results generated at the beginning of the test might be different from the ones obtained at the end of the test. Knowledge of changes in the mechanical properties of a tooth specimen left in dry conditions is crucial. Clark (1997) suggested the differences in results obtained between male and female test samples may possibly be attributable to the storage method used. It was important to evaluate the time for which the tooth specimen could be left dry without any changes of its properties. It is equally important to study the effect of storage time on the properties of tooth samples stored in de-ionised water.

Poolthong (1998) tested premolars with regards to time dependence on mechanical properties of enamel and dentine in wet and dry conditions. Premolars were disinfected in Miltons solution for 24 hrs and then embedded in epoxy resin (resin is allowed 12 hrs to set as per manufactures instructions). The premolars were then ground and polished. Indentations were made 3, 6 hours, 1, 3 days, 1, 2 weeks and 1 month and 95 days respectively.

Table 2. 6. The Physical Properties of Dentine and Enamel.

MEAN ± SD OF HARDNESS (H) AS A FUNCTION OF PLASTIC DEPTH AND ELASTIC MODULUS (E) AT THE MAXIMUM DEPTH OF ENAMEL AND DENTINE AT VARIOUS DURATION AFTER STORED IN WATER.				
	Enamel (wet)		Dentine (wet)	
Duration	H	E*	H	E*
3days	4.10±O.41(12)*	82.5±3.7(12)*	0.95±0.07(ll)*	20.2±1.7(11)*
12 days	3.99±0.33(12)*	85.3±6.1(12)*	1.00±0.09(10)*	20.6±1.8(10)*
95 days	4.lO±0.25(12)*	84.3±5.5(12)*	0.92±0.10(11)*	19.3±1.8(ll)*

The number of indentations is shown in parentheses.

* denotes that the values within the same column are not significantly different ($p < 0.05$). (Poolthong 1998)

The *H* and *E* values of both enamel and dentine when tested at 12 and 95 days after extraction were not significantly different from the values tested at 3 days.

In Poolthong's study (1998), dentine appeared to be more sensitive than enamel when the structure was left dry. Focusing on the water content, dentine has 20% by volume compared to 1% enamel. Dentinal tubules have been reported to contain approximately 75% of the total water content, with the remaining *25%* was bounded in the dentinal matrix (Van der Graf and Ten Bosch 1990). The change of H value in three-day data may be because the degree of dehydration reached a critical point which altered its properties. In tension, dentine was reported to give less fracture strain after it was left dry for seven days, but the data at the three day period were not available (Jameson *et al.* 1993). The alteration of fracture strain due to water loss may have occurred before the seven day period.

The water loss of enamel is also more difficult since water normally exists in intercrystalline spaces which are surrounded by tightly packed hydroxyapatite crystallites. By contrast, water can easily evaporate through dentinal tubules when the tooth is cut. Enamel showed no significant change up to one month. The *E* values of enamel were rather consistent though they showed a similar trend as hardness which may be attributable to lack of water loss. However, elastic modulus was observed to increase by some *15%* on drying of the enamel (Staines et al. 1981). Poolthong (1998) attributes this to the fact that in their experiment, a larger diameter spherical indenter 6350 μm instead of 40 μm, which resulted in a larger area of contact (approximately 100 times greater) and indented deeper into the enamel (50 μm instead of less than a micrometre). Such high loads may have predisposed the enamel to cracking about the impression. Poolthong (1998) adds a further possibility is that the large contact area and force in Staines work may have lead to a contribution of the underlying dentine, which is strongly moisture dependent.

As a result, the tooth specimen should not be left dry for too long, especially dentine, and the recommendation is one day without any change of hardness in dry condition. Enamel can be tested in dry conditions for up to one month without any significant change of hardness, but the elastic modulus trend was not clear.

Poolthong (1998) concluded, hardness of dentine could be altered depending on the period left in dry condition. Dentine is recommended to be tested within one day and should be kept in water in order to maintain its mechanical properties. Enamel seemed to be less sensitive to the dry condition and might be left up to one month without any significant changes to its hardness. Tooth specimen can be repeatedly and reproducibly tested over a three month period when stored in deionised water.

Water normally provides viscoelastic properties to the material. Hence, the data obtained from dentine left for one hour are expected to show more viscoelasticity than relatively dry dentine tested at one month. The dentine then became less stiff with more water. However, a trend of increasing elastic modulus with drying time was not evident in this study. Further experiment for this observation using the load/partial-unload cycle method is recommended since multiple data in terms of elastic modulus as a function of depth can be obtained. The average value of multiple data from one indentation instead of single data might be more reliable (Poolthong 1998).

Weaver (1966) investigated the microscopic hardness of bone. He found that storage at 4°C in saline solution softened the bone approximately 20%. Storage in 10% formalin increased the hardness approximately 20%. Drying and embedding the bone in methyl methacrylate increased its hardness by 30 to 40 %. He concluded that normal values should be obtained from unaltered samples.

Another storage regime was used by Bosshardt (1994). Of a large collection of human premolars, extracted for orthodontic reasons he looked at the repair of root resorption. Following extraction, the teeth were immediately fixed in half-strength Karnovsky's

fixative (Karnovsky 1965), buffered (pH 7.4) with 20 mmol/l sodium cacodylate for 24-48 h. Thereafter, the teeth were briefly washed in 0.185 mol/l sodium cacodylate buffer (pH 7.4) and exposed to a decalcifying solution containing 0.15 mol/l EDTA, 2.5% glutaraldehyde with or without supplementation with 0.2 mol/l sucrose. Decalcification was performed at room temperature over 4-6 weeks, under constant stirring. The solution was changed twice weekly. Afterwards, root slices of about 1 mm thickness were cut vertical to the root surface in a corono-apical direction. The specimens were post-fixed in 1.33% OsO4 buffered in 67 mmol/l s-collidine for 2 hours (Bosshardt 1994).

Tohda 1996, immediately after extraction, fixed the teeth in a mixture of 2.5% glutaraldehyde and 2% paraformaldehyde solution, pH 7.3, for 48 h, and cut longitudinally to produce ground sections of 50-um thickness.

Hals and Selvig (1977) fixed extracted teeth in neutral formalin, dehydrated in alcohol and embedded in polyester or epoxy resins. Semi-serial ground sections, 30-80 um in thickness, were then prepared at right angles to the long axes of the teeth.

Root cementum is variably permeable. AEFC of extracted permanent teeth of young and old subjects is permeable to water-soluble dyes such as toluidine blue which passes through the cementum diffusely and somewhat along the fibers of Sharpey (Schroeder 1986). In CMSC, the water-soluble dye penetrates mainly via canaliculi and lacunae of cementocytes, but a diffuse flow also occurs (Lindèn 1968). Stones (1934) reported that acellular cementum in which Sharpey's fibres are calcified was impermeable to dyes. However other authors disagree (Bartelstone, 1954 and Wainwright, 1952). These authors observed that radioactive Iodine could permeate cementum exposed to a periodontal pocket. If we were to except that cementum is relatively permeable then resin embedding may cause absoprtion of the methylmethacrylate resin and therefore affect the surface properties of cementum.

Since the X-ray analysis performed is essentially an analysis of the prepared surface, it is requisite that the prepared surface be truly representative of the specimen. Over the years, a number of qualitative criteria for a properly prepared surface have evolved. These are that the specimen should be polished as flat and scratch-free as possible and be analyzed in the unetched condition so as not to alter the topography or surface chemistry. Such criteria were set forth primarily for metallurgical specimens; they can be applied most directly to petrographic specimens. However, for biological specimens and hydrous materials such criteria are virtually meaningless since it is rare that a "polished" specimen is used in such work (Goldstein et al 1981).

2.9.1 The effect of Formalin, Sodium Hypochlorite and Alcohol on Cementum

Although the effect of storage is not mentioned specifically in the literature, various extrapolations can be made. Waters (1980) reported the effect of storage in Formalin would cause dehydration and also cross-linking of proteinaceous material. Also commercially available Formalin is generally acidic due to the formation of formic acid, which would result in the dissolution of the mineral component Waters (1980).

Sodium hypochlorite is one of the most commonly used in dentistry as a disinfectant. It also, is known for its protein denaturing as well as its antibacterial properties, accounting for its endodontic uses (Piskin et al., 1995).

The effect of alcohol on cementum has not been investigated, however alcohols effect on bone has been studied by many authors (Turner and Burr 1993). Alcohol is said to remove water from bone reversibly. Alcohol also has an irreversible effect in that it removes the lipids, therefore causes cell membrane damage (Lucsanasombool, 2000) Water has a great effect on the mechanical properties of the collagen fibril, but not on the hydroxyapatite mineral (Sasaki and Enyo, 1995).

3. Aims and Objectives

This study measured the physical properties of hardness and elasticity of human root cementum on first premolar teeth from male and female subjects with the use of micro-indentation analysis, and how these properties differed along the root length. To enable accurate determination of these properties, we needed to assess the effect of storage media and time on hardness and elasticity of human premolar teeth. This study provided a 3-dimensional map of hardness and elasticity. The specific objectives of this study were to:

1. To develop a method for 3-dimensional analysis of hardness and elasticity on an unprocessed tooth.

2. Formulate a 3-dimensional map of hardness and elasticity of cementum using Ultra Micro-indentation Systems (UMIS),

3. To assess storage conditions on samples of human premolar teeth,

4. To correlate the physical properties of the different areas of cementum to the structural composition at these sites; and

5. To establish baseline values for the properties of hardness and elasticity of cementum that can be used for future investigations involving similar protocol to allow assessment of changes of these properties that occur following orthodontic tooth movement.

4. Methods and Materials

4.1 Selection Criteria

4.1.1 Tooth Determination

The orthodontic treatment of patients occasionally requires the extraction of teeth to enable the final treatment objectives to be achieved. Premolar teeth were used in this study to establish a control database of the physical properties. This would allow later comparison for a similar experimental protocol involving teeth exposed to orthodontic forces. As premolar teeth are frequently exposed to orthodontic force and then extracted (e.g. Rapid maxillary expansion or arch wire expansion) these teeth therefore lend themselves to this type of experimental protocol.

Twenty first premolar teeth obtained from orthodontic patients (both genders), who require extractions as part of orthodontic treatment, were the source of samples for the storage section of this study. The age period selected was 14-18 years. This was assessed radiographically and confirmed clinically by microscopic analysis. On completion of the storage segment of the study, nine first premolar teeth were obtained from male and female orthodontic patients. On the basis of availability and sample size restrictions, male and female first premolars were used in the 3-dimensional mapping segment of this study (Fig. 4.1).

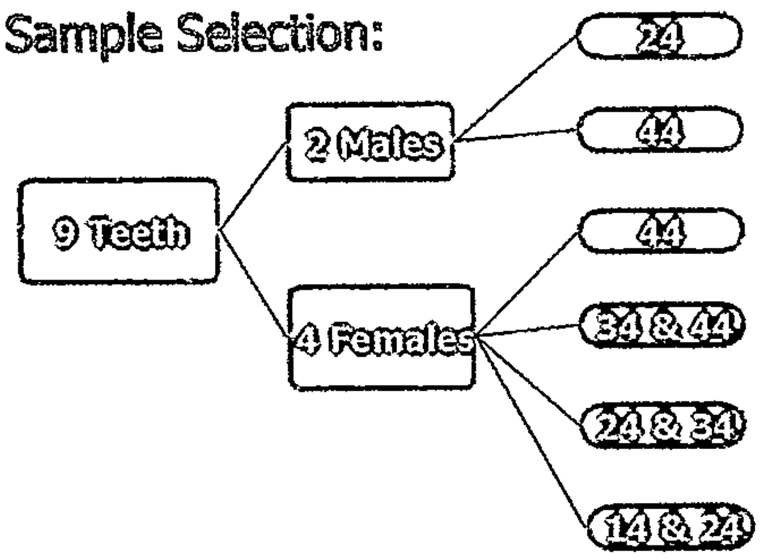

Figure 4. 1. First premolar teeth extracted from male and female patients selected to show the inter- and intra- differences for 3-D study.

4.1.2 Subject Selection

First premolar teeth were obtained from orthodontic patients requiring extractions of as part of orthodontic treatment (ethical approval - SB:cs 9293 3240). Patients meeting the required criteria were recruited off the United Dental Hospital orthodontic waiting list. These patients were invited to participate in the study.

The required criteria were biased to obtain virgin cementum. The selection criteria used was:

1) Patients had at least 2 premolar teeth to be extracted,
2) There was no reported or observed dental treatment to the teeth to be extracted,
3) There was no previous reported or observed trauma treatment to the teeth to be extracted,
4) There was no previously reported orthodontic treatment involving the teeth to be extracted,
5) There was no past or present signs or symptoms of periodontal disease,
6) There was no past or present signs or symptoms of bruxism,
7) There was no significant medical history that would affect the dentition,
8) There was no physical abnormality concerning the anatomy of the cranio-facial & dento-alveolar complexes, and
9) Root development occurred to closed apex, and
10) The patient resided in a fluoridated region during root development.

4.2 Specimen Collection

On patient consent, the teeth were extracted by forceps in the Oral Surgical department of the United Dental Hospital. Fractured teeth were excluded. Upon removal, teeth were immersed completely in an individual solution of sterilized de-ionized water (Milli Q),

from the same source, in a ten millilitre vial. The individual specimen vials were taken to an ultra sonic bath of de-mineralised and de-ionized water to remove traces of loose residual periodontal ligament (PDL) and residual soft tissue fragments and ultra-sonicated for a period of ten minutes. Following the ultra sonic bath, a damp gauze swab was then used to remove the remaining PDL. A rubbing motion was employed until all visible signs of the PDL was removed. The teeth were then disinfected in 70% alcohol for 30 minutes. Following disinfection, teeth samples were stored in Milli Q at ambient room temperature 23°C ± 1°C. These conditions were set and maintained through out the testing and storage procedures.

4.2.1 Tooth Mounting

The specimen was removed from the deionized water and allowed to dry for 1 minute to remove all traces of deionized water. The pulp chamber was opened using a diamond bur with copious water spray, and the tooth mounted via a high speed bur (Diamond Bur # 856-018 FG STD K) centre along the long axis to a standard depth, inserted through an occlusally prepared access cavity toward the root canal. The burs were cemented with light cured GIC orthodontic band cement (3M) "Transbond".

This bur served as a support against the cantilever force during UMIS machine testing. The tooth was supported at its apical end by a specially designed jig (Fig. 4.2).

4.3 Jig Assembly and Location Device

A specially designed jig was constructed to enable non-destructive, unembedded testing of teeth in 3-Dimensions (3D). This device was crucial for the relocating and assigning specific coordinates on the surface of the tooth. This simple and compact assembly is easily fitted into different instruments allowing the simple location of points on the surface of the tooth. Specific points can be targeted for further analysis, by 3-D recording of the X, Y, Z coordinate test site (Fig. 4.3 and 4.4).

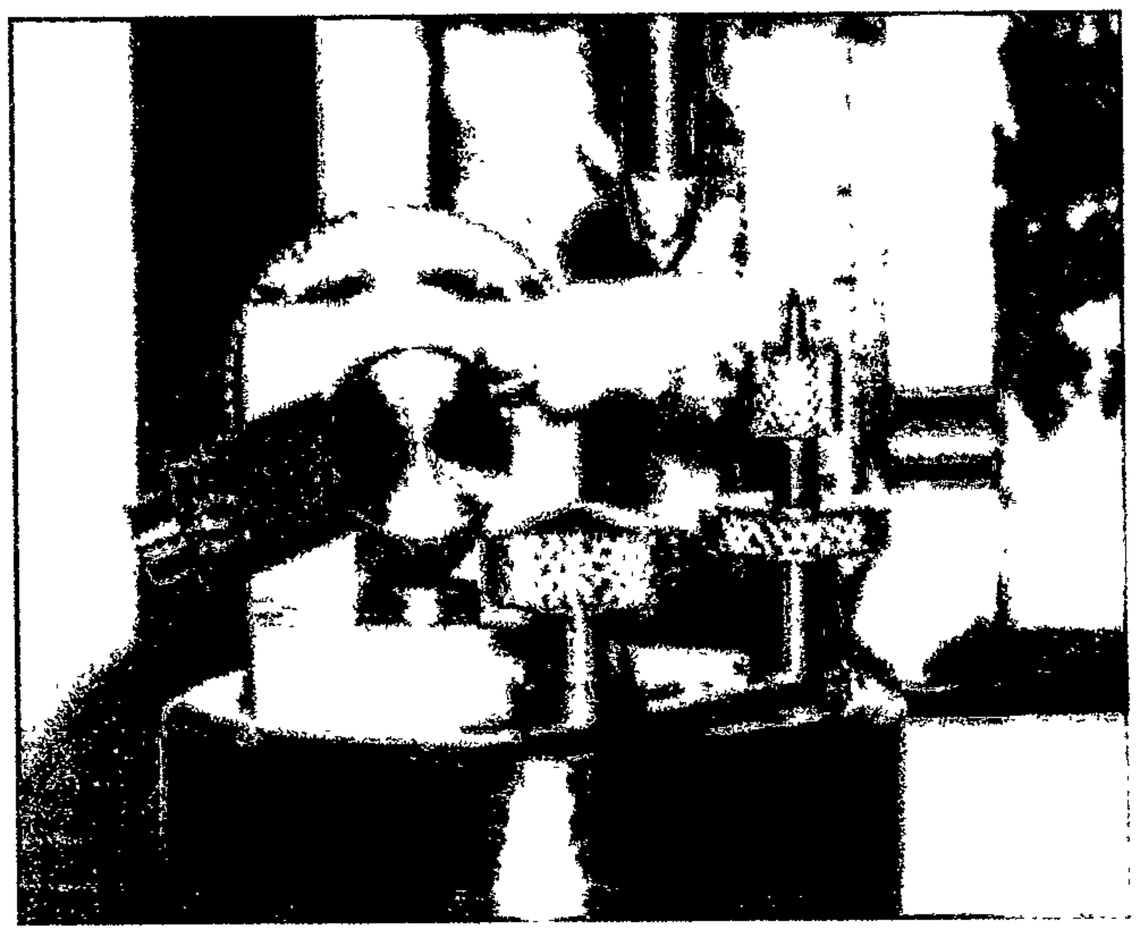

Figure 4. 2. The "Jig" assembly in operation on the Umis platform. This allowed for 360° rotation of the specimen. Both the inserted bur and the extendible arm on the Jig support the tooth from the indentation force.

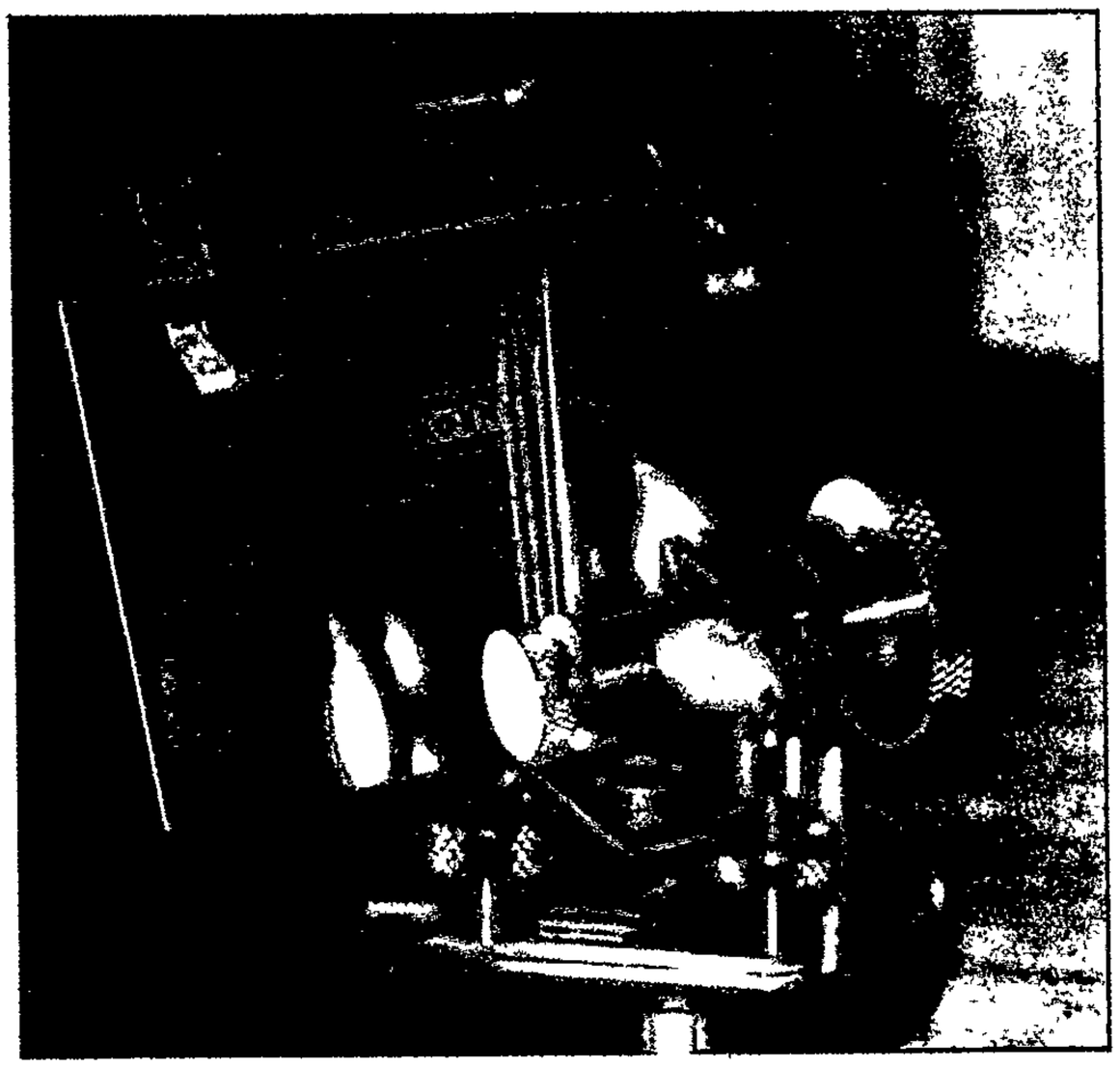

Figure 4. 3. The use of the protractor allowed measurement of the angle YZ degree coordinate to be recorded. Further analysis allowed the breakdown of vectors, both horizontal and vertical measurement from the reference point located on the Jig.

The bur is inserted into the jig at the coronal end and the tooth is supported at its apical end by an extendible arm on the Jig. The location device used allowed for further precise

identification of the test site. The X coordinate was measured to a central point of reference on the central shaft on the Jig. This measurement was obtained using vernier callipers. The Y and Z coordinates were registered by means of an angular measurement around the respective horizontal and vertical axes (Fig. 4.3 and 4.4).

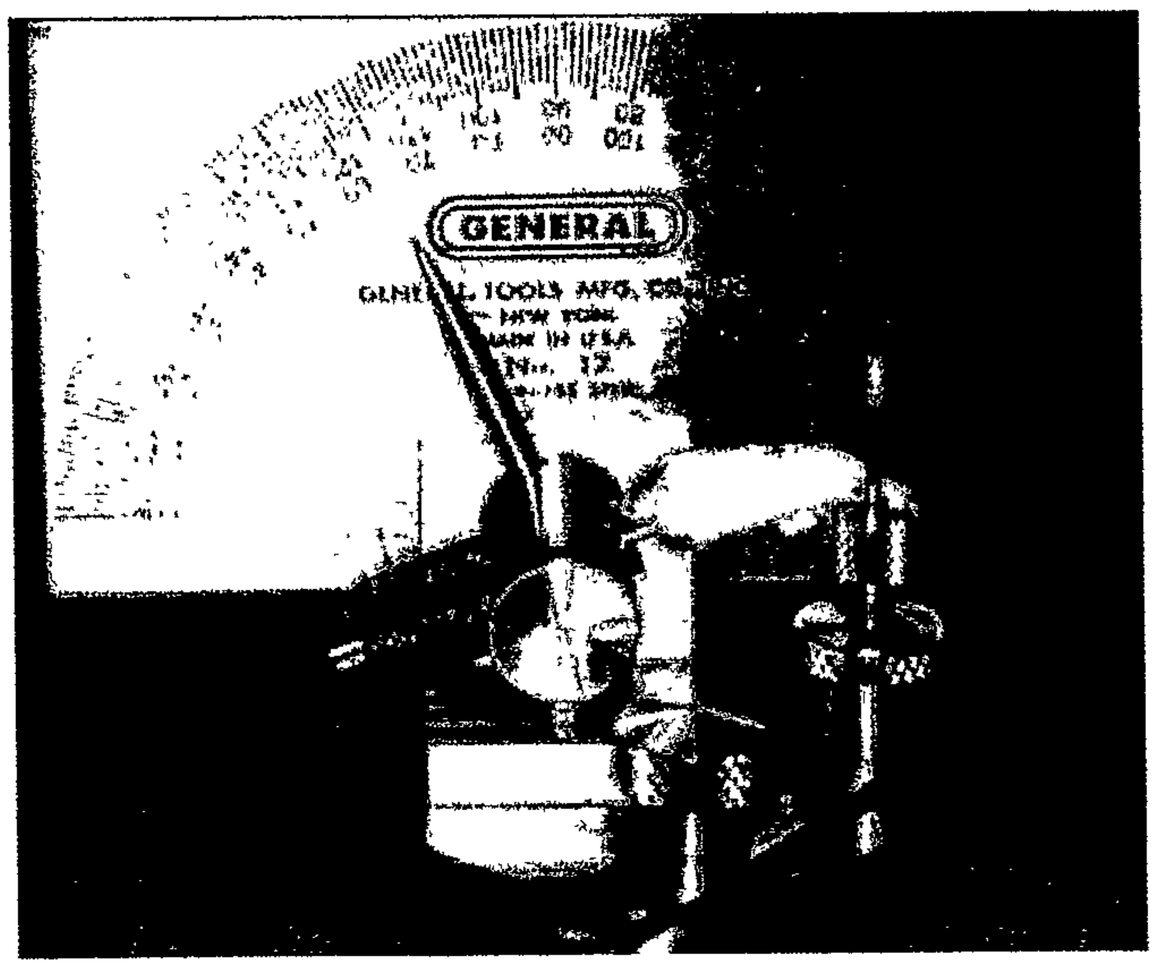

Figure 4. 4. The use of the protractor allowed measurement of the angle XY degree coordinate to be recorded. Further analysis allowed the breakdown of vectors, both horizontal and vertical measurement from the reference point located on the Jig. The X coordinate was measured directly as a horizontal millimetre measurement from the centre of the shaft of the Jig.

4.4 Measurement of the Hardness & Elasticity on the Ultra-Micro Indentation system (Umis)

The Ultra Micro Indentation System is a nano-indentation instrument for the investigation of the material properties of coatings, thin films and the near surface region of materials (Fig. 4.5). UMIS was developed at the National Measurement Laboratory in **CSIRO**. In operation, a small diamond spherical indenter is forced into the surface and the resulting depths of penetration recorded to produce a load/unload curve. From this curve, hardness, elasticity, fracture behaviour, strain index, creep and contact stress-strain and other mechanical properties can be derived.

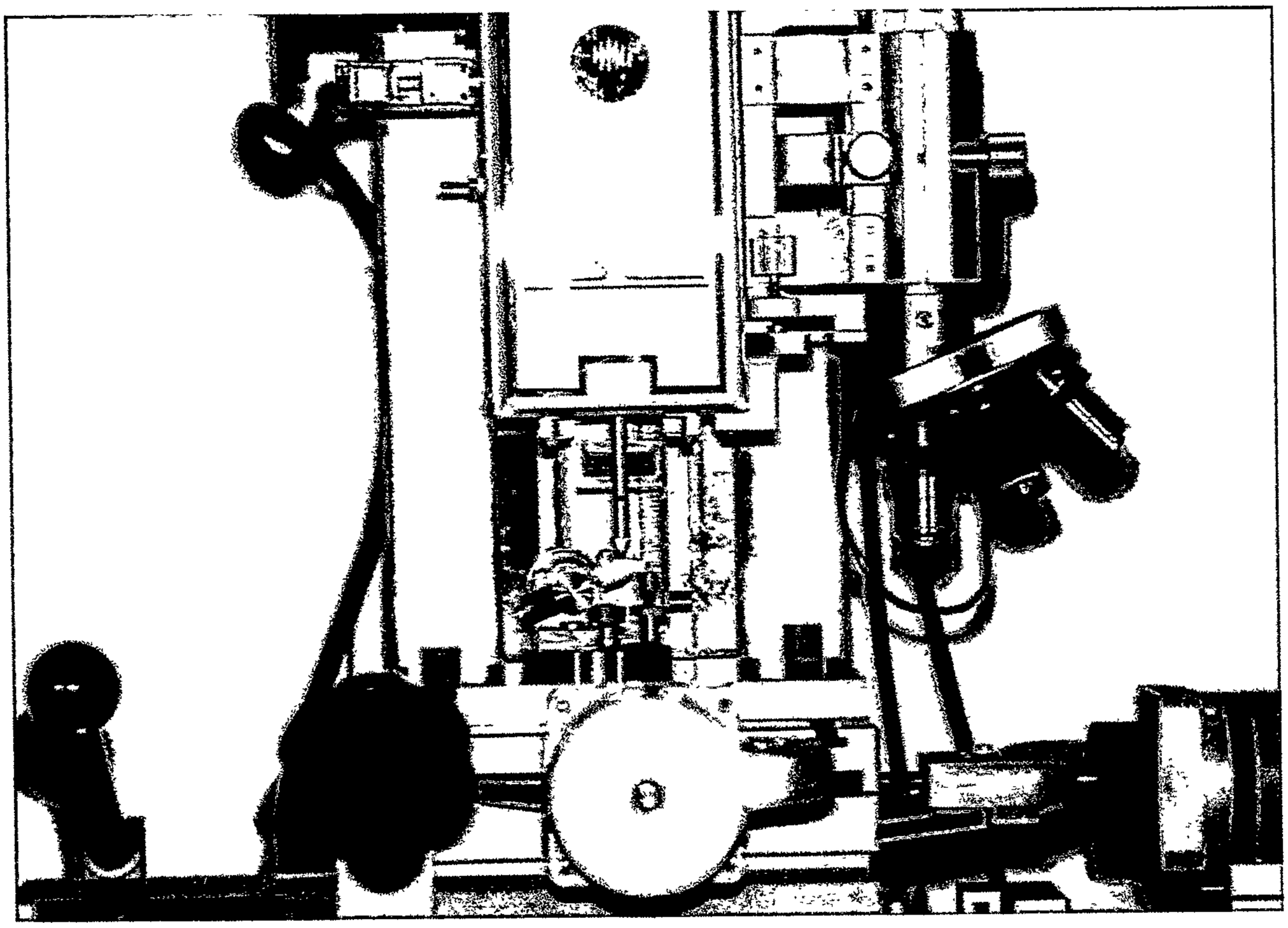

Figure 4. 5. Umis 2000 testing device.

The UMIS test was programmed at 5mN contact force (1/2 gram) with 20μm Spherical Diamond indenter penetrating the surface to a maximum force of 500mN (50 grams) in 20 indent increments. Each coordinate (as seen in Fig. 4.6) comprised of 5 individual indents in a 100 μm square array. All root surfaces were measured at 60 different sites. An additional 2 enamel sites were measured at the buccal and lingual surfaces. A 3-dimension hardness and elasticity map was constructed using an imaging programme.

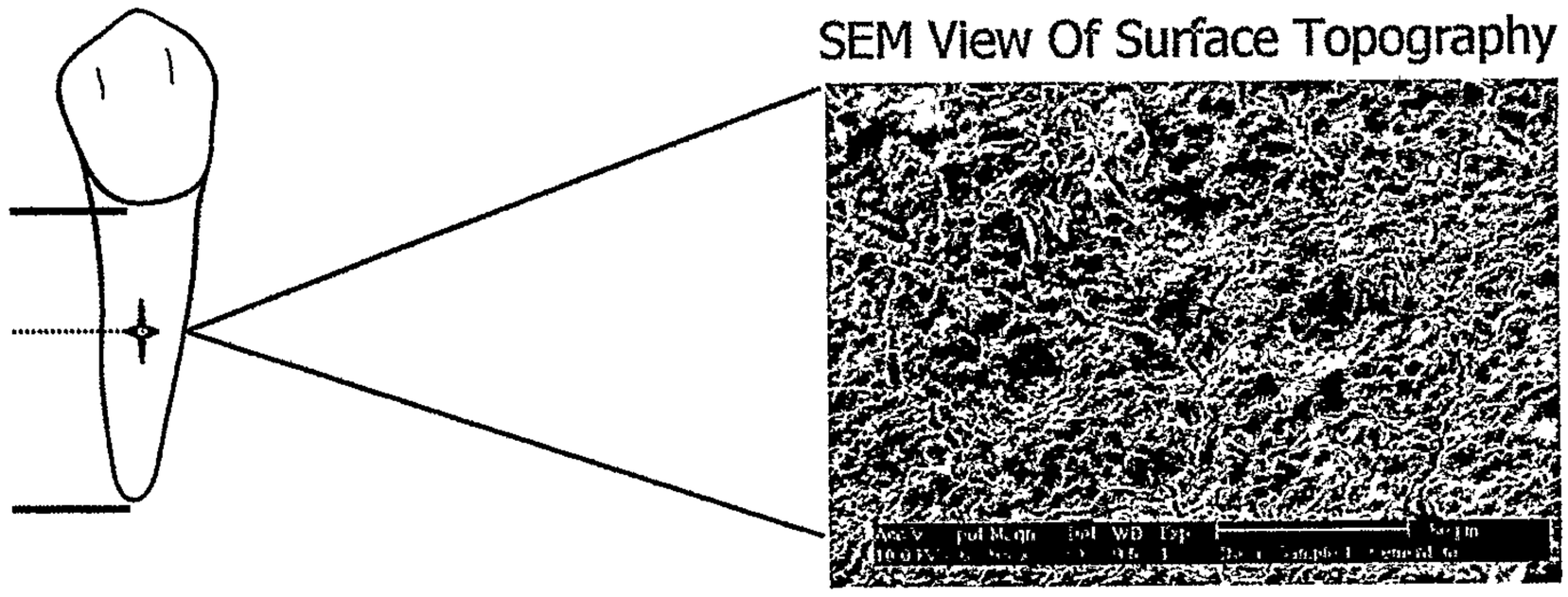

Fig. (a) Fig. (b)

Figure 4. 6. a. Diagrammatic representation of locating mid-point of buccal surface for storage study. Figure b. SEM micrograph of the buccal surface mid-point illustrating the five-point indentation array. (Magnification = 535x). The extensive cracking observed in Figure b, occurred due to the dehydration process prior to carbon coating for SEM.

4.4.1 Establishing Working Length / Site Location

A video microscope (x10 and x20 magnification, CSIRO Australia) was used to resolve surface irregularities. As the surface of the unprepared sample is irregular, the surface tested needed to be as flat as possible. The Umis allowed 25 μm working surface variation. The working length was accomplished by scanning the near region until an area is found with a similar depth of focus. This facilitated the function of the extremely sensitive instrument the UMIS 2000.

4.4.2 Selection of Indenter

The initial pilot study carried out was based on a protocol by Clark (1997). This protocol required modification, being that the teeth used were without preparation or resin embedding, however the same instrument was used to assess hardness and elasticity. In his protocol a triangular diamond indenter was used, the Berkovich indenter (CSIRO, 1993).

The results using the Berkovich indenter on the unaltered sample were highly variable. It was assumed that the heterogeneous nature of the unprepared surface of the cementum caused the sliding of the indenter as was indicated by the plots obtained.

The use of the spherical indenter appeared to eliminate problems attributed to surface asperities. Greater loads were utilized to enable the compression of the asperities and therefore compensate for the minimally prepared surface. The Umis 2000 has the ability to accept surface discrepancies of up to 25μm in a traverse without interfering with its operation. In this study a spherical indenter was used with a 20μm diameter diamond tip (CSIRO, 1993).

4.4.3 Indentation Location

Teeth are not of uniform length or shape. To standardize the sample the root was equally divided into six regions as measured on the buccal surface. The buccal surface was then divided longitudinally in two, however the apex was not divided. This enabled eleven points to be located. The lingual surface was treated similarly resulting in 11 points on the buccal and lingual surfaces respectively (Fig. 4.7a). To assist in calibration of the instrument two enamel points were utilized, one buccal and one lingual. The mesial and distal surfaces were similarly divided horizontally, however longitudinally the width varies. Dividing the tooth into apical, middle and cervical regions compensated for this. This resulted in 19 points on the mesial and distal surfaces respectively (Fig. 4.7b).

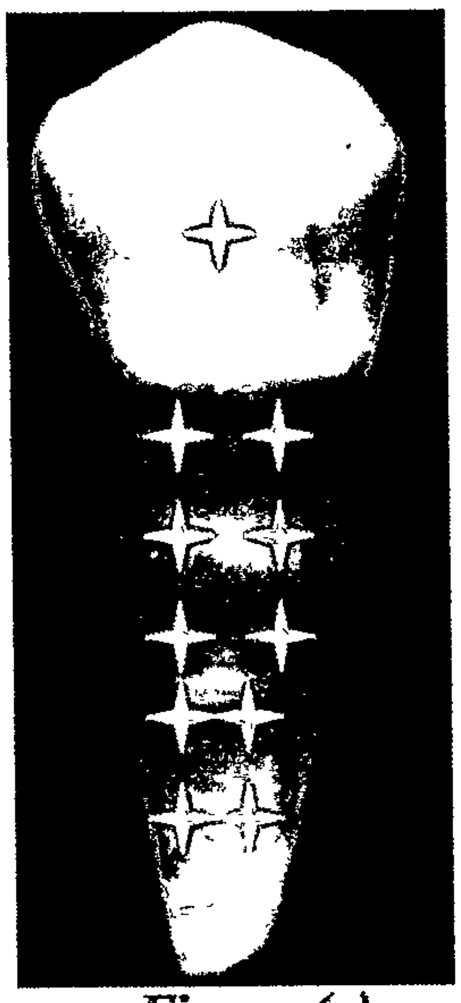

Figure (a)

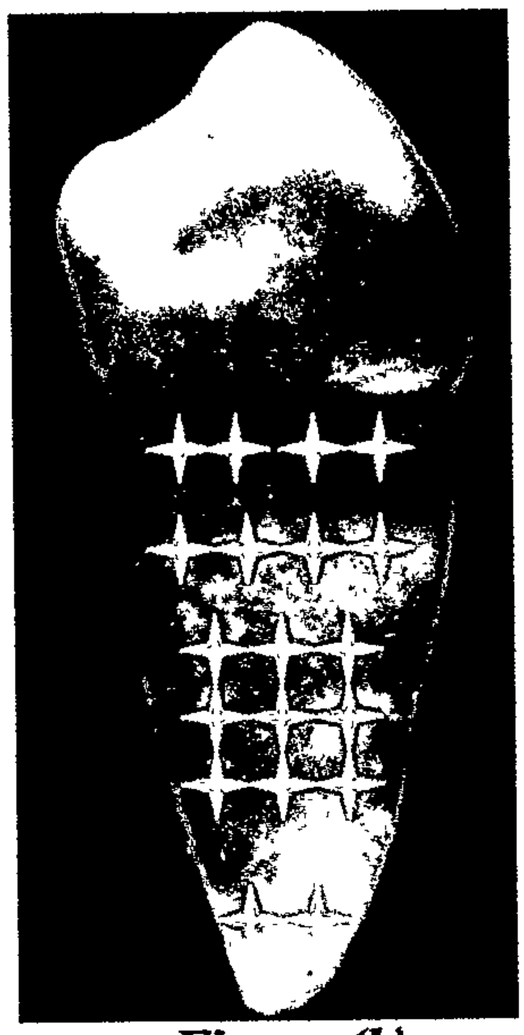

Figure (b)

Figure 4. 7. *Figure a.* Eleven points on the buccal and lingual root surfaces respectively. Two enamel points were used to allow for instrument calibration. *Figure b.* The mesial and distal surfaces were divided horizontally. The tooth was also divided into apical, middle and cervical regions. This results in 19 points on the mesial and distal surfaces respectively.

4.5 UMIS Functions

4.5.1 Multiple Partial Unloading

The UMIS used a predetermined load for its indentation testing. This load was achieved sequentially by a series of in/out (load/unload) cycles. Hardness was presented graphically as a function of depth of penetration for each individual penetration step. Hardness and the composite modulus, E*, were also presented graphically as a function of the depth of elastic/plastic penetration with the Umis software.

Indentations may have a final depth of penetration from less than 100 nm up to 40 μm or more, depending on machine configuration, with penetration measured from an initial datum established by bringing the indenter into contact with the surface with a very small force "contact force".

Specimens must have a flat, well-finished under-surface and when mounted must be parallel with the worktable. However, changes of surface level of several micrometres arising from the superposition of masked layers or other causes were automatically accommodated.

A video microscope capable of resolving surface features as small as 1 μm was attached. A precise X-Y translating mechanism allowed the viewed region to be transferred from the video microscope platform to the indenting position.

Acquisition of data by using a multiple partial unloading cycle was the technique used which is particularly suited for spherical indentation.

Multiple partial unloading gave more reliable determination of hardness and modulus as a function of the depth of elastic/plastic penetration for materials whose properties vary with distance from the surface.

To determine hardness from indentation depth it is necessary to determine the penetration of the indenter below the perimeter of contact, the remainder of the total measured depth being elastic depression of the surrounding material. The elastic contribution, obtained from unloading data was required to make these calculations (Fig. 4.8).

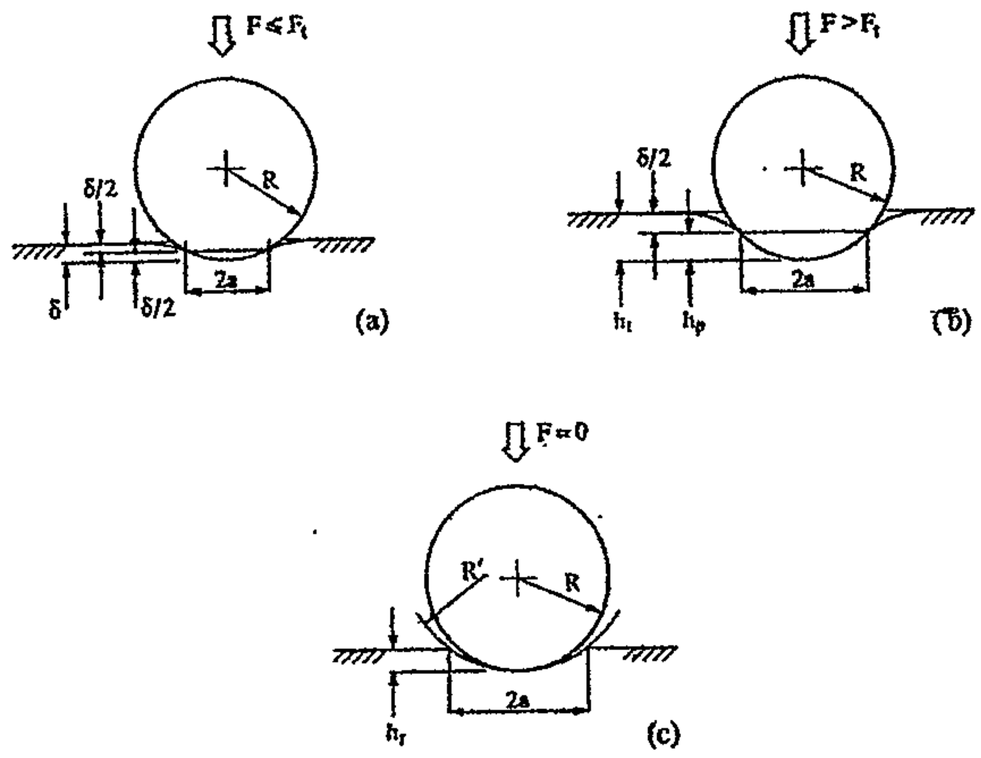

Figure 4. 8. The geometry of the indentation: a. Loaded to the elastic / plastic transition; b. Fully loaded; c. Fully unloaded.

In multiple partial unloading a single indentation was partially unloaded in one increment at each force step by an amount, which varied from 10 to 90 percent of the load step. Each force step provided two pieces of information: the total depth of elastic/plastic penetration and a measure of the recovery from that load. In this study 50% of the loading fraction was the unload increment.

In the case of indentation with a sphere, two points at each load were sufficient to fully characterize unloading from each load step (Fig. 4.9).

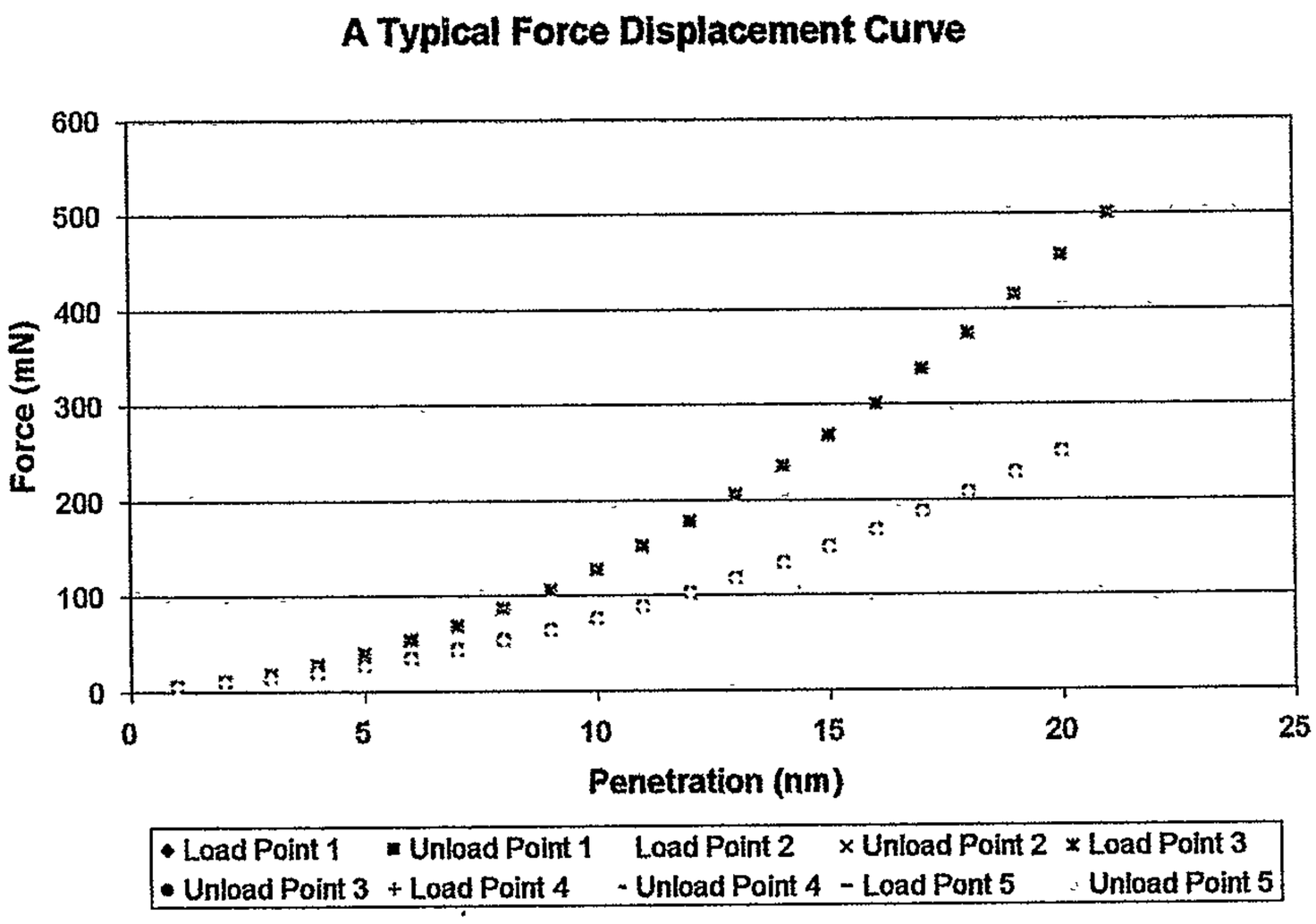

Figure 4. 9. A typical load/unload plot at point number 34 on the lingual surface of the lower left first premolar.

4.5.2 The Partial Unload Cycle

Contact with the surface and auto-zeroing sequences were initially utilized prior to load cycle data acquisition. The load was reduced by 50% of the load after the loading dwell at each load step. This, accompanied by a settling pause allowed the partially recovered depth to be measured. The load was then increased to the next step, fully reinstating the elastic recovery before producing a new increment of elastic/plastic indentation.

4.5.3 Spherical Indentation

Mean pressure is synonymous with Meyers hardness and the critical condition for transition (from elastic to elastic/plastic behaviour) and is assumed to exist when the mean pressure equals the critical pressure for the development of plastic flow of the surface layer under consideration. There is no definitive value of this situation for a spherical indenter. This arises because the contact strain increases with load, whereas for a pointed indenter it remains constant. We can relate the equivalence of the spherical indenter to the spherical indenter hardness by comparing contact pressures at the same strain.

Spherical Indenters. ε (strain) = a (constant)/ R(radius)

Pyramid / Cone Shaped Indenters. ε (strain) = Tan β(contact angle).

Stepwise loading a ball in contact with a semi-infinite half space up to the transition load and stepwise unloading it again should result in completely reversible displacements.

The depth of indentation below the circle of contact (h_p) at any load greater than the transition load, may be calculated from simple geometry knowing 'a' and the indenter radius *(R)*, then:

$$h_p = R - \sqrt{(R^2 - a^2)}$$

On unloading, the elastic recovery accounts for almost all of this displacement. The unrecovered portion is accounted for by an almost imperceptible spherical depression in the recovered surface; the radius of, which is very large, compared to that of the ball. Due to the sphero-conical indenter geometry the useful range of plastic penetration of the indenter at the maximum load is about one third of the sphere radius. Penetration beyond this depth is determined by the conical form of the indenter and is no longer able to be analysed correctly by the software.

4.5.3.1 Determination of Hardness from Spherical Indentations

The measured depths are corrected for the contribution made to them by the structural compliance of the instrument, which adds a small displacement, proportional to the force (F). The residual recovered indentation depth (h_r), the elastic deflection of the surface ($\delta/2$) and the depth below the circle of contact (h_p) are then calculated for each load step and plotted as a function of the depth below the circle of contact.

Hardness is calculated as a function of depth below the circle of contact by:

$$H = \frac{F}{\pi a^2}$$

where $a = (2R\,hp - hp)$

and $hp = ht - \delta/2$

4.5.3.2 Determining Elastic Modulus from Partially Unloaded Spherical Indentation Data

The analysis package for partial unload cycle data provides for the extraction of E^* at each step. Young's modulus for the test material may be determined only if Young's modulus for the indenter material and Poisson's ratio for both are assumed. Elastic recovery of a spherical indention is governed by:

$$\delta = \left[\frac{9}{8}\right]^{\frac{1}{3}} \left[\frac{1}{E^*}\right]^{\frac{2}{3}} \left[\frac{1}{D_i} - \frac{1}{D_m}\right]^{\frac{1}{3}} F^{\frac{2}{3}}$$

It is therefore possible to determine the value of the composite elastic modulus from the recovery on partial unloading:

$$E^* = F\left[\frac{9}{8}\right]^{\frac{1}{2}}\left[\frac{1}{D_i} - \frac{1}{D_m}\right]^{\frac{1}{2}}\delta^{-\frac{3}{2}}$$

D_i is the diameter of the spherical indenter and D_m is the diameter of the residual spherical depression (2R'). F is the total load at each step, and h_t is the corresponding total penetration.

4.5.4 Umis Calibration

Prior to testing procedure the Umis 2000 was calibrated by the use of a standard with known properties. The standard chosen was fused silica. A typical run using the same force and indentor was used. The poison's ratio was imported into the programme and compared to the test result.

4.5.5 Jig Compliance Testing

So as to ensure no errors were introduced in to the Umis parameters, the compliance of the designed jig was tested. A prepared sample was chosen and used as a standard. A known sample, a highly polished piece of enamel in cross-section from a human premolar, was used. This particular sample has been investigated previously (Poolthong 1998). The results obtained were compared and cross-referenced to the tooth mounted on a jig. The results from Berkovich and Spherical indenters were also compared.

A bur was placed into the tooth sample and the tooth sectioned, polished and mounted on the jig. The results obtained were compared and cross-referenced.

PROTOCOL

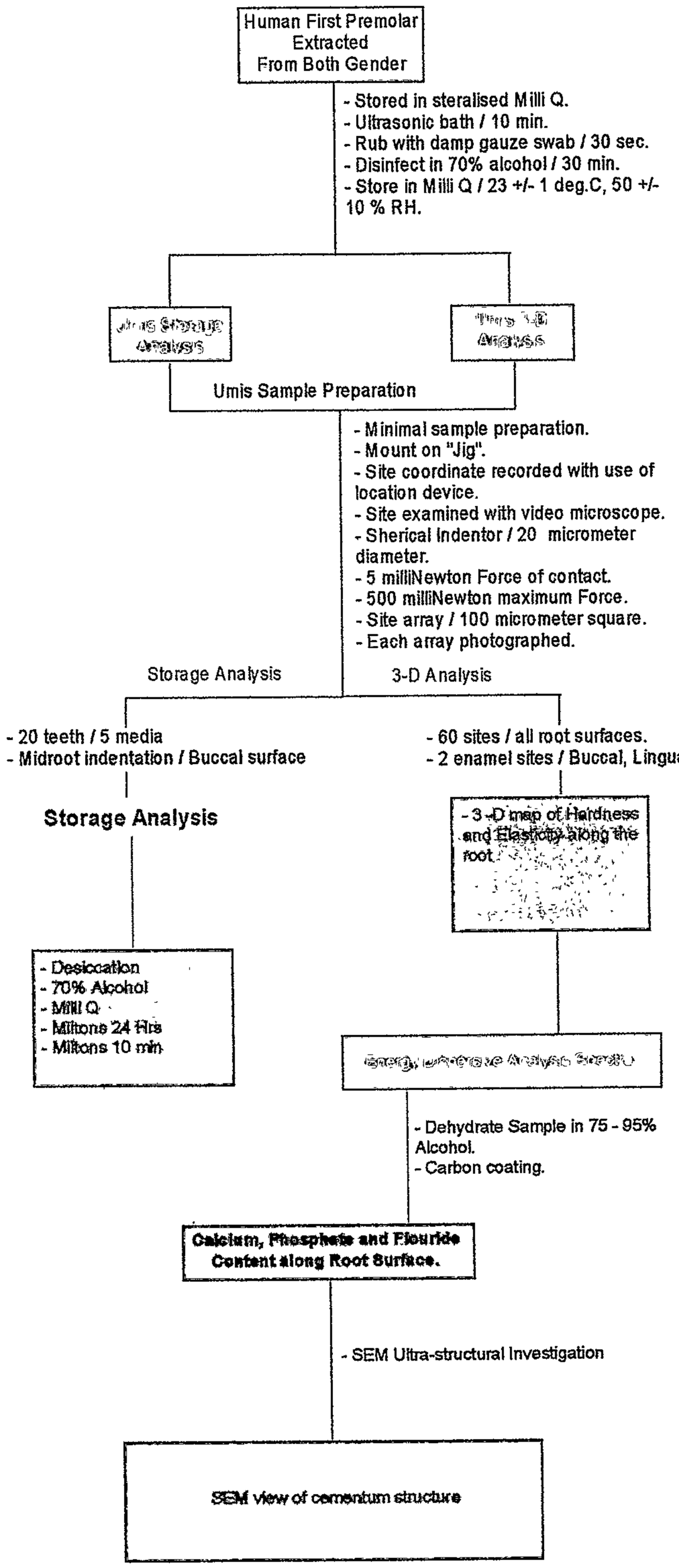

Figure 4. 10. Study outline.

4.6 Storage

4.6.1 Storage Study

The aim of the storage study was to test the effects of time and storage media on the hardness and elasticity of cementum. The variables include:

- Time (Initial test carried out after 6hrs, followed by 1-month intervals for 4 months).
- The 5 Storage media are:
    1. Desiccation
    2. 70% Alcohol
    3. De-ionized Water (Milli Q)
    4. Miltons (24 hrs)
    5. Miltons (10 mins.)

One point mid-way along the buccal surface of the root tooth surface was selected for testing. The mid-point of the buccal surface was determined by bisecting the longitudinal axis determined by a tangent to the CEJ and the apex (Fig. 4.6a).

Twenty teeth were collected and mounted as per protocol (Fig. 4.10) and divided into the respective groups, with four teeth in each group.

The samples were tested within 6hrs of extraction to establish baseline data. They were then stored for one (1) month at constant ambient room temperature 23 ± 1°C their respective media. After one month, the teeth were systematically tested and every month thereafter for the three-month period. The samples for the 3-Dimensional analysis were stored in the media that produced the least change in the physical properties of cementum. The buccal midpoints of the favoured storage media were re-tested at the completion of the 3-D analysis to confirm the effect of time on the physical properties of cementum.

4.7 3-Dimensional Measurement of Hardness and Elasticity

The nine teeth extracted from the six patients were analyzed for hardness and elasticity at the sixty sites along the root surface, which comprised of five individual indent arrays as seen in Fig. 4.6b. The same operating conditions, as for the storage analysis were set and maintained during 3-D testing. From the data obtained a 3-D map was plotted from the apex of the tooth to the CEJ on all four root surfaces.

Data was acquired by a multiple partial unloading cycle. This technique was particularly suitable for spherical indentation.

4.8 3-Dimensional Measurement of the Calcium X-ray Absorption (Energy Dispersive Analysis Spectra) on SEM

The specimen was dehydrated using different concentrations of alcohol (75%-95%) and is prepared for SEM (carbon coated). The calcium X-ray absorption was measured on the SEM.

The scanning electron microscope (Phillips XL30) with the use of the EDAX (energy dispersive analysis spectra) enabled the Calcium, Phosphate and Fluoride concentrations along the divided portions of the root to be determined. The resultant concentrations allowed for ready comparison to the hardness and elasticity values along different regions of the root.

The parameters used were, 20KVp, spot size 5, magnification x500 and a 50-second absorption period measured at a constant distance of 10mm. As the sample was not polished constant computer driven manipulation of the sample / source distance was required to enable standardization of results for ease of comparison.

Resultant concentrations were stored and downloaded into Microsoft Excel v5 in preparation for statistical analysis.

4.8.1 Preparation for EDAX Investigation

Originally platinum was chosen for coating of the samples. This coating promoted a superimposition of the platinum EDAX peak on to the phosphate peak, which would therefore produce errors in the counts obtained for the phosphate in the samples. As a result carbon coating was chosen to eliminate this error.

The coatings were obtained with the use of two carbon rods sharpened to a point with a conventional pencil sharpener and were positioned in such a way so that the points were in contact. Under the conditions of a vacuum a current was past through the carbon electrodes to produce arching. A centrifugally spinning device allowed for even carbon coating to be placed on the samples.

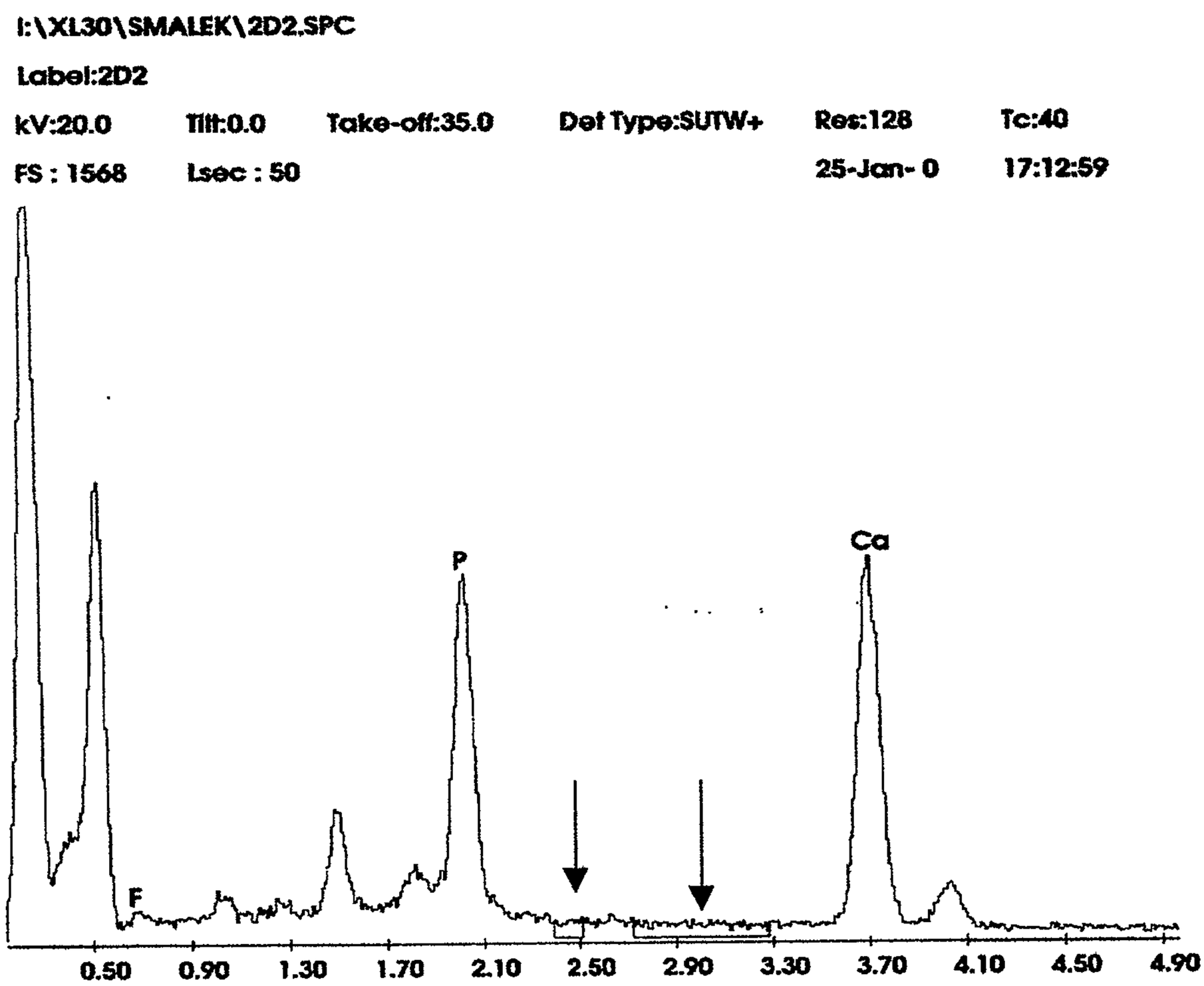

Figure 4. 11. A typical spectrum obtained with the use of EDAX. This spectrum is representative of Sample 2, position 2, on the distal surface. Note the two integration windows which were used to obtain the ratio of the peak to background ratio.

4.8.2 Determination of Calcium, Fluoride and Phosphate Concentrations

Calcium, Fluoride and Phosphate concentrations were reported as relative values of the samples as the samples were not embedded and polished flat. Two integration windows (fixed references) of the background were manually assigned in regions of minimal absorption to enable estimation of peak to background ratios. The same fixed integration windows were used for all samples. This prevented the software (self determined) interpretation of the peak to background ratio. The use of the two integration windows of the background reduced the possibility of error, which was estimated at approximately 5%, in the qualitative measurements of concentration.

The integration windows were chosen so as not to interfere with those counts of Calcium, Fluoride and Phosphate. They were also chosen in areas of little variation throughout the test areas chosen. The first window, designated 'Window 1' was between 2.39 and 2.51 Kilo electron volts (KeV). The second window, designated 'Window 2' was between 2.72 and 3.28 (KeV) (Fig. 4.11).

Results were obtained midway along all specimens, on all surfaces. The demarcations were the same as those used in the 3-D segment of the study. The first sample, which was Platinum coated, was used only for Calcium and Fluoride analysis. The phosphate ratio could not be calculated with certainty due to the phosphate-platinum overlap, and so was disregarded.

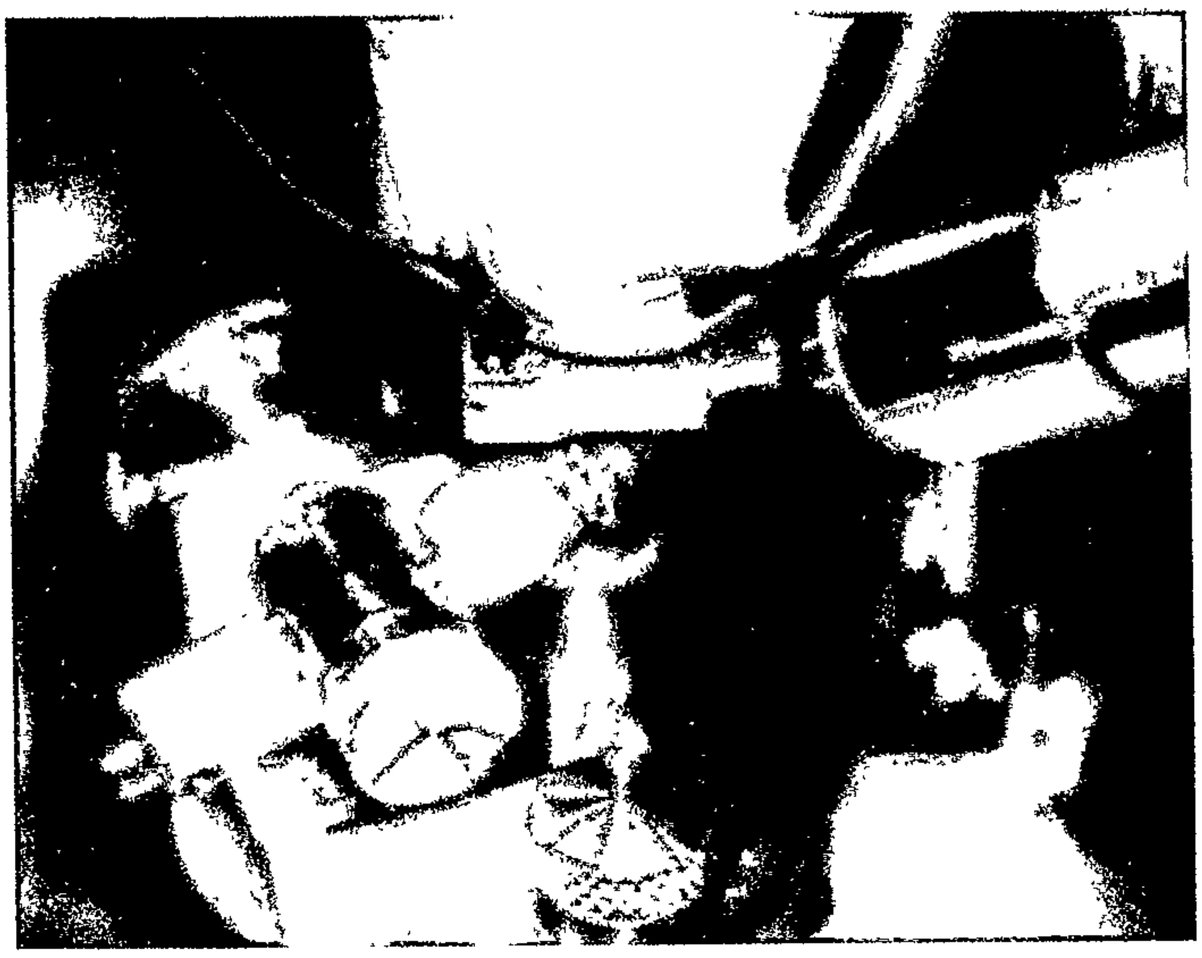

Figure 4. 12. The inside of the SEM chamber with the tooth attached and mounted to the location "jig". The electron beam was delivered from above (centre), while the EDAX sensor is located at the right hand of the photo.

4.9 Ultra - Structural Investigations using the SEM

Attempts were made to develop a protocol of fracture of the teeth to enable SEM imaging of the cementum ultra-structure. Various methods were considered such as a controlled fracture and a fracture using liquid nitrogen.

The specimens were finally fractured so that the cemental structural components could be related to the varying areas of hardness and elasticity. The structural components were visualized using the SEM as per protocol. This allowed for correlation of the physical properties of the different areas of cementum to the structural composition at these sites. Using stereo microscopy and image analysis techniques, the cemental structure was related to the location on the root.

Attempts were made initially using a scored fracture technique, in which a scribe mark was made and an osteotome inserted and twisted to complete separation (Schroeder 1993). This produced mixed results. A second attempt to produce a fractured surface for examination involved the use of liquid nitrogen.

Firstly a controlled fracture involved longitudinal scoring of the tooth with a diamond disc until the opposite surface was almost reached. A small osteotome was inserted and twisted to split the remaining surface, which included the cementum. The surface was cleaned with Miltons and the coated for SEM investigation as per protocol.

The second attempt involved the tooth being inserted into liquid nitrogen on to a metal platform, and once bubbling stopped, which indicated that a uniform subzero temperature was reached. A small household razor blade was placed on its surface in a longitudinal orientation. One firm blow with a mallet fractured the tooth, however this produced multiple pieces. It was difficult to determine the location of the individual pieces. The surfaces were cleaned with Miltons and the coated for SEM investigation as per protocol.

Finally, the nine premolar samples were embedded in "Epofix" (Struers, Denmark). Approximately 500 ml of "Epofix" embedding and impregnation resin was used to 'mount' all specimens. This consists of a resin of bisphenol-Adiglycidylether with molecular weight <700 and a hardener of triethylenetetramine. The epofix resin is soluble in alcohol and acetone. The epofix hardener was soluble in alcohol, acetone and water and resistant to acids, bases, acetone and alcohol. The resin was mixed as per the manufacturers' instructions (ie. 25 parts resin and 3 parts hardener by weight) and the resin was poured around each tooth. The resin was allowed to bench cure for a minimum of 48 hours at ambient room temperature of 23 ± 2^0C.

This mounting was a final attempt to produce images to enable correlation of structure to the physical properties previously obtained (Fig. 4.13).

The mounted and sectioned teeth were analyzed using transmitting light microscopy, SEM and confocal microscopy. Microscopic sections (100μm) were obtained to allow a protocol to be developed. Attempts were made using reflective microscopy, fluorescent imaging both stained with eosin and unstained. There was insufficient time to perfect the development of this method or for further analysis.

The parameters used were 20KVp and a spot size 5. Images were digitally recorded then downloaded and stored via a TIFF format on to a CD-Rom.

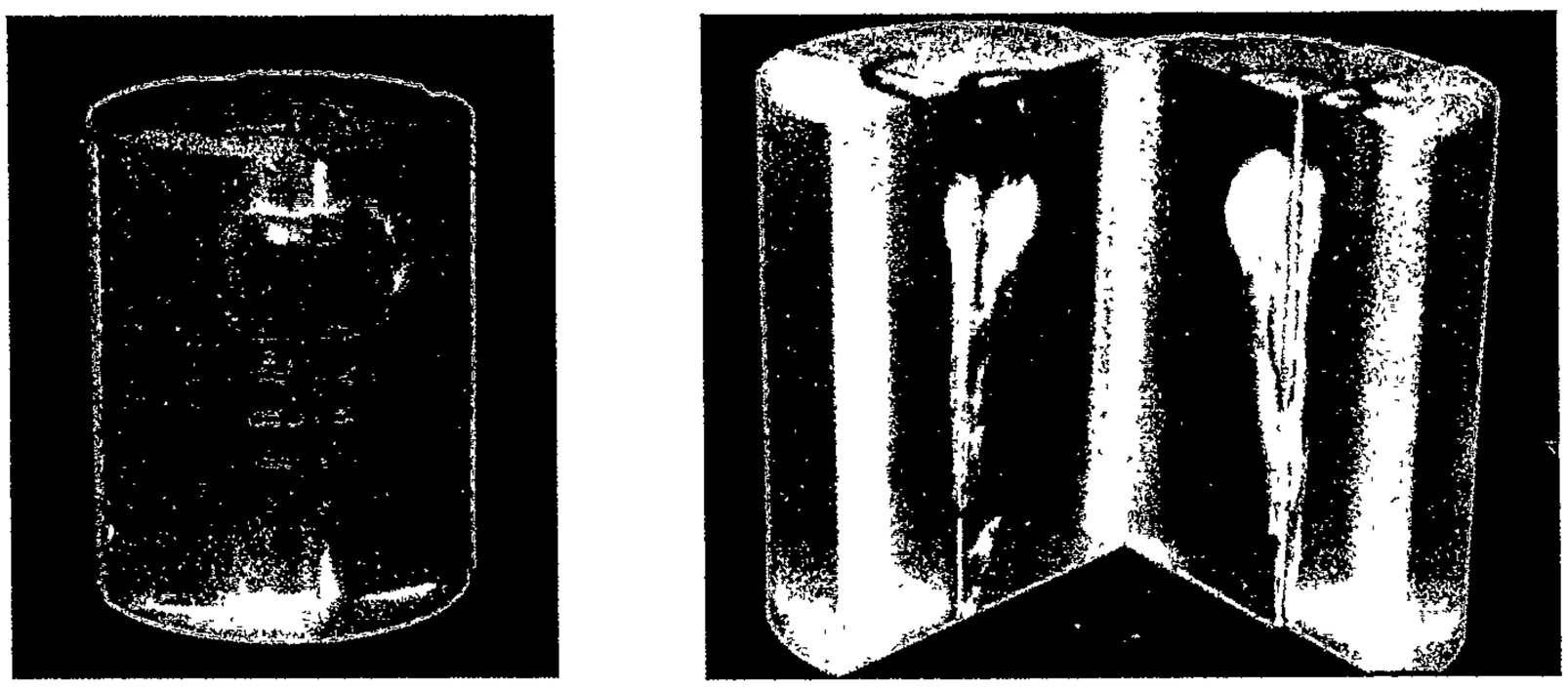

Figure 4. 13. Samples mounted and sectioned for structural analysis using SEM.

4.10 Statistical Analysis

SPSS (Statistical Package for Social Sciences) was used via a conversion of the UMIS data to an Excel download to allow statistical analysis of the data. The conversion allowed for a text data format from an ASCII file format used in the Umis programme.

A multivariate general linear model was chosen to express the interrelationships between the multiple factors (SPSS). A general linear model is basically an equation that expresses values of the variable in terms of other variables.

Variables included: Sex, Patient (sex), Side, Upper/Lower, Layer (surface), Surface, Calcium content.

4.10.1 Statistical Storage Analysis

Using multivariate testing of a general linear model designed to intercept; media, time and media*time (* denotes intersect). A general linear model was then considered to attempt to factor out any confounding differences in hardness that may be due to natural differences in tooth variations. Media, teeth within the media, time, media*time were run in a general multivariant linear model. Additionally, the same general linear model was re-run so as to remove confounders due to the minimally tested media sample group

4 (Miltons 24 hrs.). However to show the media which produced the least change in the hardness and elasticity values over time, and therefore the most ideal storage media to be used in the analysis of the physical properties of cementum, the standard deviations of each tooth were calculated and compared. The media were divided into the three main groups assessed (alcohol, desiccation and Milli Q). The standard deviations of hardness and elasticity over time were computed by means of a general linear model to determine whether the standard deviations of hardness and elasticity were significantly different over time.

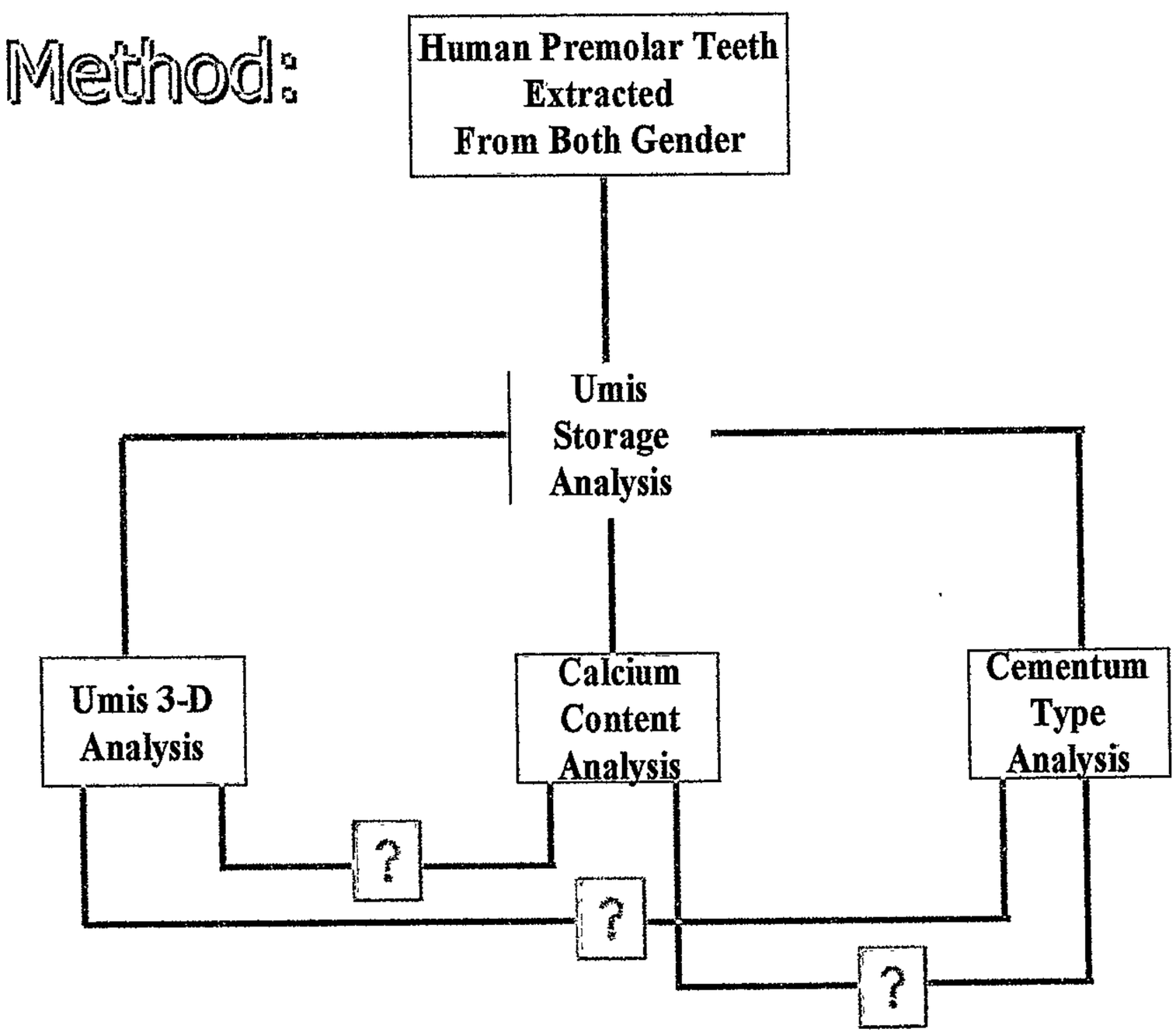

Figure 4. 14. Method components and interrelations studied.

4.10.2 Statistical 3-D Analysis

Sixty hardness measures along with their approximate (x, y, z) coordinates were imported into a software visualization package **AVS/Express** (Advanced Visual Systems, OpenViz). The coordinate data was originally modelled in **Houdini** (Side

Effect Software). Hardness is mapped to a colour, blue is soft, red is hard. The hardness values were then bilinearly interpolated to produce the contour map.

4.10.3 Method Error

There are generally two types of errors, Systematic errors and Random errors. Systematic errors are those derived as a result of biased or unrepresented sample (for example, measuring with the machine incorrectly calibrated, or using teeth that have been taken from patients with a disease that causes teeth to soften). This is a result of the sample group being in some way not representative of the wider population.

Random errors are errors due to the nature of using a sample to estimate values from a population – they are in no way mistakes, and cannot be eliminated, only controlled. One source of random error is the error of measurement, the plus-or-minus introduced by the actual measurement process (the point you pick, the way you hold the machine, the plus-or-minus in the machine reading, etc). It is measured from the variability in repeated measurements made at a particular point and under a particular condition. These errors due to measurements are calculated as pooled standard deviation (sd), in which the sd is squared and multiplied by the number of observations minus one (in this case there were five indentations, $(sd)^2$ is multiplied by four). This value is then divided by the total number of observations (that is $4.(sd)^2$). Finally the square root of this value will reveal the pooled standard deviation. This is given by the formula:

$$S = \sqrt{\frac{\Sigma (Xi - \breve{x})^2}{n - 1}}$$

Where S is the pooled standard deviation, Xi is the number of individual cases, n is the number of observation and $\breve{x}$ is the mean value obtained.

The random errors are measured by the standard deviations (standard errors of the mean) as reported. These are the variability due to chance. The possibility that the natural

variability of these observations obscuring the real differences seen is unlikely in this study. The increase in observations, such as the five arrays at one point is an attempt to reduce random errors (Dixon and Massey 1983, Bulman and Osborn 1989).

5. Results

The hardness, elasticity and the calcium content values of teeth at sixty points on the root surface as well as two enamel locations were obtained. A 3-D colour coded map of hardness, elasticity and calcium content was obtained and the data was also statistically analyzed.

5.1 Selection of Indenter

The effect of different indenters on unpolished cementum was examined in order to establish the working conditions needed for the evaluation of hardness and elastic modulus of the root surface.

The choice of indenters was influenced by a number of factors, primarily their behaviour on cementum. The UMIS provided quantitative values for hardness and elastic modulus in units of GPa. The results using the Berkovich indenter on the unpolished cementum were highly variable (Fig. 5.1). This force / penetration data generated using the Berkovich indenter on the unpolished cementum was found to produce considerable scatter. Ideally the force / penetration curve should only exhibit small deviations with similar maximum force penetration peaks. The Berkovich programme on the UMIS does not present data as multiple load / unload plots, but as continuous load and continuous unload plots.

The use of the spherical indenter, on unpolished cementum appeared to eliminate problems attributed to surface asperities (Fig. 5.2). This was seen by the reproducibility of the load / partial unload curves. The load curve is represented by the force with the greater magnitude, while the unload curve is plotted at 50% of the loading force.

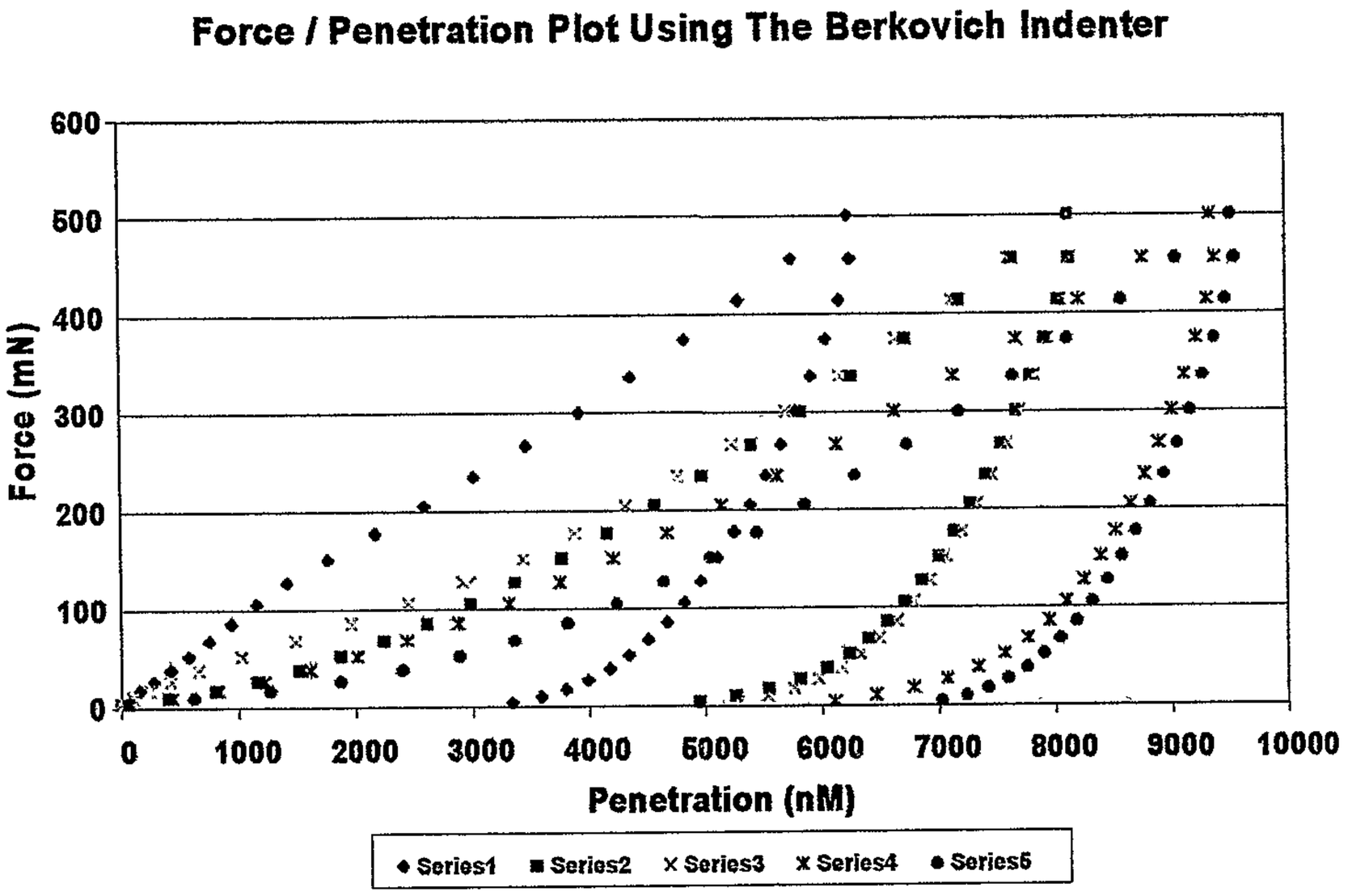

Figure 5. 1. Load / unload data plot demonstrating the scatter obtained by the Berkovich indenter on the unpolished cementum surface of sample 9. The series plots 1-5 represent the indents at the same location.

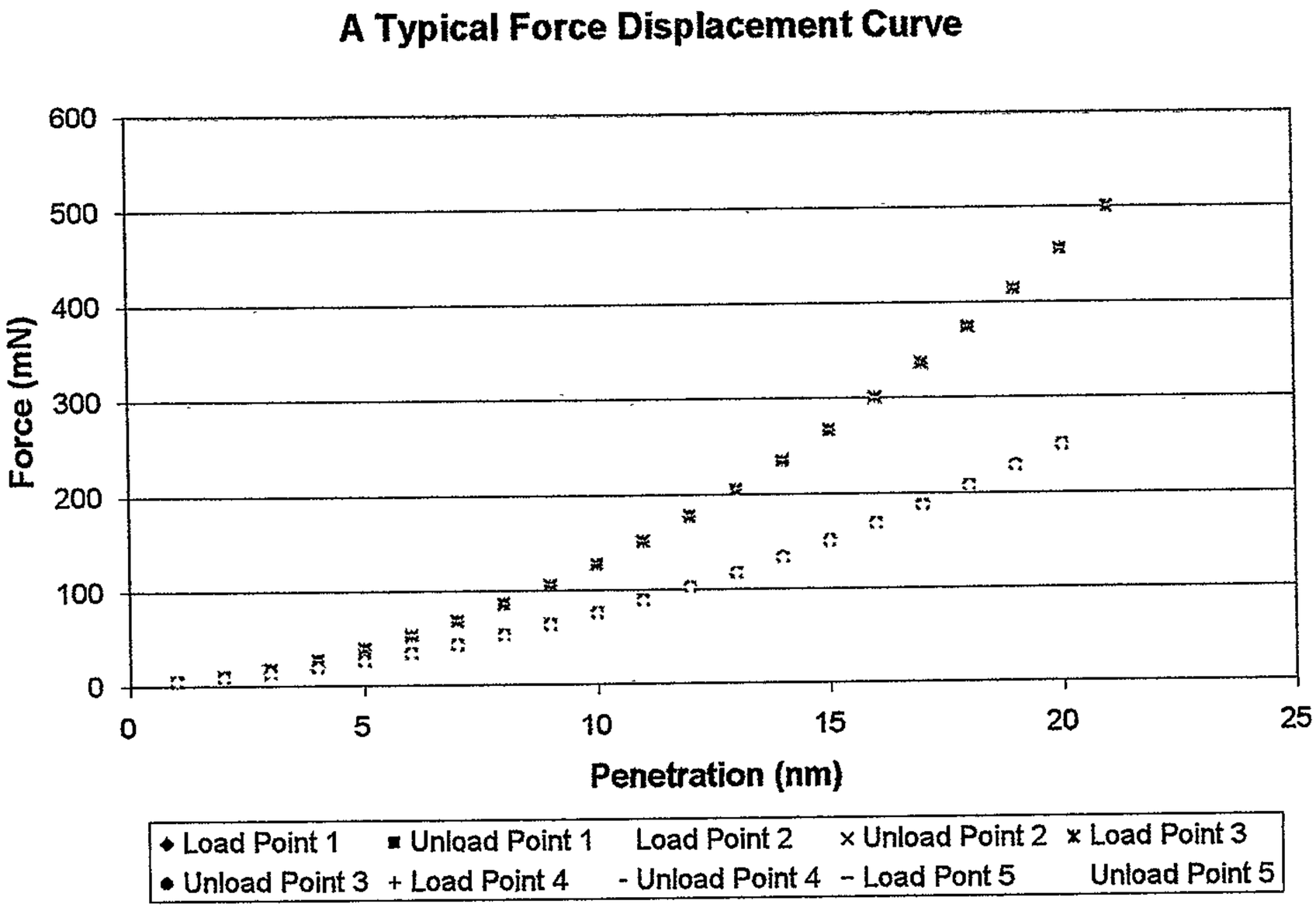

Figure 5. 2. Load / partial-unload curve using the spherical indenter on unpolished cementum at point number 34 on the lingual surface of a lower left first premolar.

5.2 Jig Compliance and Umis Calibration

The effects of different parameters such as load, type of indenter and jig design were evaluated using a known substance that is enamel. Enamel was chosen as an internal standard since its properties have been previously investigated and its availability on the sample renders it an ideal choice. The enamel surface is minimally affected by methods of preparation such as embedding and polishing.

5.2.1 The Effect of Different Loads with the Berkovich Indenter

The hardness and elasticity of enamel, obtained by the Berkovich indenter varied with increasing force levels on a highly polished sample. With testing at low loads (50mN) the hardness values ranged between 4.18 - 4.95 GPa and elastic modulus values between 77.18 - 89.00 GPa. With higher loads (150mN), the hardness values ranged between 3.95 - 3.98 GPa and elastic modulus values between 79.77 - 81. 77GPa. At loading with maximum loading (500mN) the hardness values decreased to 3.20 - 3.58 GPa and elastic modulus values to between 67.38 - 71.35 GPa. Cracking was detected with the use of the video-microscope. As a crack propagates hardness and elasticity both decrease as the force increases.

5.2.2 The Effect of Different Loads with the Spherical Indenter

The same highly polished enamel surface was tested with the spherical indenter. As the force increased, the contact pressure (Meyers hardness) increased and the elastic modulus decreased. At low loads (50mN) the mean hardness value was 1.80 GPa and mean elastic modulus value was 58.62 GPa. With higher loads (150mN) the mean hardness value was 2.64 GPa and mean elastic modulus value was 65.60GPa. At loading maximum force (500mN) the hardness values increased to 3.20 - 3.50 GPa and elastic modulus values to 49.35 - 50.46 GPa. No cracking was observed with the use of the spherical indenter.

5.2.3 The Effect of Jig Mounting on the Unpolished Enamel Surface

Table 5.1 is a summary of data obtained using Berkovich indenter with the load - unload cycle on unpolished enamel, which is mounted on the jig. At maximum force of 500mN, hardness of unpolished enamel mounted on the jig was 3.20 GPa. An example of the contact pressure (Meyers hardness) displacement plot versus depth of penetration, from the spherical indenter on the same unpolished enamel is seen in Fig.5.3. The spherical indenter gave a similar hardness value of 3.20 GPa at a maximum force of 500 mN (Fig 5.3) to the Berkovich indenter (Table 5.1).

Berkovich Enamel Results - Jig Mounted

***- SUMMARY OF RESULTS**	
Indenter (code)=	**GO->04**
Maximum force (mN)	**= 500.07**
Contact force (mN)	**= 5.04**
Initial penetration (nm)	**= 220.71**
Adjusted total penetration (nm)	**= 3033.62**
Adjusted plastic penetration (nm)	**= 2522.18**
Elastic recovery (nm)	**= 681.92**
Elastic recovery rate (dP/dH)	**= 1.36**
Hardness (at maximum depth)(GPa)	**= 3.20**
Equivalent Vickers hardness(Kg/mm²)	**= 93.80**
E* At maximum depth (GPa)	**= 51.99**
E/(1-v^2) At maximum depth (GPa)	**= 54.72**
E*/H At maximum depth (GPa)	**=16.5**
Returned energy ratio	**= 0.39**
Additional compliance correction	**= 0.00**

Table 5. 1. Summary of data using Berkovich indenter for an unpolished, jig mounted enamel. Hardness at the maximum force of 500mN is 3.20 GPa on the lingual surface of Sample 9.

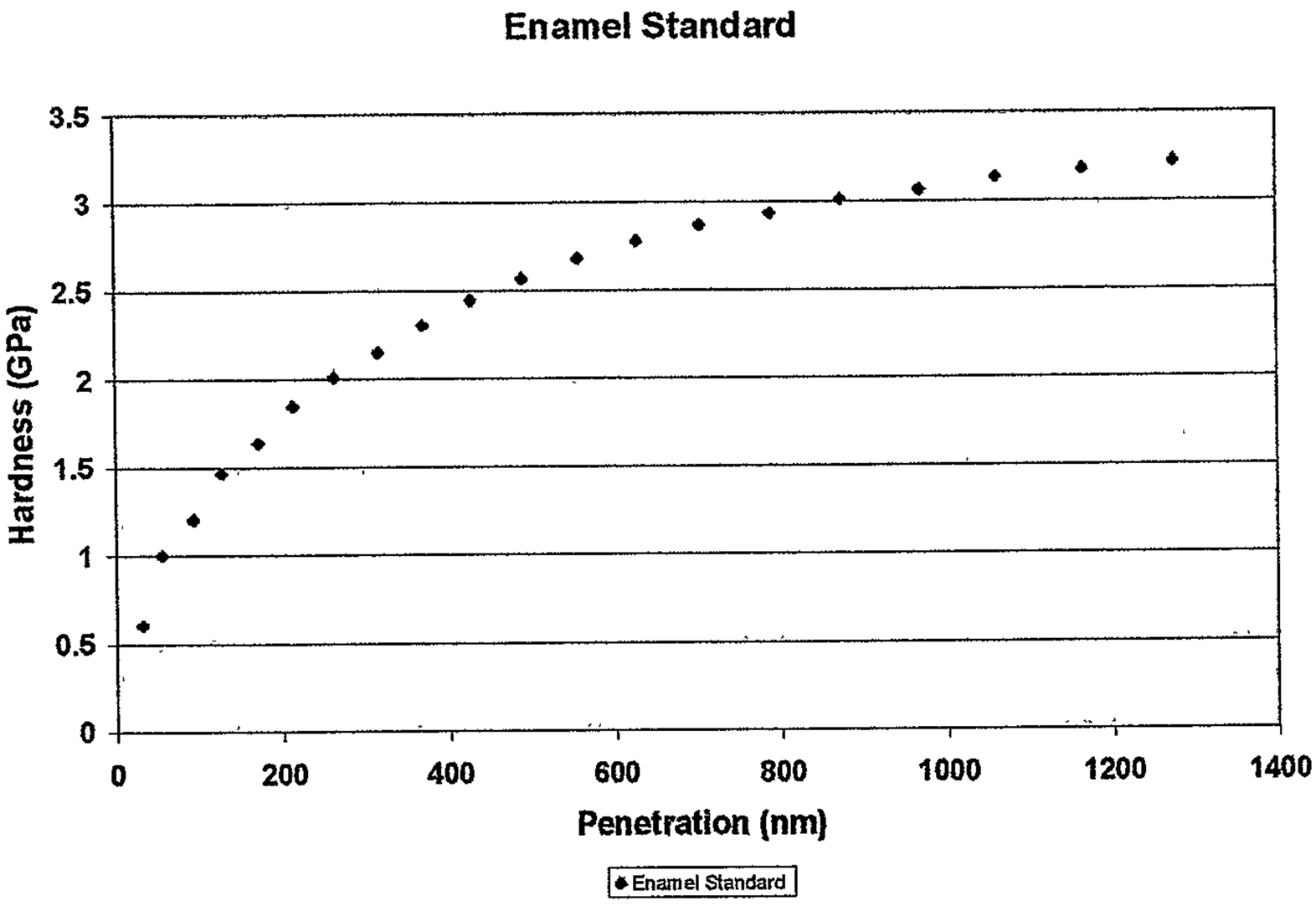

Figure 5. 3. Hardness plot using a Spherical indenter on the unpolished enamel standard which is jig mounted. Note similar values were obtained at maximum load using the Berkovich indenter and the Spherical indenter.

5.3 Storage

The physical properties of cementum may be affected by different chemical solutions used for storage over time. This experiment investigated the hardness and elastic modulus on five storage media; alcohol, desiccation, Milli Q and both Miltons 24hr and 10-minute soak (Appendix table 9.3). Initial hardness values were recorded within six hours of extraction (time = 0) and the samples re-analysed every month for three months. Two teeth stored in alcohol were analysed at four months for hardness and elastic modulus. Four teeth stored in Milli Q were analysed at nine months for hardness and elastic modulus.

Examples of the hardness and elastic moduli versus penetration plots generated with the spherical indenter loaded to 500mN are presented (Fig 5.4 and 5.5).

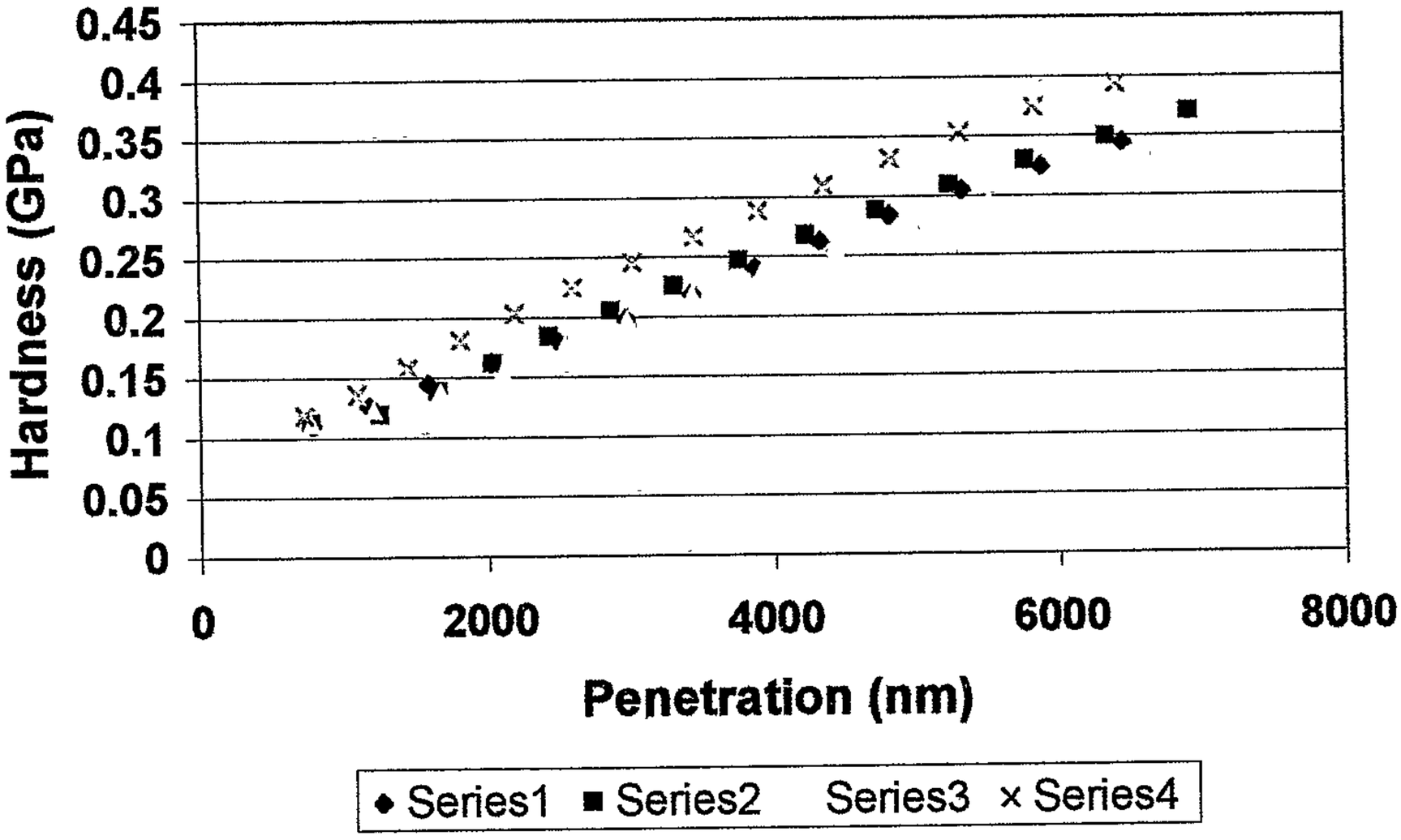

Figure 5. 4. The hardness versus penetration plot showing hardness increasing at a linear rate with increasing depth of penetration. The Series 1-4 represents the box array of indentation, 100μm^2. The hardness (GPa) is reported as the maximum allowable penetration between 6000-7000nm.

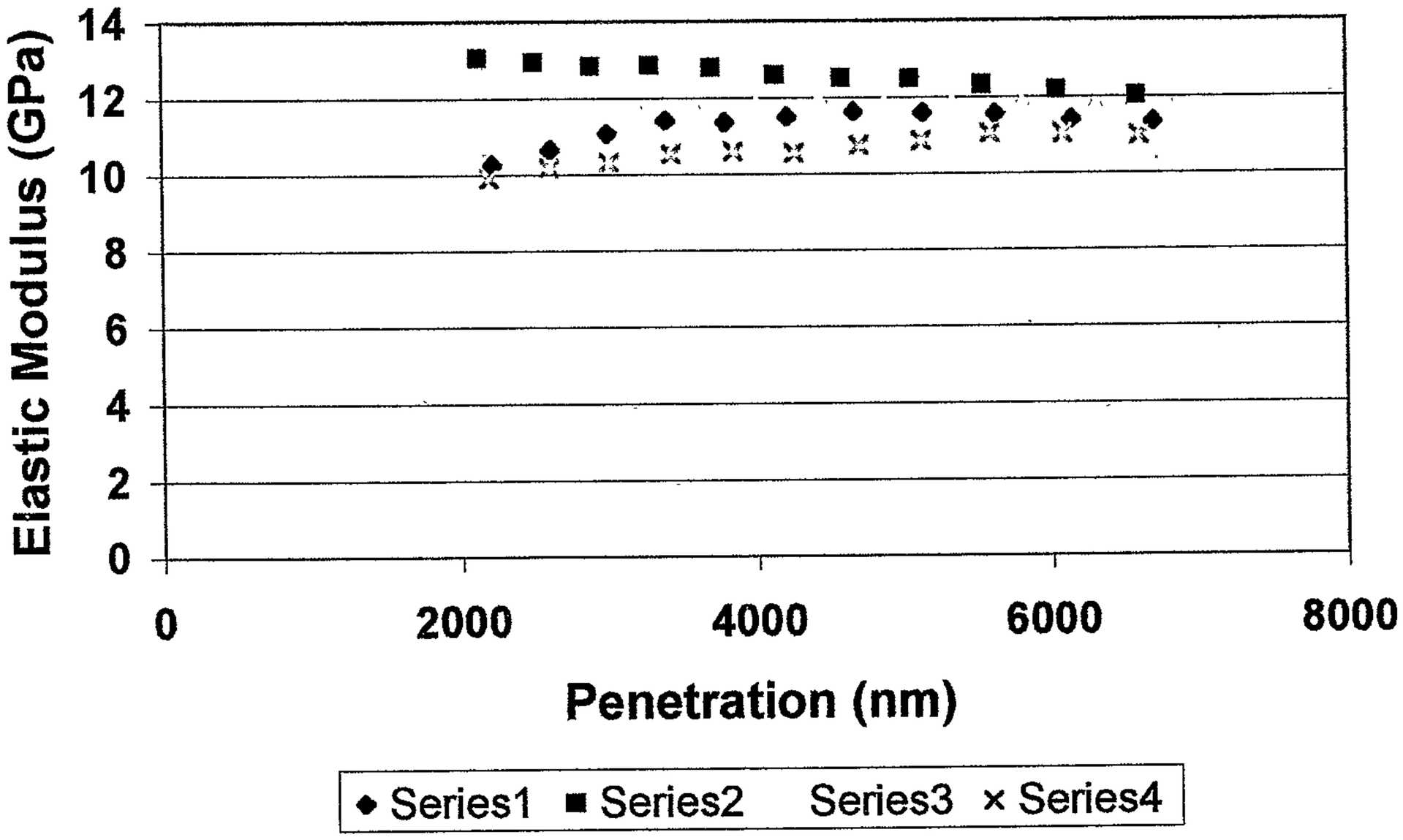

Figure 5. 5. The elastic modulus versus penetration plot showing a constant plateau with increasing depth of penetration. The Series 1-4 represents the box array of indentation, 100μm^2. The elasticity (GPa) is reported as that recorded between 2000nm and the maximum allowable penetration between 6000-7000nm.

A multivariant general linear statistical comparative model for hardness and elastic modulus in terms of media, tooth within media, time and influence of media and time were compared (Appendix table 9.4).

The SPSS statistical programme using multivariate general linear was used to evaluate storage results. The results suggested that media ($p < 0.01$) and time ($p < 0.01$) significantly affected hardness and elasticity. Statistically the variable tooth within the media was considered to eliminate the possibility of similar teeth being stored in the same media. An example of this would be soft teeth being stored in the same group while hard teeth were in another group. This was not the case as seen statistically ($p > 0.05$).

More specifically the media affected hardness ($p < 0.01$) more so than elasticity ($p > 0.05$) (Table 9.5). The breakdown of significance seen in Appendix Table 9.5 reported the individual statistical relationships of the two dependant variables (hardness and elastic modulus) and the fixed factors (media, tooth within the media, time and the influence of media and time).

The same model was formulated in which the data for time four months and nine months were excluded initially for ease of comparison (Table 9.6). Additionally, the same multivariant general linear model was re-run so as to remove confounders due to the minimally tested media sample group 4 and group 5 (Miltons 10mins. and Miltons 24 hrs.) (Appendix Table 9.7).

The SPSS statistical summary is presented (Appendix table 9.8) using the modified model. Hardness and elasticity are again viewed as the dependant variables, while media, tooth within the media, time and the influence of media and time are considered as the fixed factors. The media was again seen to significantly affect hardness and elasticity $p=0$. The interaction between media and time was now not significant ($p>0.05$).

The breakdown of the individual dependant variables and their significance are presented in Appendix Table 9.9. This shows the individual statistical relationships of the hardness and elasticity and their interrelationships to the fixed factors. The multivariate general linear model suggested a significant interaction between media and time in relation to hardness ($p < 0.01$) but not elastic modulus ($p>0.05$). Again the individual natural variation of the teeth within the media is not significant ($p>0.05$). The media significantly affected hardness ($p < 0.01$) and did not significant affect elastic modulus ($p > 0.01$).

The overall mean hardness and elastic moduli, generated with the spherical indenter loaded to 500mN are presented for all storage samples tested (Table 9.9). The mean changes can be seen in Figures 5.6 - 5.10.

Effects Of Different Storage Media on the Average Hardness and Elastic Modulus

Report

MEDIA Media	TIME	AVER.H			AVER.E		
		Mean	sem	N	Mean	sem	N
1.00 Alcohol	.00	.3018	.056	4	5.737	1.48	4
	1.00	.3324	.070	4	6.668	1.72	4
	2.00	.4199	.014	4	7.353	1.49	4
	3.00	.4244	.037	4	7.901	1.12	4
	4.00	.4317	.030	2	11.79	.2272	2
	Total	.3765	.024	18	7.457	.7141	18
2.00 Desiccation	.00	.2498	.040	4	4.320	1.05	4
	1.00	.3999	.062	4	8.064	.9275	4
	2.00	.4732	.047	4	7.821	1.78	4
	3.00	.4452	.054	4	9.150	1.36	4
	Total	.3920	.032	16	7.339	.7532	16
3.00 Milli Q	.00	.3420	.049	4	7.023	1.08	4
	1.00	.2787	.035	4	7.997	.9352	4
	2.00	.3508	.028	4	9.298	1.18	4
	3.00	.2862	.049	4	7.490	1.03	4
	9.00	.2936	.030	4	6.412	.9693	4
	Total	.3103	.017	20	7.644	.4705	20
4.00 Miltons 24Hrs	.00	.4574	.026	4	8.820	1.20	4
	1.00	.2818	.022	4	8.150	.4116	4
	Total	.3696	.037	8	8.485	.6009	8
5.00 Miltons 10 mins	.00	.4722	.014	4	7.669	1.01	4
	1.00	.5021	.018	4	8.444	1.47	4
	Total	.4871	.012	8	8.057	.8378	8
Total	.00	.3646	.025	20	6.714	.5877	20
	1.00	.3590	.027	20	7.865	.4913	20
	2.00	.4146	.023	12	8.157	.8224	12
	3.00	.3852	.033	12	8.180	.6512	12
	4.00	.4317	.030	2	11.79	.2272	2
	9.00	.2936	.030	4	6.412	.9693	4
	Total	.3730	.013	70	7.669	.3035	70

Table 5. 2. The effects of different storage media on the average hardness and elasticity over the set time periods are reported. (sem: standard error of the mean, N = number of tests analyzed).

A general linear model was then considered to attempt to identify the differences between the media in relation to the standard deviations observed from baseline. This proved that different storage media affected the teeth in a different way that there were significant differences in respect to hardness ($p = 0.014$) but no significant differences due to elasticity between the three different main storage media; alcohol, desiccation and Milli Q (Appendix tables 9.9 and 9.10).

To show the media which produced the least change in the hardness and elasticity values over time, and therefore the most ideal storage media to be used in the analysis of the physical properties of cementum, the standard deviations of each tooth were calculated for each time frame. The media were divided into the three main groups assessed (alcohol, desiccation and Milli Q). The standard deviations of hardness and elasticity over time were computed by means of a general linear model to determine whether the standard deviations of hardness and elasticity were significantly different over time. Values were found to be significantly different between the media ($p=0.014$) in respect to hardness but not so with respect to elasticity ($p=0.220$). The deviations in the hardness testing of the Milli Q samples were significantly lower than the other media (alcohol and decsiccation) (Appendix Table 9.9 and 9.10).

The narrower the window of variation (standard error) the more optimal the storage media. This media was then chosen for the 3-D section of the study. Milli Q exhibited the lowest standard error of the mean for hardness (SE = 0.013) and elasticity (SE = 0.305) than the other storage media tested (Table 5.3).

Mean Standard Deviations

MED

Dependent Variable	MED	Mean	Std. Error	95% Confidence Interval	
				Lower Bound	Upper Bound
SDH	1	.098	.018	.058	.137
	2	.116	.018	.076	.155
	3	.044	.013	.017	.072
SDE	1	2.799	.431	1.867	3.731
	2	2.537	.431	1.605	3.469
	3	1.893	.305	1.234	2.552

Table 5. 3. The mean standard deviations for the three media tested. 1: Alcohol, 2: Desiccation, 3: Milli Q. Note the smallest deviation occurred in the Milli Q group for both hardness and elasticity.

5.3.1 Effects of 70% Alcohol Storage on Cementum Hardness

Hardness changes over time of samples stored in 70% alcohol (Fig.5.6) showed that the mean hardness over the range of teeth tested was similar from baseline (within 6 hours

of extraction) and again at 1 month. There was a 30 - 40% increase in mean hardness from time period 1 to time period 2 and 3, which then remained constant at the third month. Paired T - tests were carried out between time periods: Baseline, Time period 1, Time period 2, Time period 3 and with regards to alcohol and Time period 4. Significant differences were seen within time period 2 and 3 ($p>0.01$) (Table. 5.2 and Fig. 5.6).

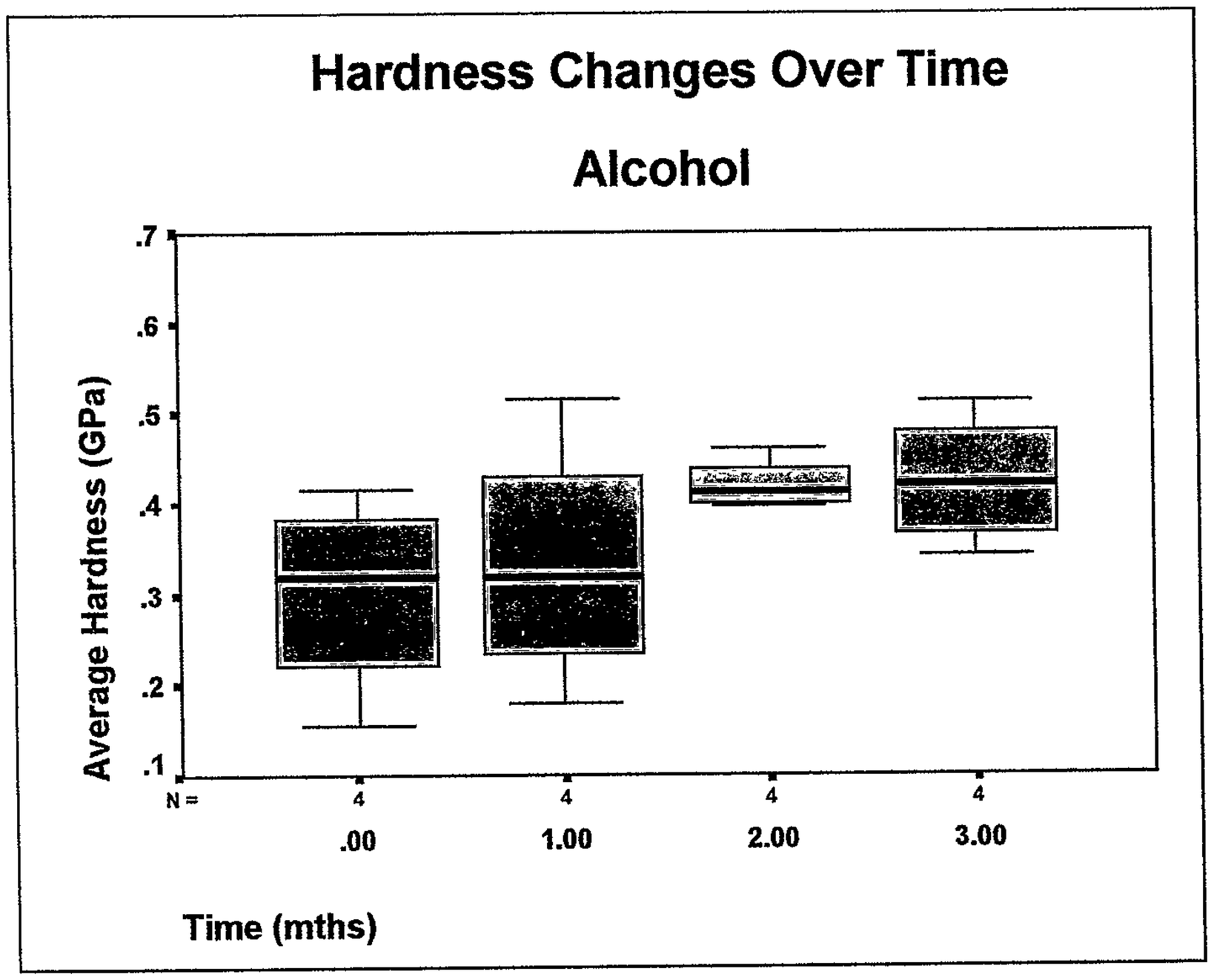

Figure 5. 6. Hardness changes over time of samples stored in 70% alcohol. The thick black line within the boxes represents the median hardness value (GPa) of the teeth. The coloured region represents quartiles, while the thin vertical line represents the range (outer quartiles). (N = Number of tests analyzed).

5.3.2 Effects of Desiccation Storage on Cementum Hardness

Hardness changes over time of samples stored in a desiccator produced a progressive increase in the hardness values obtained. The hardness increased in the first month and continued to increase at time period 2. It appeared to plateau with a slight decrease at the final testing at time period 4 (Table. 5.2 and Fig. 5.7).

Paired T - tests were carried out between time periods: Baseline, Time period 1, Time period 2, Time period 3. Significant differences were seen within all time periods with respect to hardness ($p>0.01$) (Fig. 5.7).

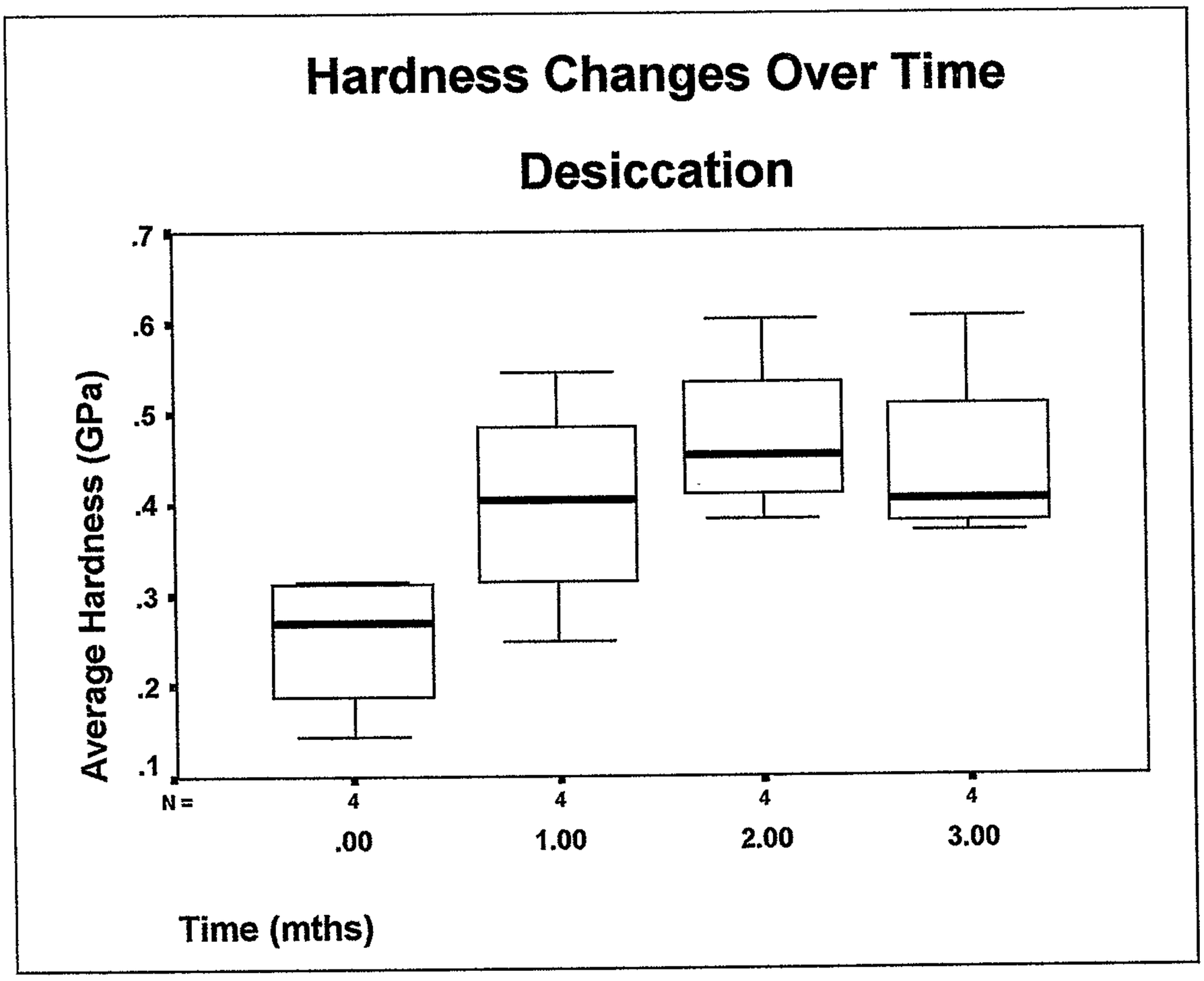

Figure 5. 7. Hardness changes over time of samples stored in a desiccator. The thick black line within the boxes represents the median hardness value (GPa) of the teeth. The coloured region represents quartiles, while the thin vertical line represents the range (outer quartiles). (N = Number of tests analyzed).

5.3.3 Effects of Milli Q Storage on Cementum Hardness

Hardness changes over time of samples stored in MilliQ produced only minor fluctuations in the hardness values obtained. The hardness remained stable for up to nine months (Table. 5.2 and Fig. 5.8)

Paired T - tests were carried out between time periods: Baseline, Time period 1, Time period 2, Time period 3 and Time period 4 and Time period 9. No significant differences were seen within the time periods tested ($p<0.05$). The teeth stored in MilliQ therefore did not differ in hardness from baseline to 9 months (Fig. 5.8).

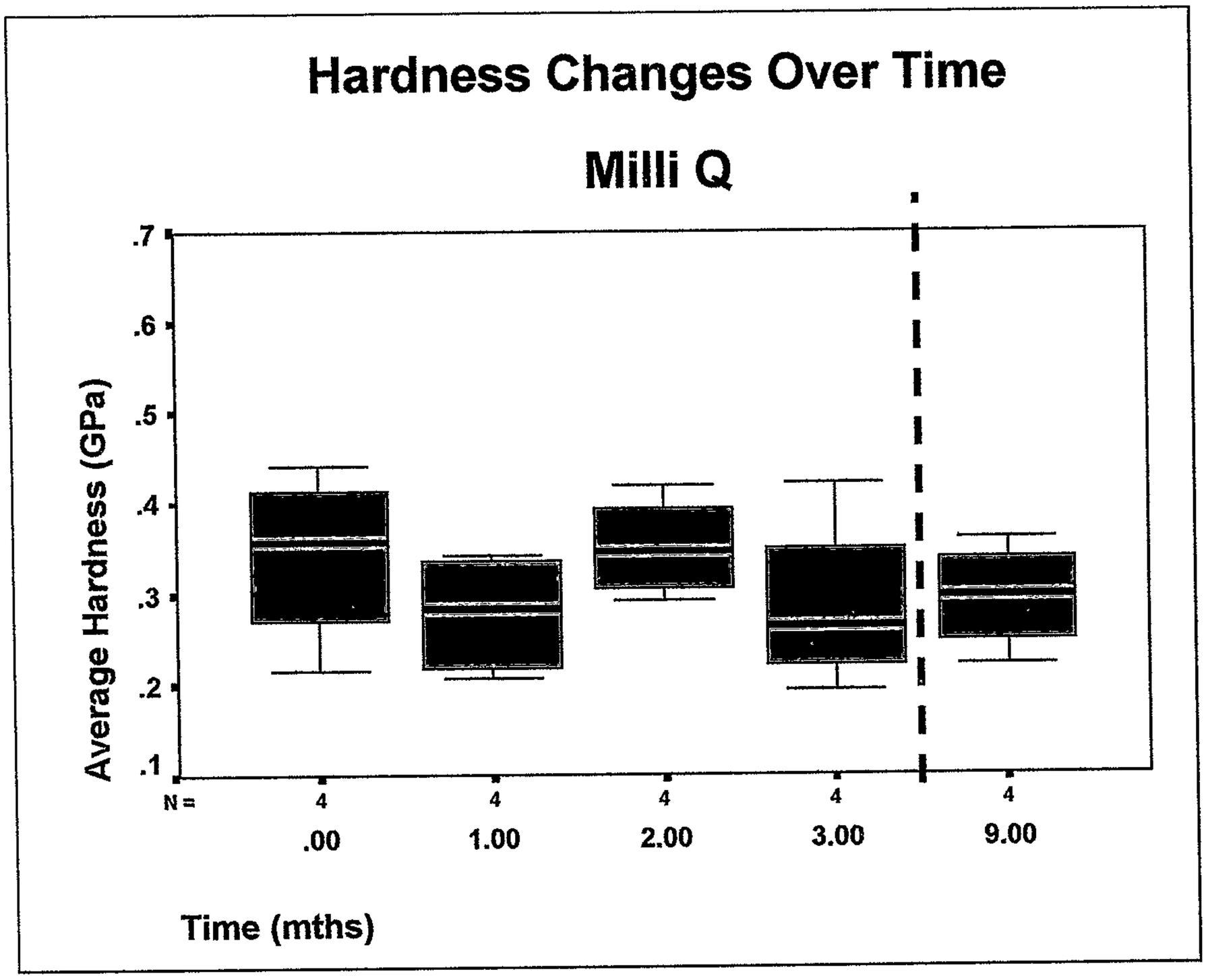

Figure 5. 8. Hardness changes over time of samples stored in Milli Q. The thick black line within the boxes represents the median hardness value (GPa) of the teeth. The coloured region represents quartiles, while the thin vertical line represents the range (outer quartiles). (N = Number of tests analyzed).

5.3.4 Effects of Miltons 24Hr Storage on Cementum Hardness

Hardness changes over time of samples stored in Miltons for a 24hr period produced a decrease in the hardness values obtained (Table. 5.8 and Fig. 5.9). The decrease in hardness was approximately 50%. There also appeared a significant amount of erosion on the surface of root surface as demonstrated in Figure 5.11. This was not visible to the unaided eye; instead the surface appeared clean.

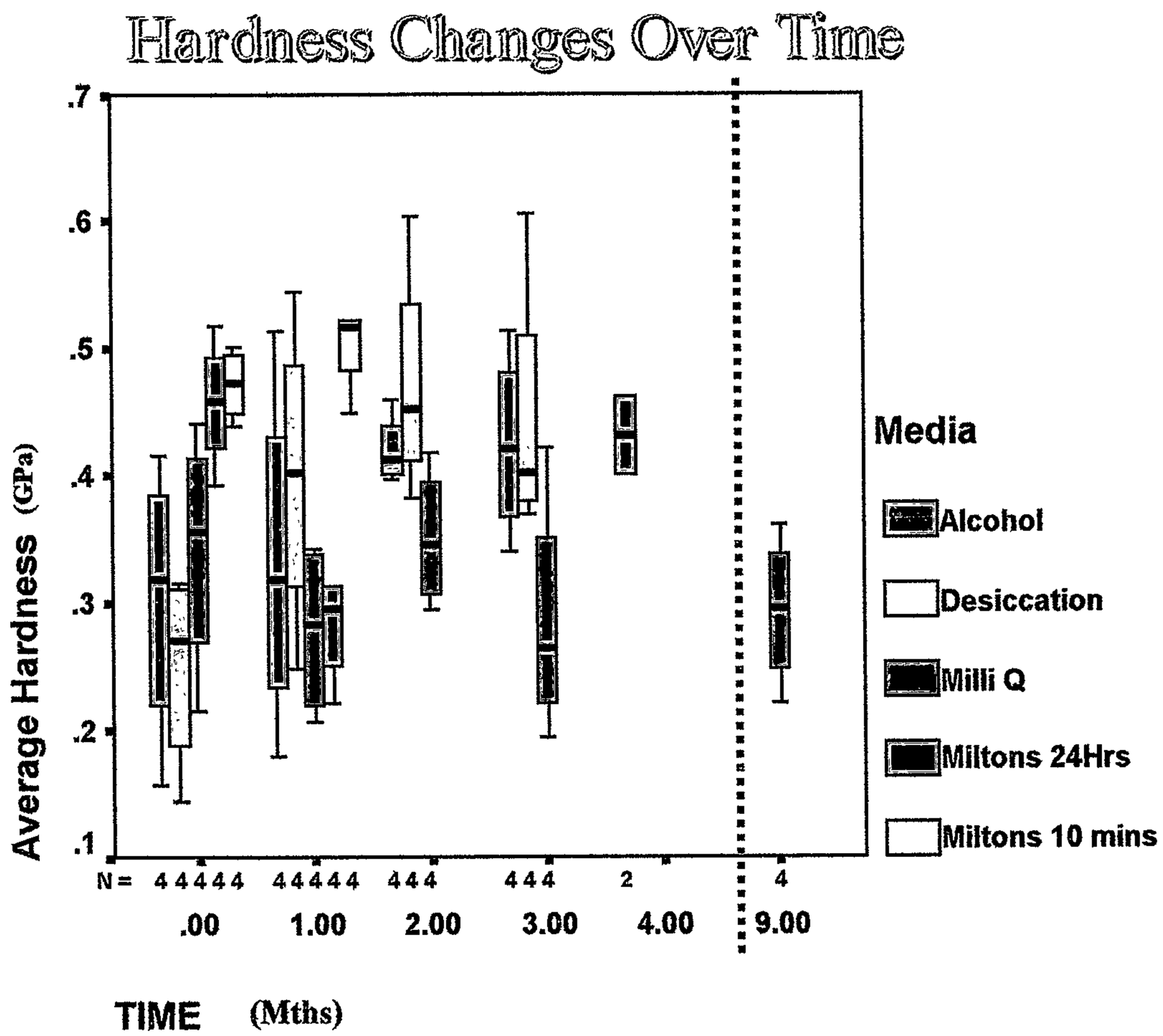

Figure 5. 9. Average hardness over time with respect to all the storage media tested. Note the minimal variations in the Milli Q group as compared to the variations in the other groups. The Milli Q group was also tested at time period nine months post extraction. The thick black line within the boxes represents the median hardness value (GPa) of the teeth. The coloured region represents quartiles, while the thin vertical line represents the range (outer quartiles). Note the insignificant change in the Milli Q group. (N = Number of tests analyzed).

5.3.5 Effects of Miltons 10 Minute Storage on Cementum Hardness

The storage media (Miltons 10 minutes and Miltons 24 hours) were assessed to study possible alternative in the removal of the periodontal ligament. The results of the 10 minute Miltons rinse showed a slight difference between time zero and the subsequent tests.

Hardness change over time of samples stored in Miltons for a 10 minutes period produced a slight increase in the hardness values (Table. 5.2 and Fig. 5.9).

5.3.6 Effects of Storage on the Elastic Modulus of Cementum

Of all the five groups of media tested, the storage media did not significantly affect the modulus of elasticity obtained by UMIS testing (Table. 5.2, Fig. 5.10 and Appendix table 9.8).

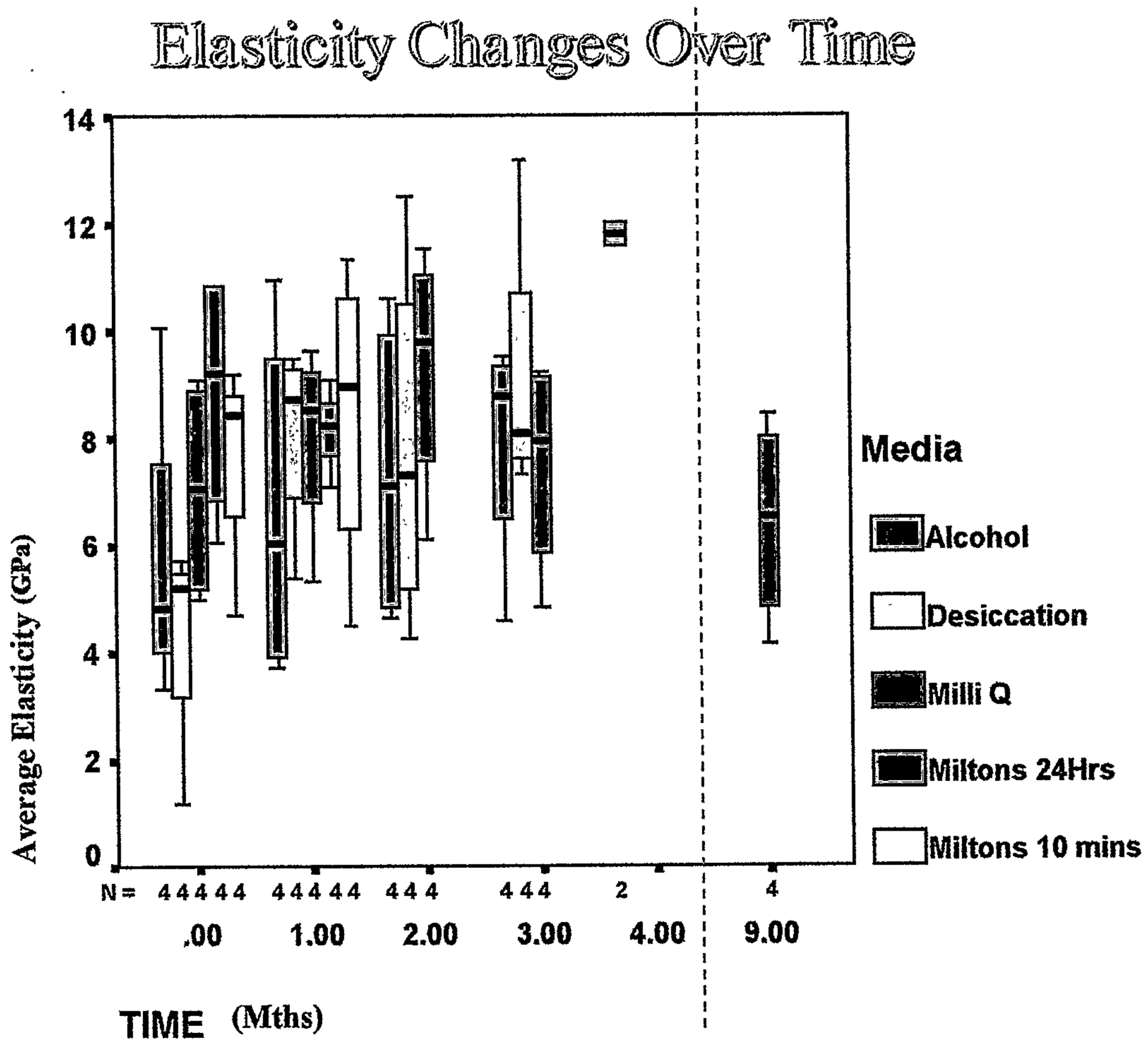

Figure 5. 10. Average elasticity over time with respect to all the storage media tested. Note the similarities in all groups tested. The Milli Q group was also tested at time period nine months post extraction. (N = Number of tests analyzed).

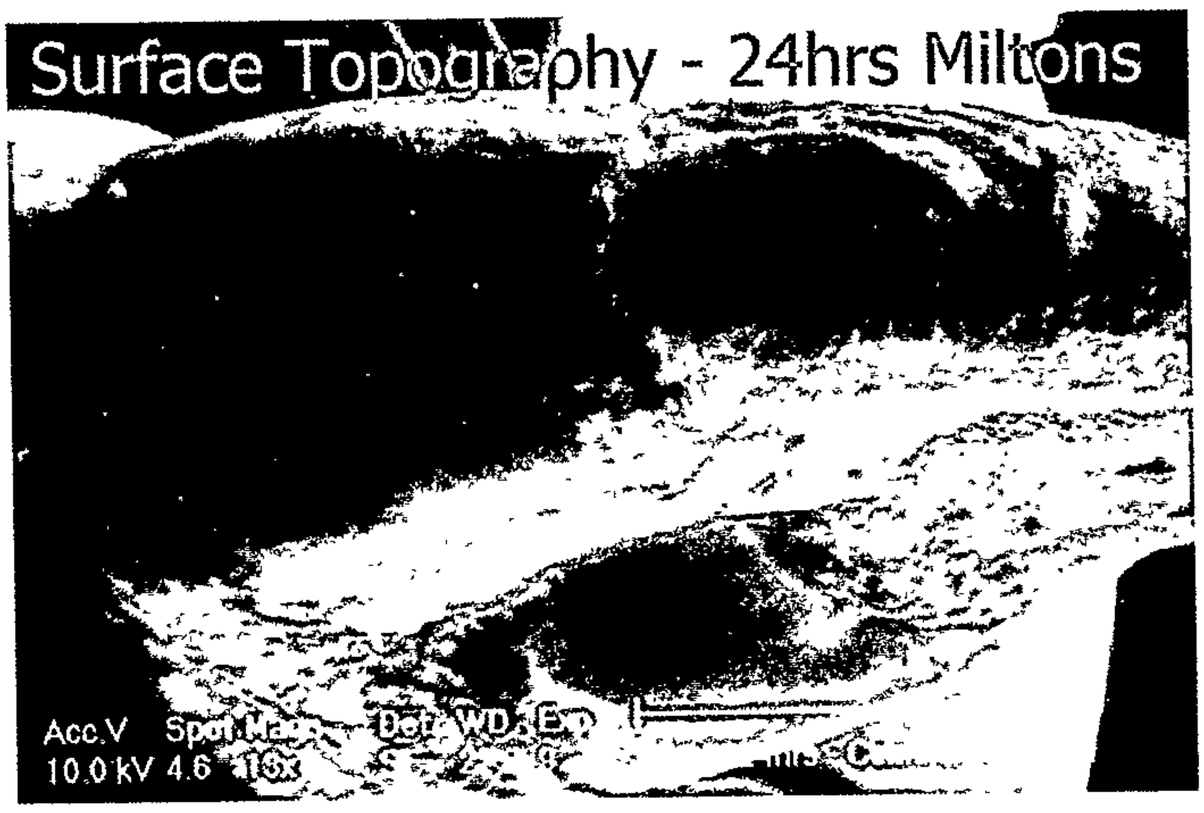

Figure 5. 11. The Effect of 24 hour Miltons soak on a human premolar cementum. Scanning Electron Micrograph. Magnif. = X13.

5.4 3-Dimensional Evaluation of the Tooth

The analysis of cementum properties along the root surface from the apex to the CEJ showed that hardness and elasticity varied from location point to location point. Statistical analysis was used to determine trends between position, surface, layer, sex and the quadrant form which the tooth was extracted. Further investigation resulted in calcium correlation to the physical properties.

A multivariate testing of a general linear model designed to show the inter-relationships of; sex, patient within sex, side, top/bottom, layer within surface, surface calcium to cementum hardness and elasticity was implemented. It was shown that the hardness and elasticity acted differently with regard to these factors.

Sex, patient within sex, surface, layer within surface were all significant with respect to hardness and elasticity at $p = 0$. Calcium content in relation to hardness and elasticity was significantly correlated at $p = 0.019$. Side, that is left or right was only mildly correlated to hardness and elasticity with $p = 0.033$. Maxillary or mandibular teeth had no difference in regard to hardness and elasticity with $p=0.337$ showing no significance (Appendix Tables 9.35, 9.36 and 9.37).

5.4.1 Hardness and Elastic Modulus Relative to Sex

Sex was found to affect both hardness and elasticity ($p<0.01$ and $p<0.05$ respectively). Of the nine teeth studied (two male and seven female teeth, from two male and four female subjects) the distal and lingual surfaces appeared softer in males. The buccal surface in males appeared harder than females (Fig. 5.12).

The average hardness of the sixty points produced an overall mean value for males slightly harder than females (Table. 5. 5). The average hardness for males was 0.37 ± 0.008GPa, while for females the average hardness was calculated as 0.35± 0.005GPa.

The mean elastic modulus of the sixty points produced an overall mean value for males slightly lower than females (Table. 5.5). The mean elastic modulus for males was 5.55 ± 0.19GPa, while for females the average modulus was calculated as 6.09± 0.12GPa.

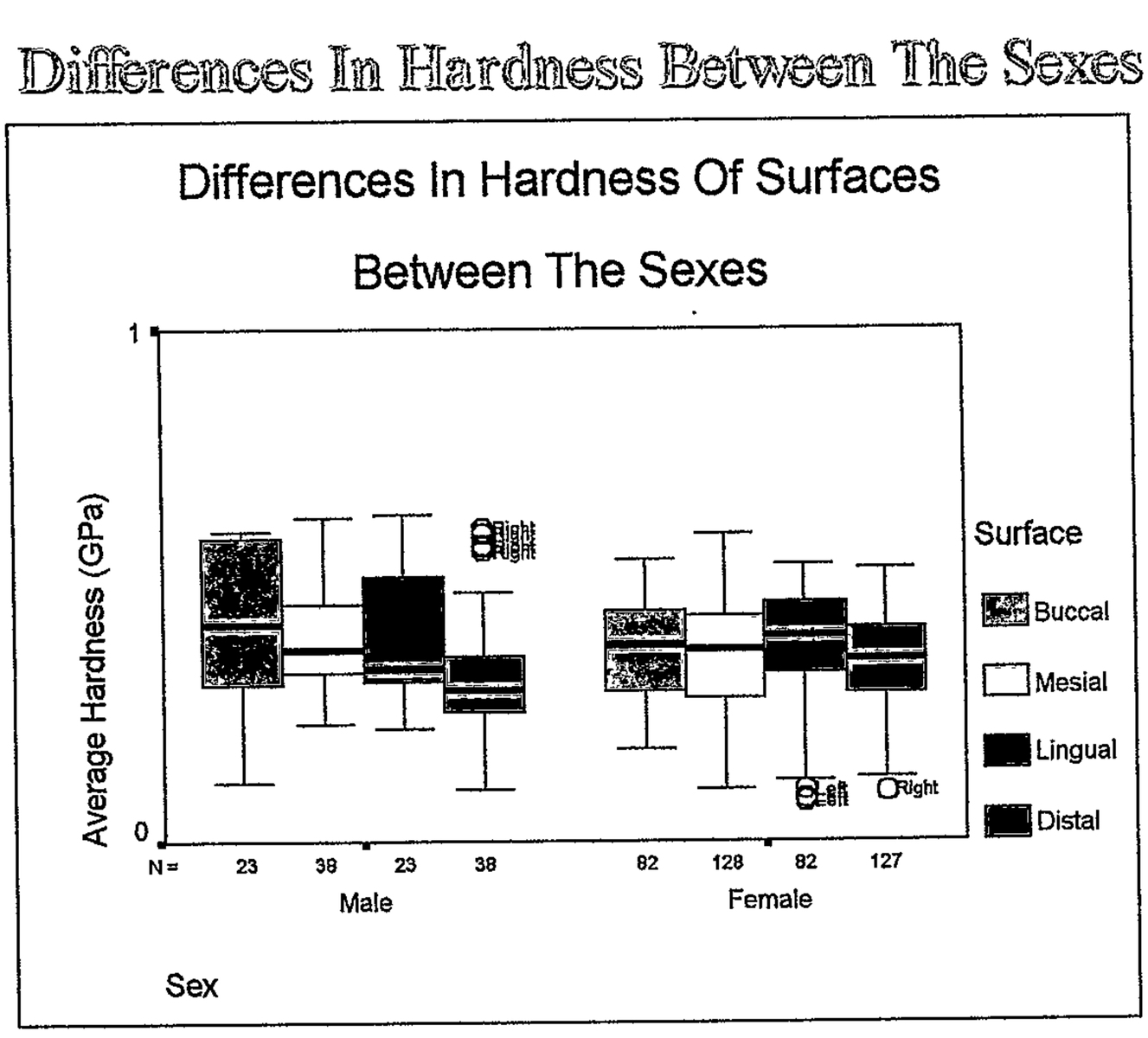

Figure 5. 12. This graph compared male and female cementum hardness at the respective surfaces. The mean hardness values suggested that males have harder buccal cementum, but softer lingual and distal cementum. (N = Number of tests analyzed).

5.4.2 Individual Variation Relative to Hardness and Elastic Modulus

Individual variation was found to affect both hardness and elasticity ($p=0.000$). The average hardness of the sixty points produced considerable variation between patients (Table. 5.6). The average hardness ranged from 0.30 ± 0.02 - 0.43 ± 0.02 GPa (Fig. 5.13).

The mean elastic modulus of the sixty points produced considerable variation between patients (Table. 5.6). The mean elastic modulus ranged from 4.92 ± 0.35 - 7.29 ± 0.27 GPa (Fig. 5.19).

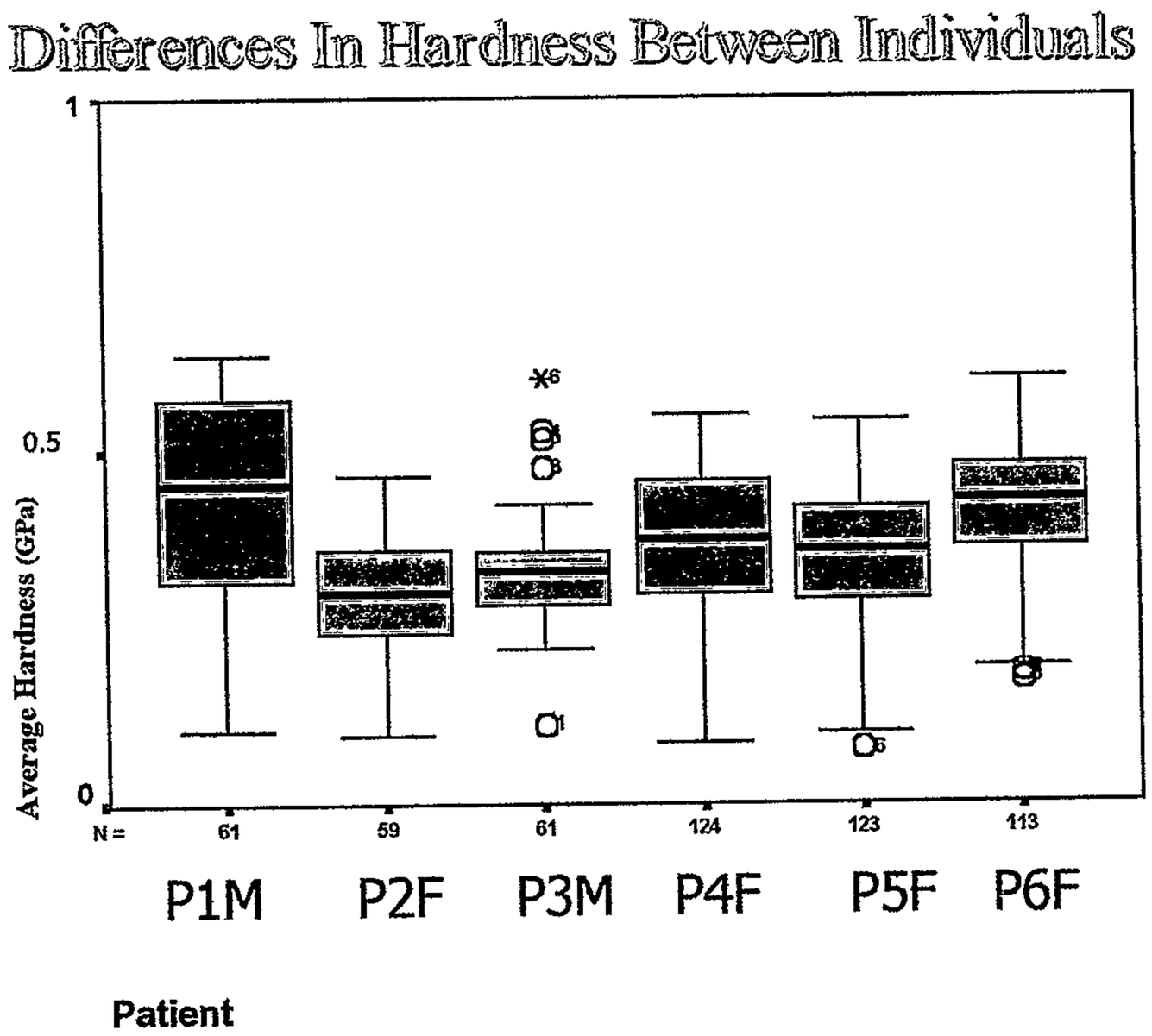

Figure 5. 13. The average hardness is plotted for the six individuals studied at the 60 sites. It can be seen that hardness is specific to the individual. P = patient, M = male and F = female. (N = Number of tests analyzed).

5.4.3 Side Relative to Hardness and Elastic Modulus

Side (left and right) was found to affect both elastic modulus but not hardness ($p<0.01$ and $p>0.05$ respectively). Of the nine teeth studies (four right and five left) the right side

teeth appeared marginally harder than the teeth obtained from left hand side (Fig. 5.14). The elastic modulus appeared lower on the left-hand side than the right-hand side.

The average hardness of the sixty points produced an overall mean value for the left-hand side and the right-hand side teeth (Table. 5.7). The average hardness for right-hand side teeth was 0.36 ± 0.007GPa, while for left-hand side teeth the average hardness was calculated as 0.35± 0.007GPa.

The mean elastic modulus of the sixty points produced an overall mean value for right-hand side teeth was 6.24 ± 0.17GPa (Table. 5.7). The mean elastic modulus for left-hand side teeth was 5.57 ± 0.18GPa.

The differences in hardness between left and right sides at different layers along the root were marginally different with a slightly steeper change in mean hardness values on the right hand side when compared to the left hand side (Figure.5.15).

Differences In Hardness Between Sides

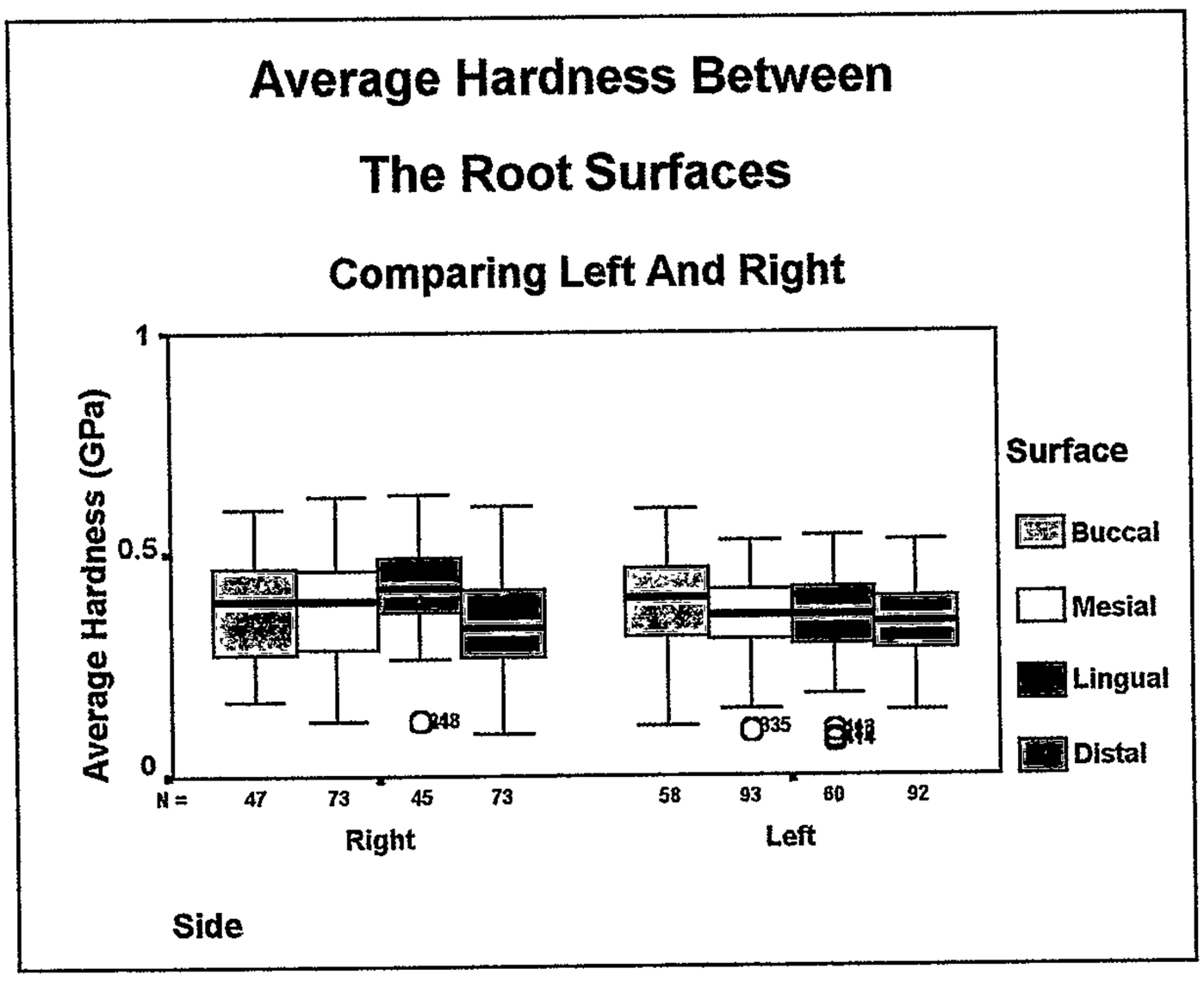

Figure 5. 14. Mean cementum hardness comparing left and right root surfaces. Showed little difference between left and right. (N = Number of tests analyzed).

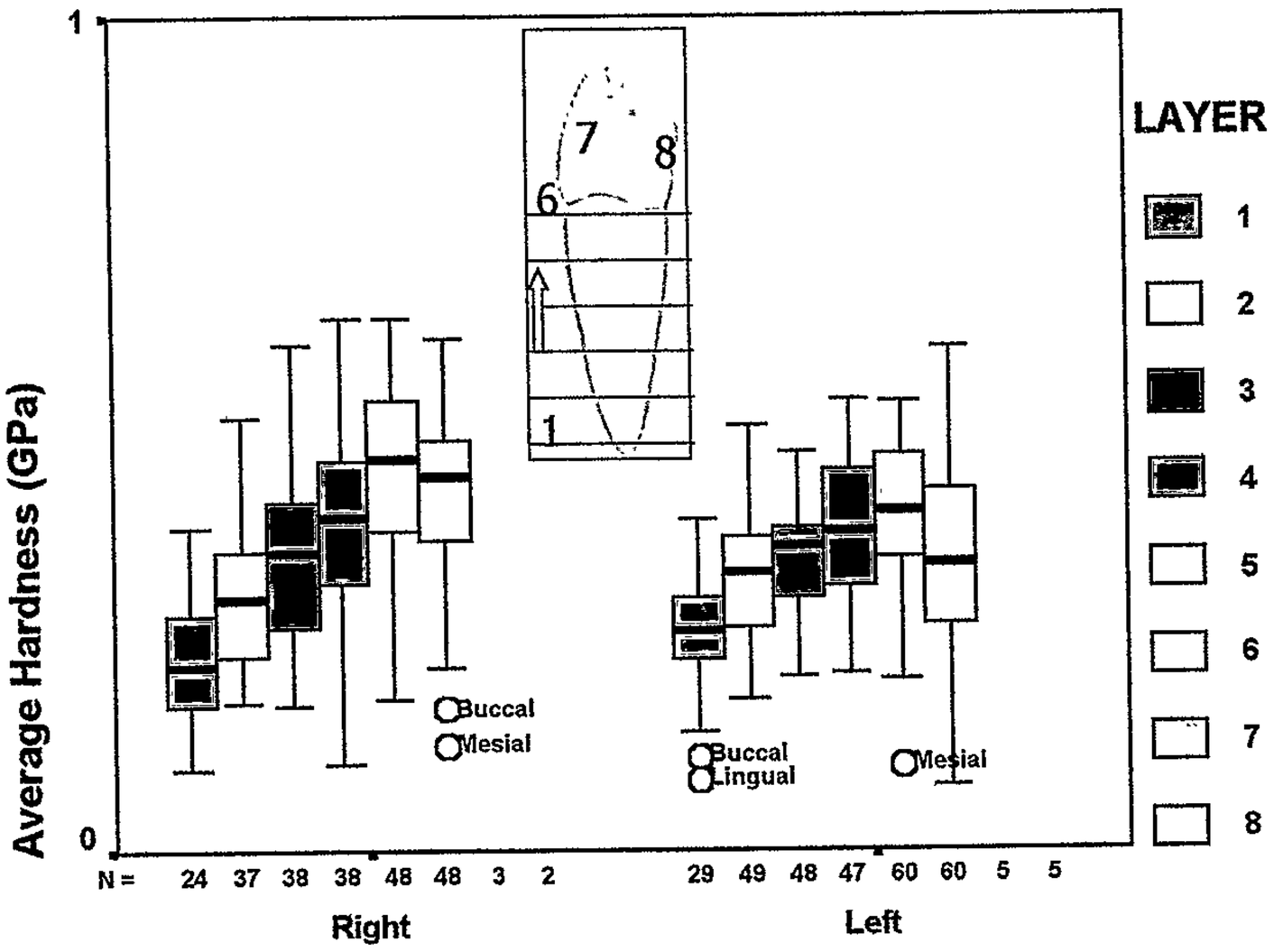

Figure 5. 15. The differences in hardness between left and right sides at different layers along the root. The marginal difference seen showed a slightly steeper change in mean hardness values on the right hand side when compared to the left hand side. (N = Number of tests analyzed).

5.4.4 Maxillary And Mandibular Teeth Relative To Hardness And Elastic Modulus

Maxillary and mandibular teeth were not found to affect hardness or elastic modulus ($p>0.05$) (Fig.5.16). Of the nine teeth studied (four maxillary and five mandibular) the maxillary teeth appeared marginally harder than the mandibular teeth (Table. 5.8). The elastic modulus appeared lower in the mandibular teeth than the maxillary teeth.

The average hardness of the sixty points produced an overall mean value for the maxillary and mandibular teeth (Table. 5.8). The average hardness maxillary teeth was 0.37 ± 0.01GPa, while for mandibular teeth the average hardness is calculated as 0.34 ± 0.008GPa.

The mean elastic modulus of the sixty points produced an overall mean value for the maxillary teeth of 6.12 ± 0.24GPa, while for mandibular teeth, the mean elastic modulus for left-hand side teeth was 5.69 ± 0.18GPa (Table. 5.8).

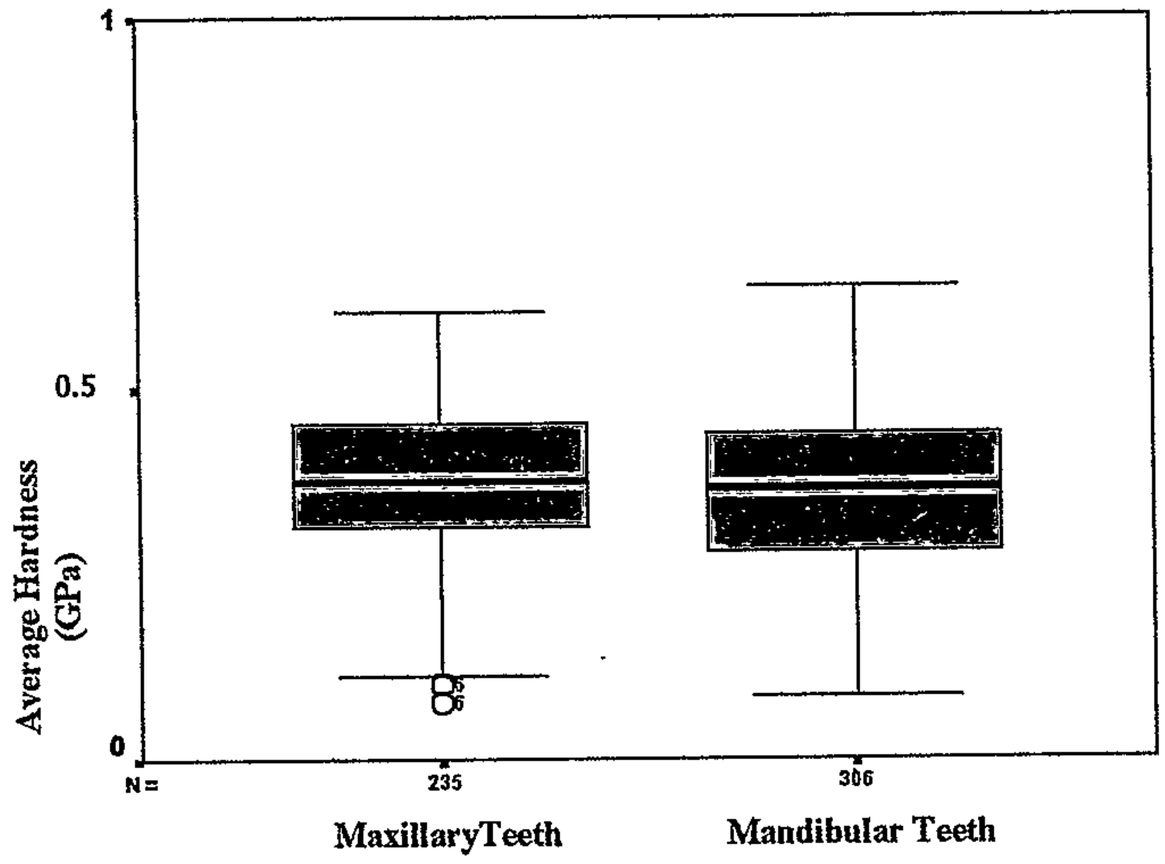

Figure 5. 16. The average hardness was plotted for the maxillary and mandibular teeth. Of the nine teeth studied there appeared to be no difference between maxillary and mandibular teeth. (N = Number of tests analyzed).

5.4.5 Layer within the Surface of Teeth Relative to Hardness and Elastic Modulus

Of the six layers described each layer was found to have a different mean hardness and elastic modulus (p=0). Averaging the points of each respective layer produced the average hardness of the six layers. There was considerable variation between the layer (Table. 5.9). The average hardness ranged from 0.25 ± 0.01 - 0.43 ± 0.01 GPa (Fig. 5.17 and 5.18).

The mean elastic modulus of the six layers produced considerable variation between respective layers (Table. 5.9). The mean elastic modulus ranged from 4.07 ± 0.30 - 7.30 ± 0.21 GPa (Fig. 5.19).

Of the 2790 indents the average hardness appeared to increase from the apex (layer "1") to the CEJ (layer "6"). The lingual enamel is surprisingly harder on average than the buccal enamel. The average hardness was plotted for the nine teeth studied, broken down by surfaces. The distal surface was consistently lower in mean hardness values than the other surfaces tested (Fig. 5.12, 5.13 and 5.18).

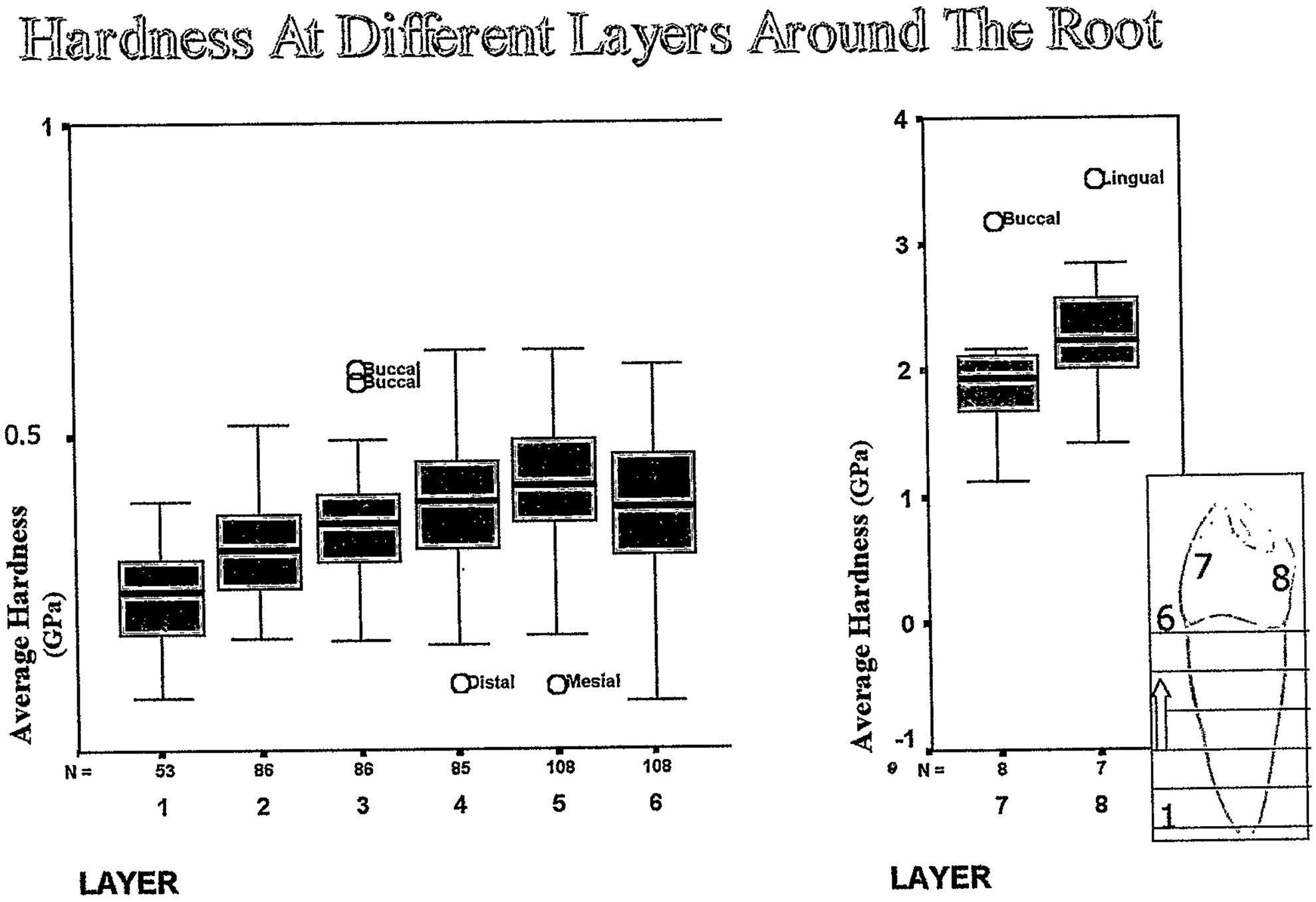

Figure 5. 17. The average hardness was plotted for the nine teeth studied. Of the 2790 indents the average hardness appeared to increase from the apex (layer "1") to the CEJ (layer "6"). The lingual enamel was surprisingly harder on average than the buccal enamel. (N = Number of tests analyzed).

5.4.6 Surface of Teeth Relative to Hardness and Elastic Modulus

Surface (buccal, mesial, distal and lingual) were found to affect both hardness and elastic modulus ($p<0.01$ and $p=0$ respectively). Of the nine teeth studies the distal surface appeared marginally softer than all the other surfaces (Fig. 5.14 and Fig. 5.18).

The average hardness of the eleven points on all the buccal and all lingual surfaces and the nineteen points on all the mesial and all distal surfaces produced an overall mean value for average hardness (Table. 5.10). The average hardness for the buccal, mesial and lingual surfaces was 0.36 ± 0.008GPa, while for the distal surfaces of teeth the average hardness was 0.33± 0.007GPa.

The mean elastic modulus of the buccal surfaces produced an overall value of 6.61 ± 0.22 GPa. The mean elastic modulus of the mesial surfaces produced an overall mean value of 5.39 ± 0.17 GPa. The mean elastic modulus of the lingual surfaces produced an overall mean value of 6.04 ± 0.21 GPa, while the mean elastic modulus of the distal surfaces produced an overall mean value of 5.59 ± 0.16 GPa (Table. 5.10).

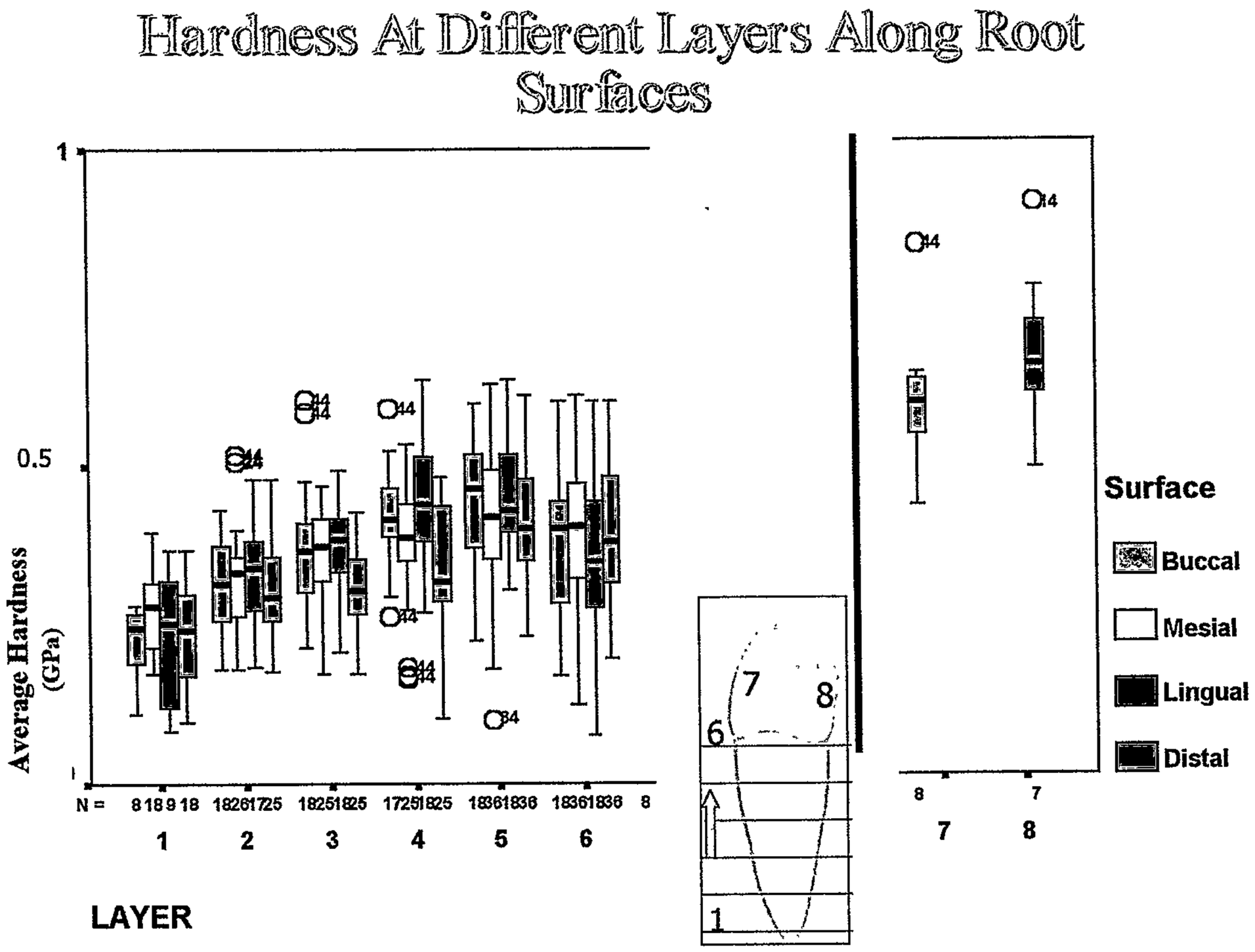

Figure 5. 18. The average hardness was plotted for the nine teeth studied, broken down by surfaces. The distal surface was consistently lower in mean hardness values than the other surfaces tested. (N = Number of tests analyzed).

Elasticity At Different Layers Along Root Surfaces

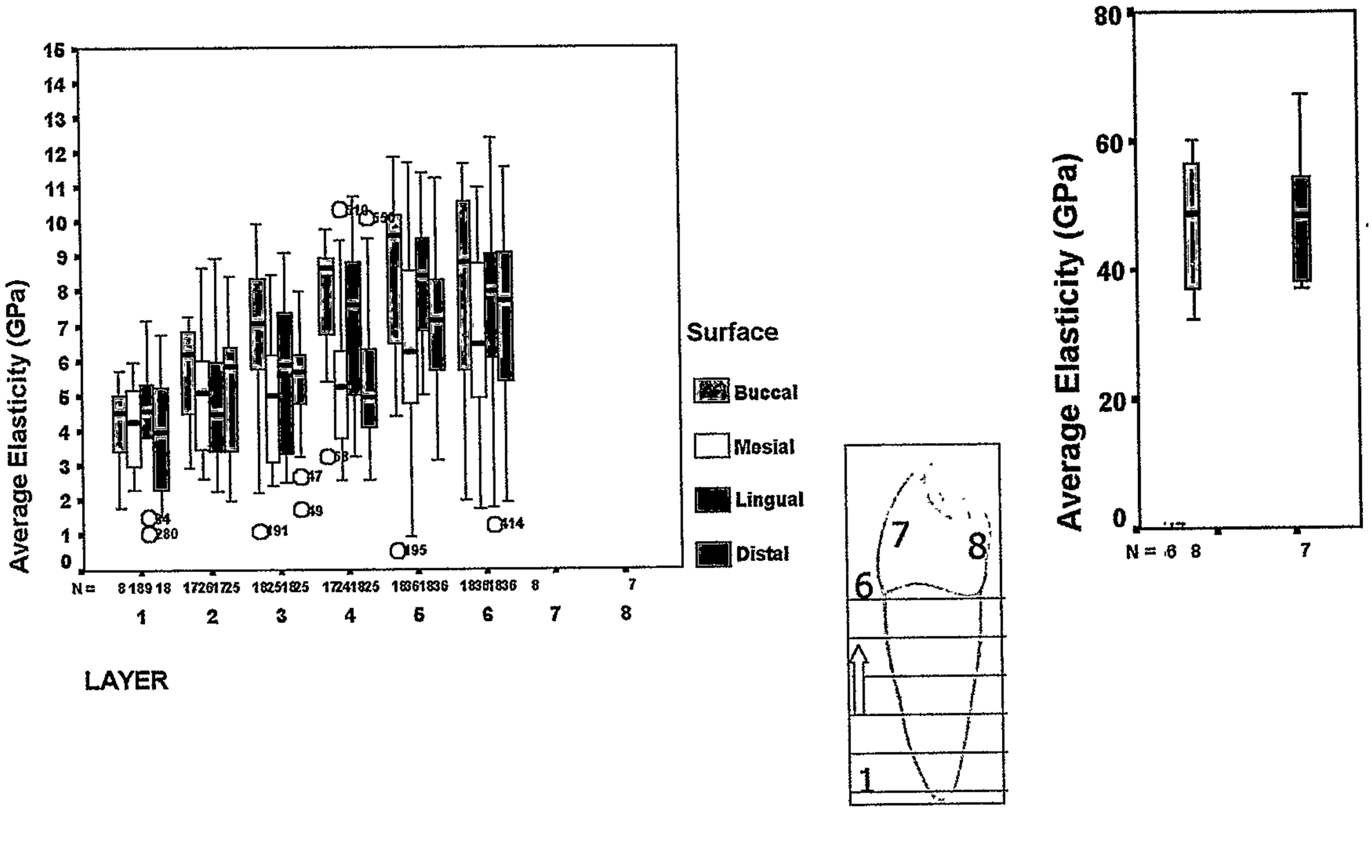

Figure 5. 19. The average elasticity was plotted for the nine teeth studied, broken down by surfaces. The large ranges are clearly visible. (N = Number of tests analyzed).

1. Grand Mean

Dependent Variable	Mean	Std. Error	95% Confidence Interval	
			Lower Bound	Upper Bound
ave.h	.355[a,]	.004	.346	.363
AVE.E	5.906[a,]	.103	5.702	6.109

a. Evaluated at covariates appeared in the model: CA2 = 7.048E-02.

b. Based on modified population marginal mean.

Table 5. 4. The average hardness and elasticity of all 9 teeth studied over all surfaces. Totals number of all indents = 2790.

2. Sex

Dependent Variable	Sex	Mean	Std. Error	95% Confidence Interval	
				Lower Bound	Upper Bound
ave.h	Male	.374[a,]	.008	.357	.390
	Female	.345[a,]	.005	.335	.355
AVE.E	Male	5.547[a,]	.192	5.169	5.925
	Female	6.085[a,]	.118	5.853	6.317

a. Evaluated at covariates appeared in the model: CA2 = 7.048E-02.

b. Based on modified population marginal mean.

Table 5. 5. The average hardness and elasticity values calculated for male and female subjects.

3. Patient

Dependent Variable	Patient	Mean	Std. Error	95% Confidence Interval	
				Lower Bound	Upper Bound
ave.h	Genc, Mr M	.429[a,]	.016	.398	.459
	Guo, Miss Si Y	.296[a,]	.015	.266	.326
	Edlbi, Mr	.319[a,]	.015	.289	.348
	Gahli, Miss M	.360[a,]	.011	.338	.383
	Lin, Miss Yi Mei	.345[a,]	.010	.325	.364
	Vernon, Miss M	.380[a,]	.012	.356	.403
AVE.E	Genc, Mr M	5.809[a,]	.358	5.106	6.512
	Guo, Miss Si Y	4.917[a,]	.349	4.230	5.603
	Edlbi, Mr	5.285[a,]	.343	4.610	5.959
	Gahli, Miss M	6.051[a,]	.261	5.538	6.564
	Lin, Miss Yi Mei	6.077[a,]	.228	5.629	6.526
	Vernon, Miss M	7.294[a,]	.273	6.758	7.830

a. Evaluated at covariates appeared in the model: CA2 = 7.048E-02.

b. Based on modified population marginal mean.

Table 5. 6. Mean hardness and elasticity values for the individual patients.

4. Side

Dependent Variable	Side	Mean	Std. Error	95% Confidence Interval	
				Lower Bound	Upper Bound
ave.h	Right	.362[a,]	.007	.348	.377
	Left	.347[a,]	.007	.333	.361
AVE.E	Right	6.243[a,]	.167	5.914	6.572
	Left	5.568[a,]	.167	5.240	5.896

a. Evaluated at covariates appeared in the model: CA2 = 7.048E-02.

b. Based on modified population marginal mean.

Table 5. 7. Mean hardness and elasticity values comparing left and right sides of the mouth.

5. Top/Bottom

Dependent Variable	Top/Bottom	Mean	Std. Error	95% Confidence Interval	
				Lower Bound	Upper Bound
ave.h	Upper	.366[a,]	.010	.346	.387
	Lower	.343[a,]	.008	.328	.358
AVE.E	Upper	6.123[a,]	.239	5.654	6.592
	Lower	5.688[a,]	.180	5.334	6.042

a. Evaluated at covariates appeared in the model: CA2 = 7.048E-02.

b. Based on modified population marginal mean.

Table 5. 8. Mean hardness and elasticity values comparing the average maxillary and mandibular results.

6. LAYER

Dependent Variable	LAYER	Mean	Std. Error	95% Confidence Interval	
				Lower Bound	Upper Bound
ave.h	1	.246[a,]	.013	.220	.271
	2	.321[a,]	.010	.302	.340
	3	.355[a,]	.010	.336	.374
	4	.394[a,]	.010	.375	.413
	5	.428[a,]	.009	.410	.446
	6	.384[a,]	.009	.366	.402
AVE.E	1	4.067[a,]	.299	3.480	4.654
	2	5.015[a,]	.224	4.575	5.456
	3	5.474[a,]	.221	5.041	5.908
	4	6.301[a,]	.225	5.859	6.744
	5	7.275[a,]	.207	6.868	7.682
	6	7.300[a,]	.216	6.876	7.725

a. Evaluated at covariates appeared in the model: CA2 = 7.048E-02.

b. Based on modified population marginal mean.

Table 5. 9. Of the 2790 indents the average hardness and elasticity values were obtained for the six layers of the teeth of the nine teeth studied. The apex corresponds to level 1, extending to the CEJ, which was level 6.

7. Surface

Dependent Variable	Surface	Mean	Std. Error	95% Confidence Interval	
				Lower Bound	Upper Bound
ave.h	Buccal	.362[a,b]	.009	.344	.381
	Mesial	.362[a,b]	.007	.348	.376
	Lingual	.362[a,b]	.009	.344	.380
	Distal	.333[a,b]	.007	.318	.347
AVE.E	Buccal	6.607[a,b]	.217	6.181	7.034
	Mesial	5.388[a,b]	.166	5.061	5.715
	Lingual	6.041[a,b]	.212	5.625	6.457
	Distal	5.585[a,b]	.164	5.262	5.908

a. Evaluated at covariates appeared in the model: CA2 = 7.048E-02.

b. Based on modified population marginal mean.

Table 5. 10. Of the 2790 indents the average hardness and elasticity values are obtained for the four surfaces of the nine teeth studied. The Standard Error of the Mean in relation to hardness and elasticity for all surfaces of the root is shown.

Average Hardness (GPa) * Layer

ave.h

LAYER	Mean	N	SD
1	.2475	53	.0803
2	.3180	86	.0803
3	.3523	86	.0818
4	.3899	85	.1004
5	.4247	108	.0998
6	.3835	108	.1177
7	1.9721	8	.5895
8	2.3362	7	.6717
Total	.4128	541	.3278

Average Hardness (GPa) * Surface

ave.h

Surface	Mean	N	SD
Buccal	.3748	97	.1121
Mesial	.3683	166	.1084
Lingual	.3752	98	.1136
Distal	.3450	165	.1039
Total	.3635	526	.1092

			Sex			
			Male		Female	
			Mean	Std Deviation	Mean	Std Deviation
Surface	Buccal	ave.h	.60	.68	.47	.39
	Mesial	ave.h	.40	.10	.36	.11
	Lingual	ave.h	.47	.42	.52	.56
	Distal	ave.h	.33	.13	.35	.10

Table 5. 11. Mean reported hardness, averaged over all 2790 indents, presented in terms of Layer, Surface and Sex. (N = Number of tests analyzed).

Average Elasticity (GPa) * Layer

AVE.E

LAYER	Mean	N	SD
1	4.1069	53	1.4752
2	5.0915	85	1.7618
3	5.5042	86	2.0203
4	6.3239	84	2.2824
5	7.2337	108	2.4875
6	7.1716	108	2.7108
7	47.162	8	10.54
8	48.236	7	11.28
Total	7.2833	539	7.4548

Average Elasticity (GPa) * Surface

AVE.E

Surface	Mean	N	SD
Buccal	7.0112	96	2.6289
Mesial	5.6465	165	2.3653
Lingual	6.4010	98	2.5731
Distal	5.9317	165	2.2801
Total	6.1274	524	2.4719

Table 5. 12. Mean reported elasticity values, averaged over all 2790 indents presented in terms of Layer and Surface. (N = Number of tests analyzed).

5.4.7 3-D Description of Composite Data

Sixty hardness measures along with their (x, y, z) coordinates were imported into a software visualization package **AVS/Express** (Advanced Visual Systems, OpenViz). The coordinate data was originally modelled in **Houdini** (Side Effect Software). Hardness was mapped to a colour, blue was soft, red was hard. The hardness values were then bilinearly interpolated to produce the contour map. A 3-D plot for the elastic modulus of the respective coordinates was also compiled using **AVS/Express** (Advanced Visual Systems, OpenViz) (Fig. 5.20 - 5.27).

The statistically significant variables of different characteristics analyzed were also presented. All surfaces of the first premolar tooth are divided into six layers with hardness and elasticity represented in colour.

Further representations are available in multimedia format on our web page. The Internet address is http://www.vislab.usyd.edu.au/gallery/dentistry/.

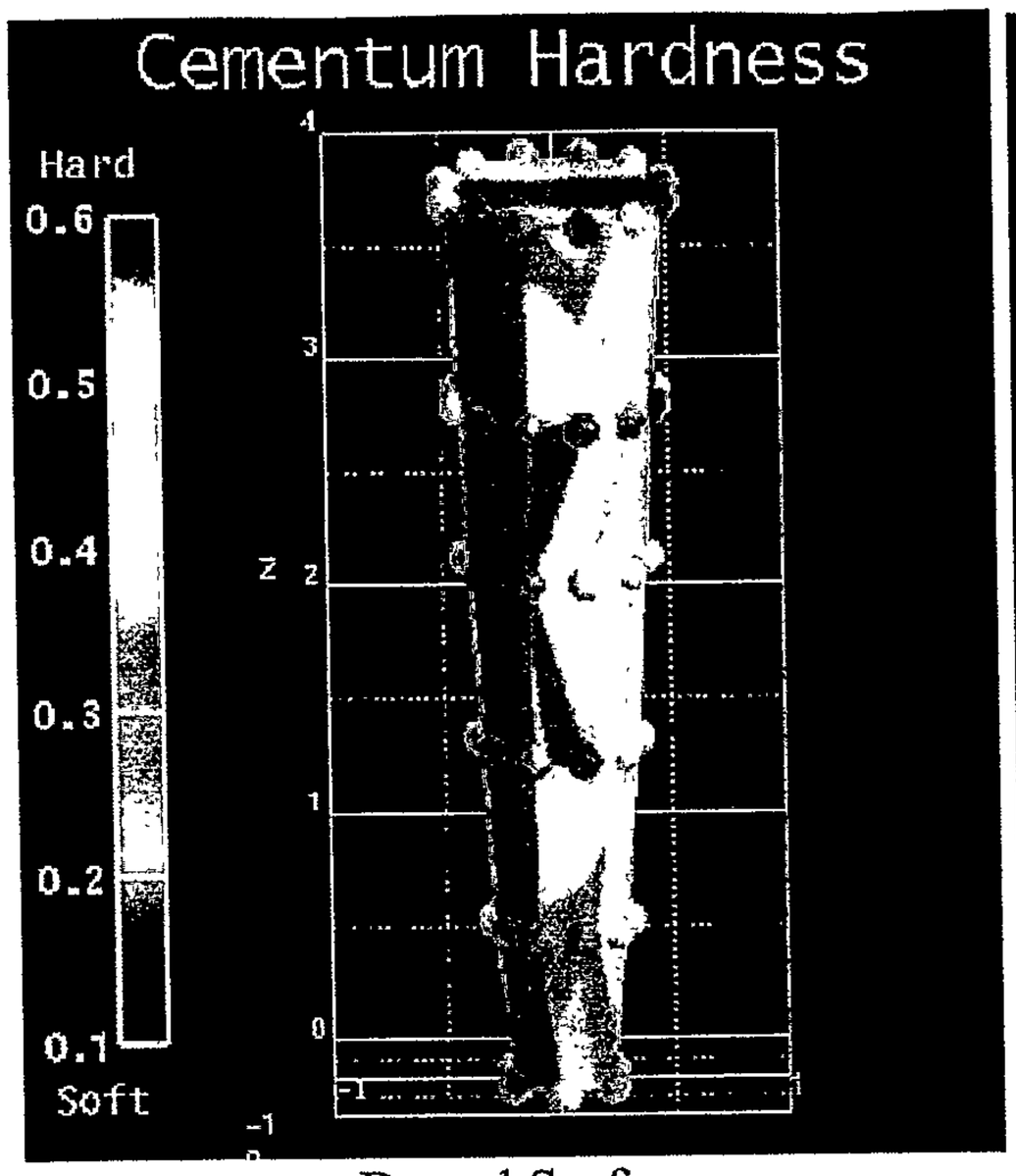

Buccal Surface

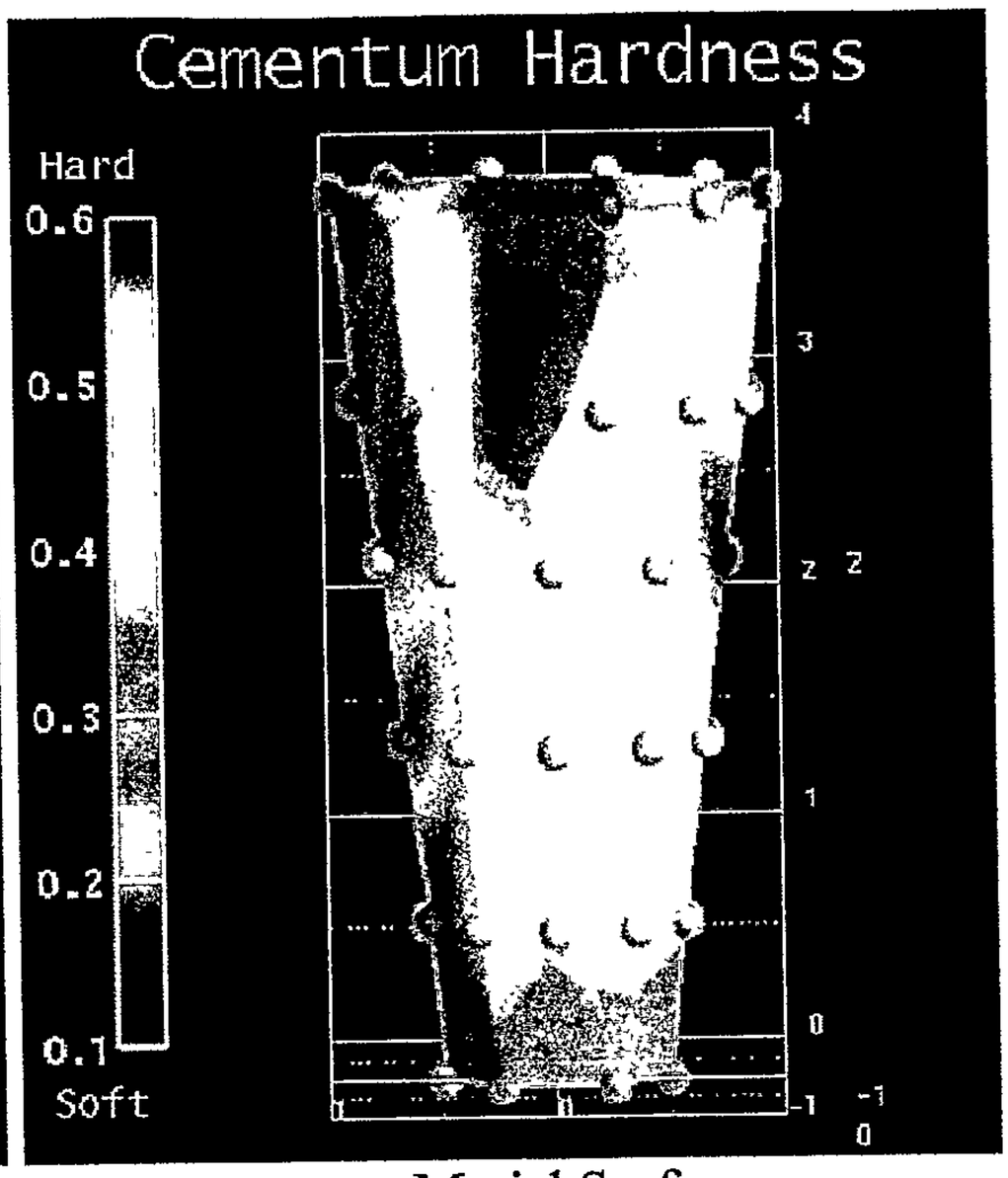

Mesial Surface

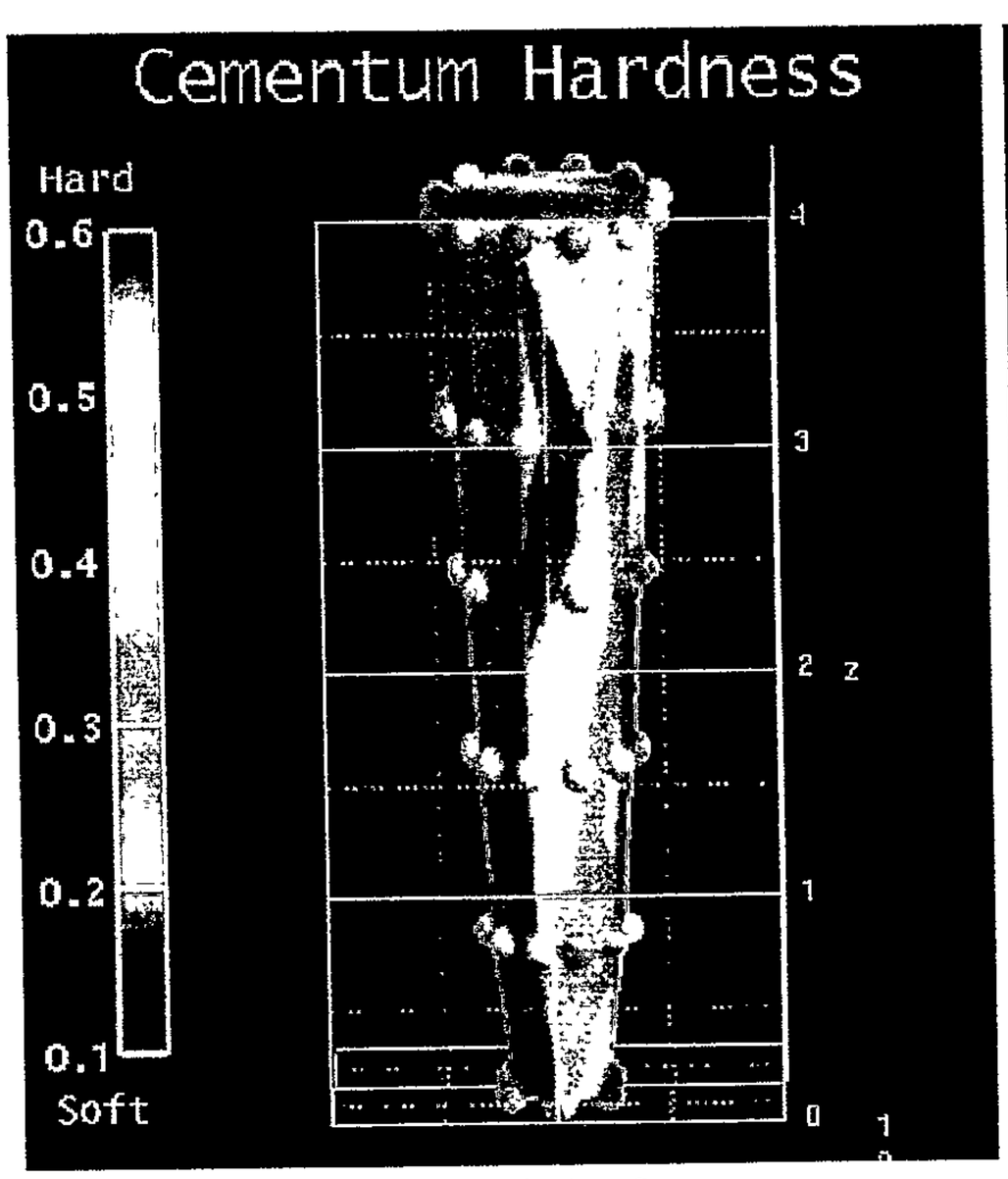

Lingual Surface

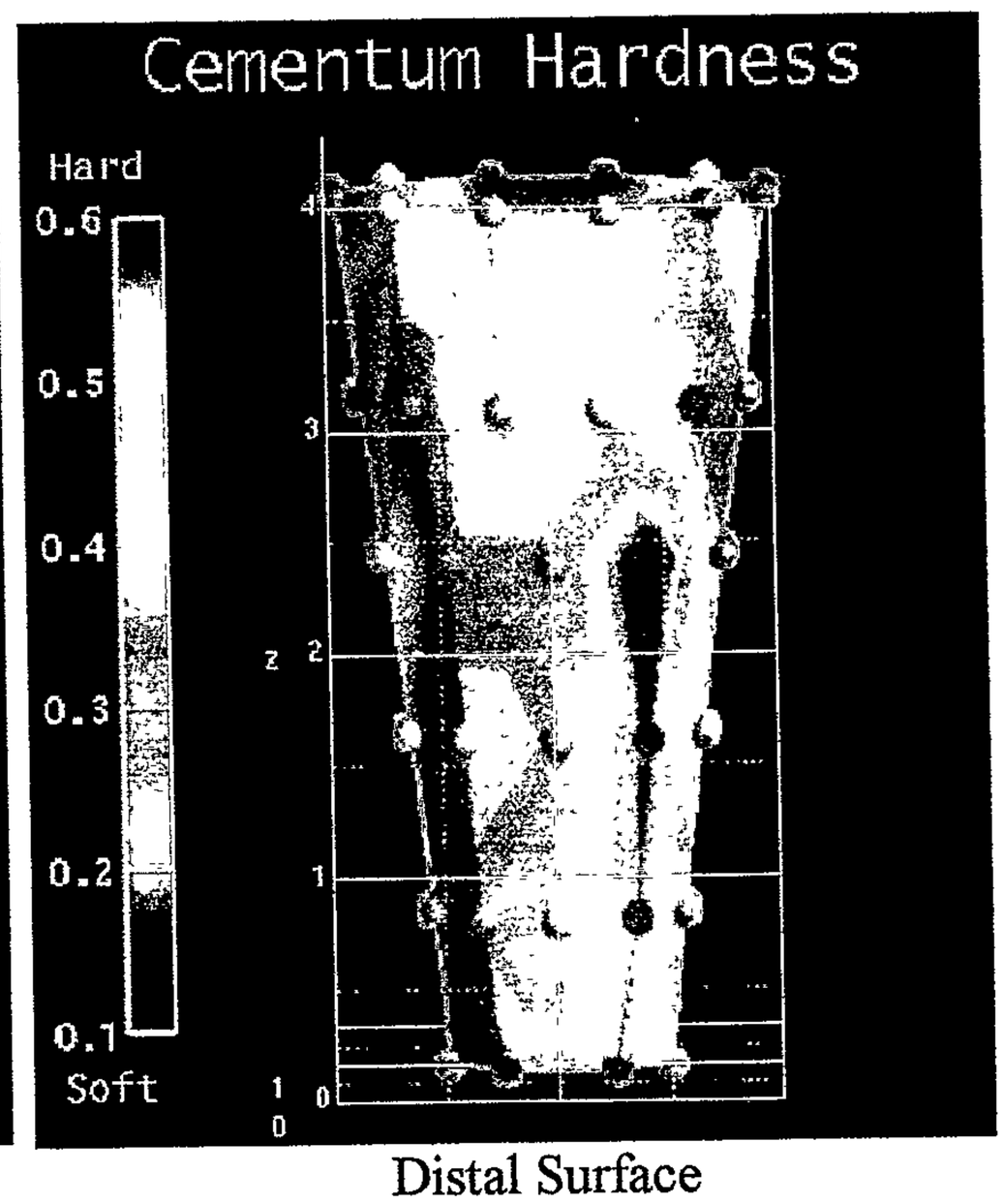

Distal Surface

Figure 5. 20. Sample 1 Hardness. All surfaces of the lower right first premolar were divided into six layers with hardness represented in colour. Blue is soft and red is hard. The sixty sites tested on this root are depicted by the spheres.

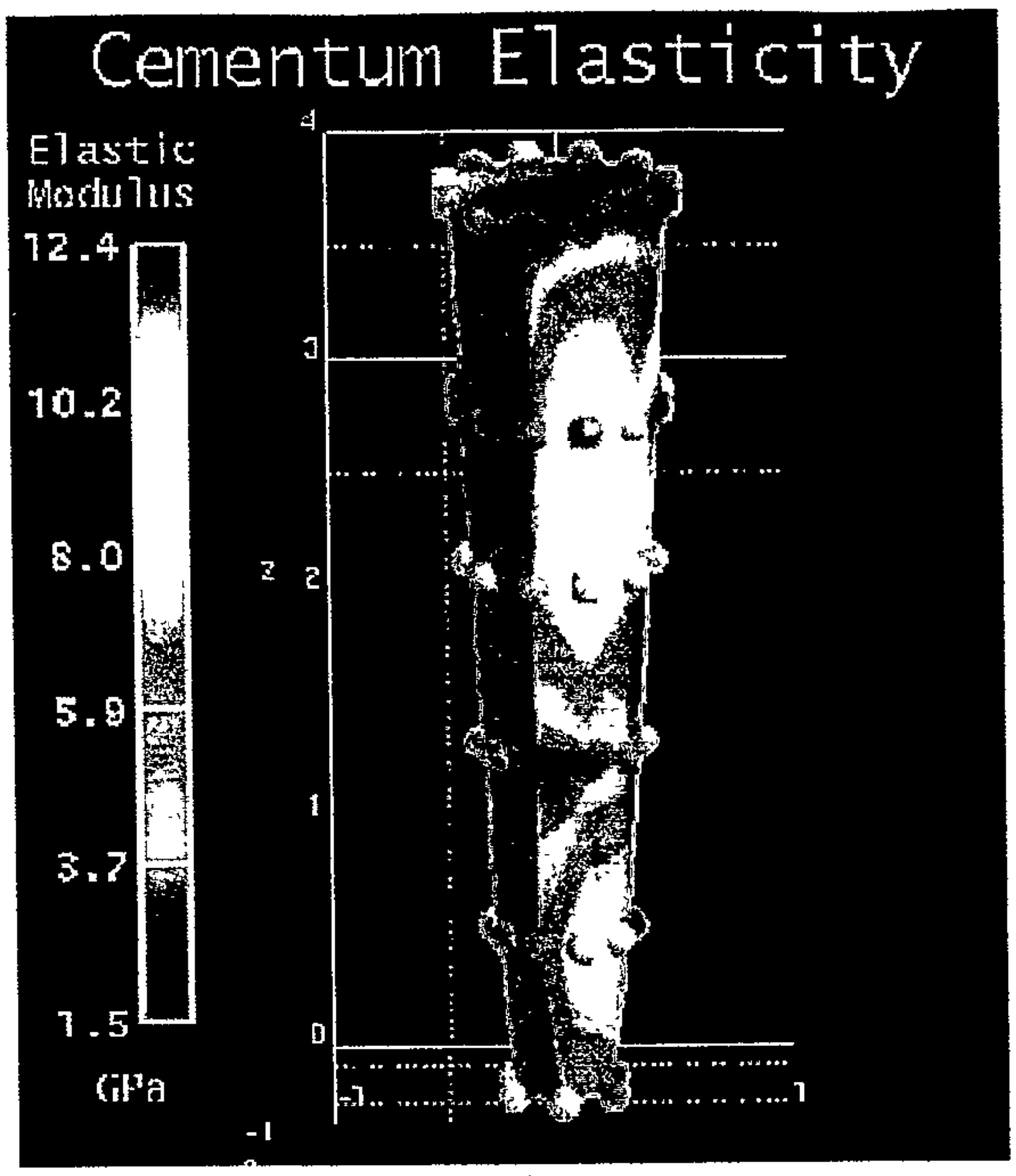

Buccal

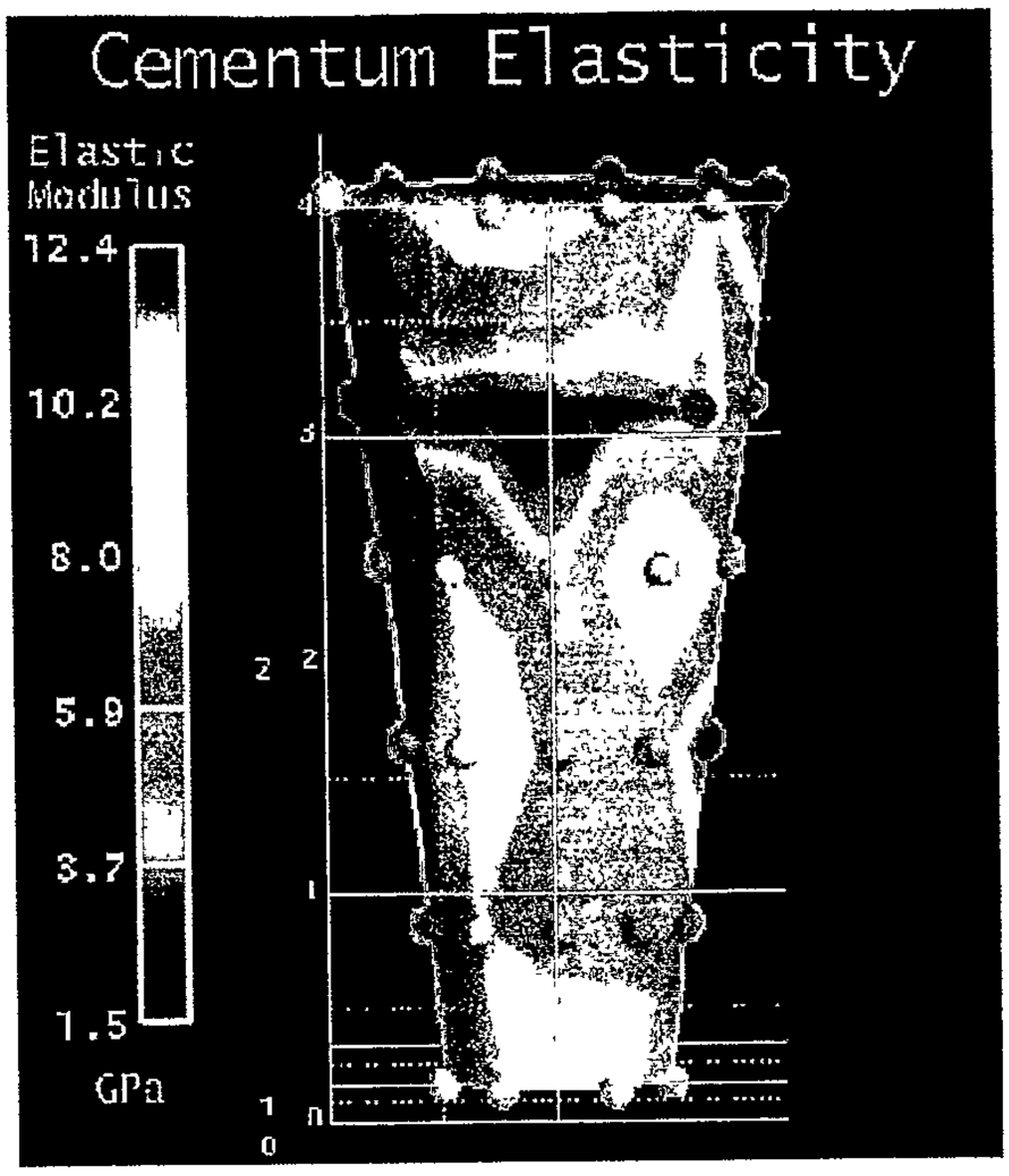

Mesial

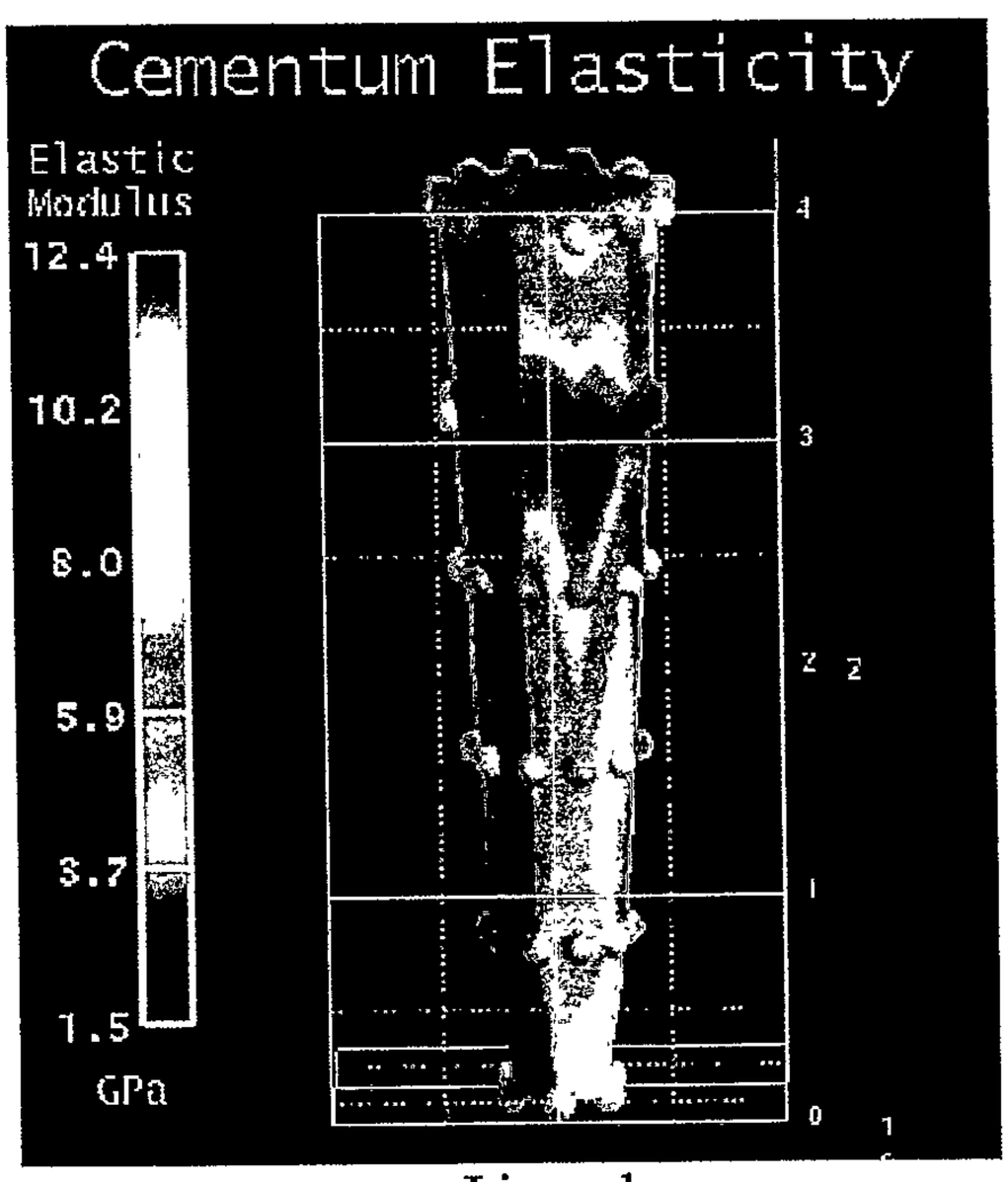

Lingual

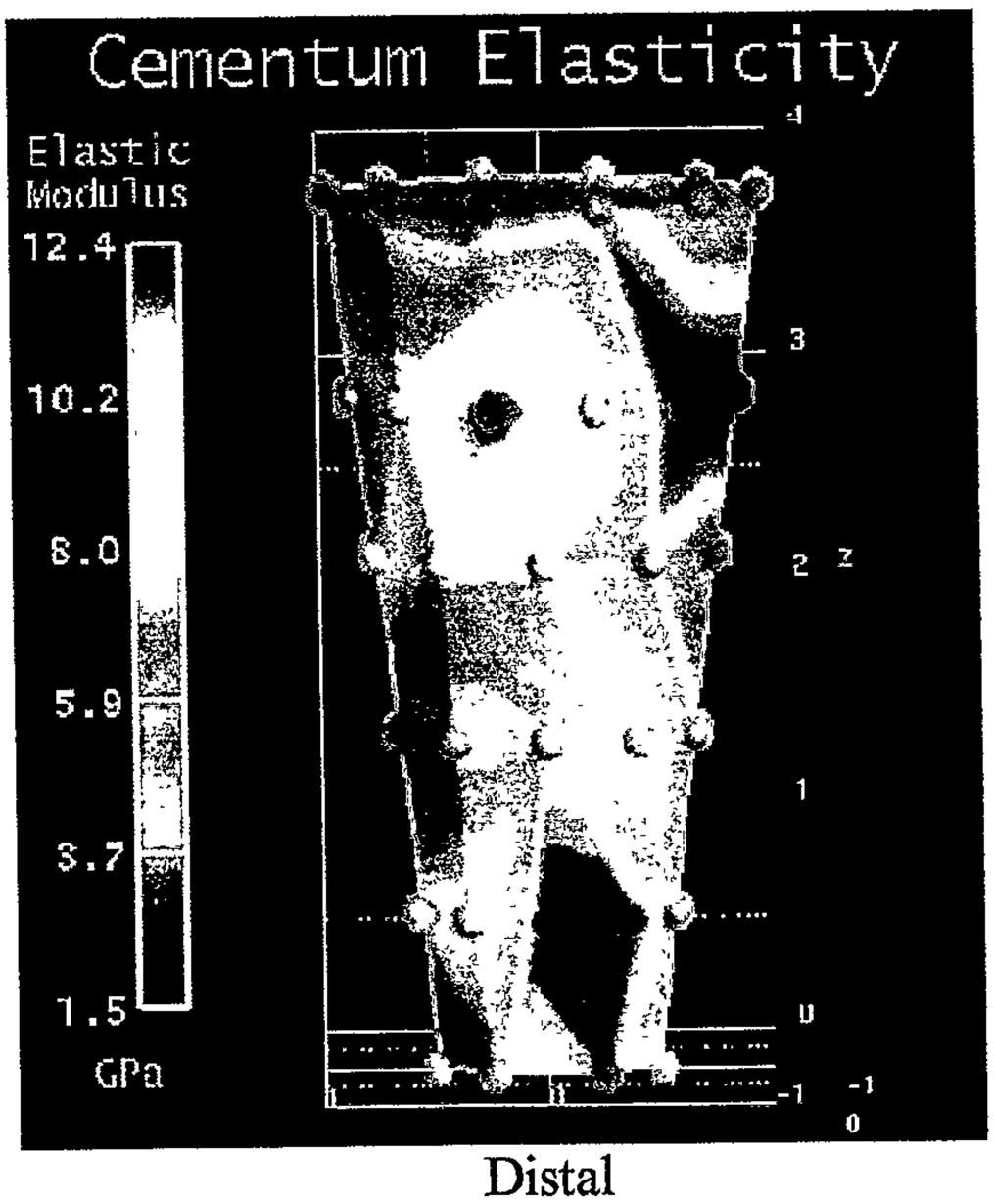

Distal

Figure 5. 21. Sample 1 Elastic Modulus. All surfaces of the lower right first premolar were divided into six layers with Elastic Modulus represented in colour. Blue is low and red is hard. The sixty sites tested on this root are depicted by the spheres.

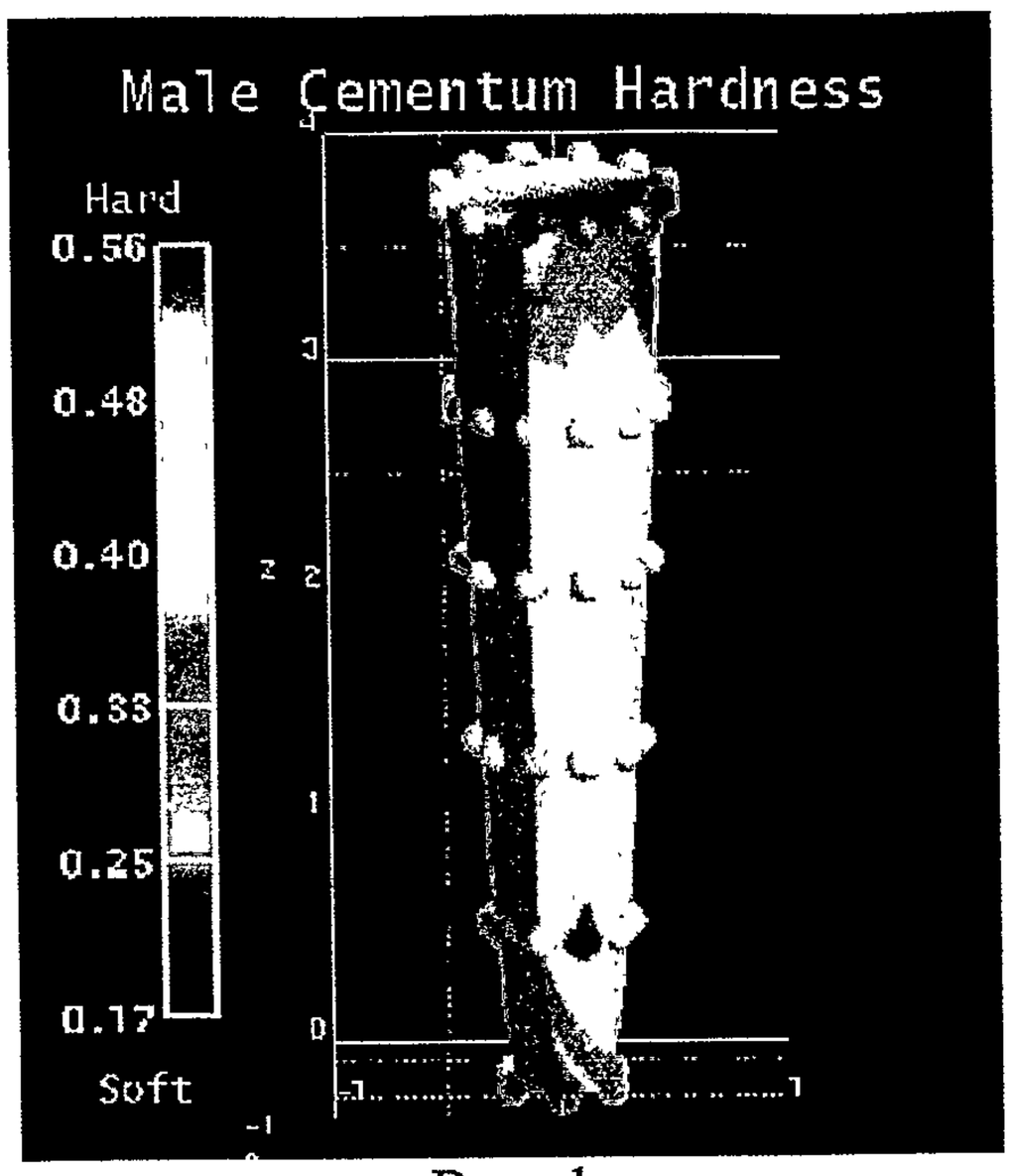

Buccal

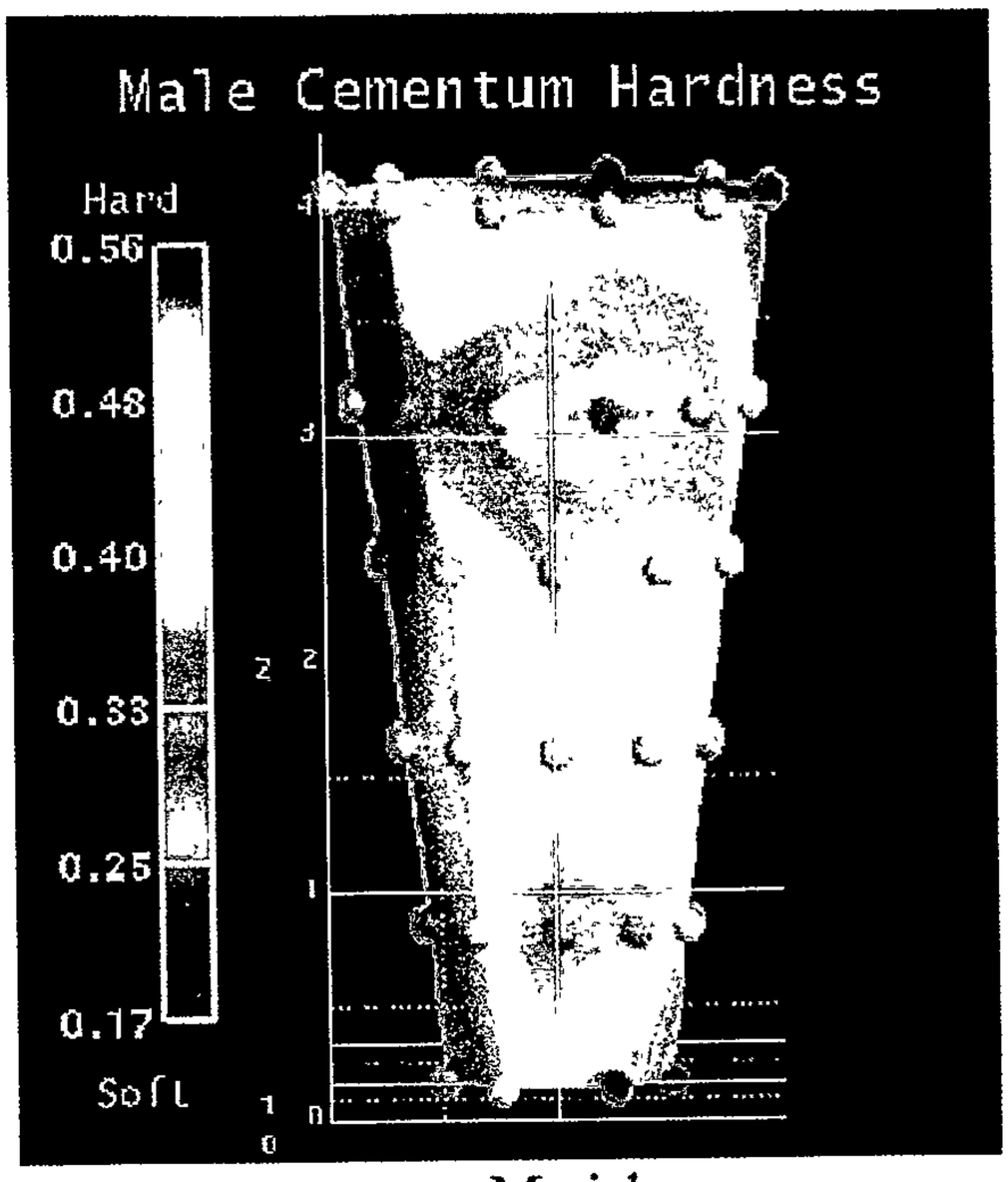

Mesial

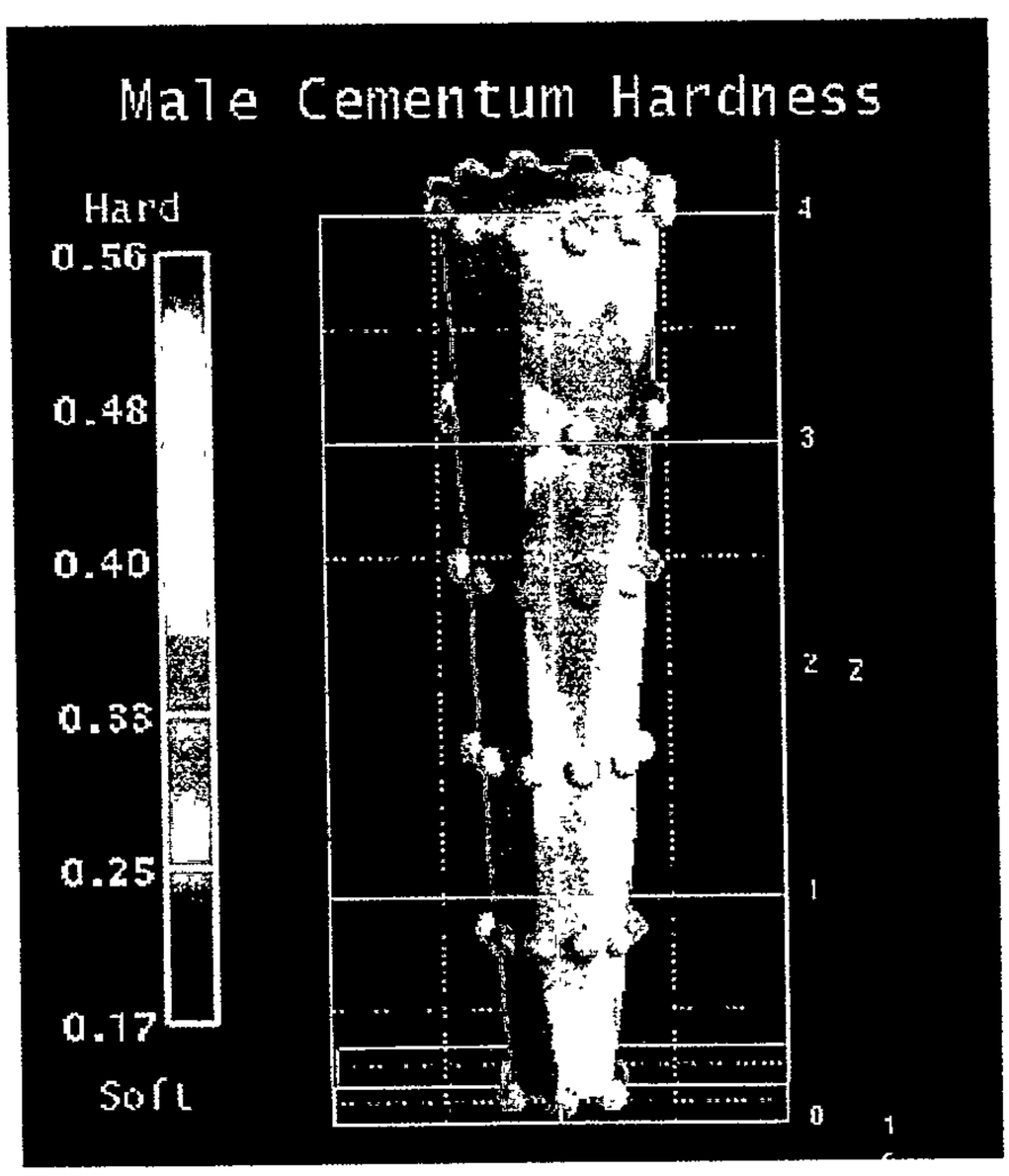

Lingual

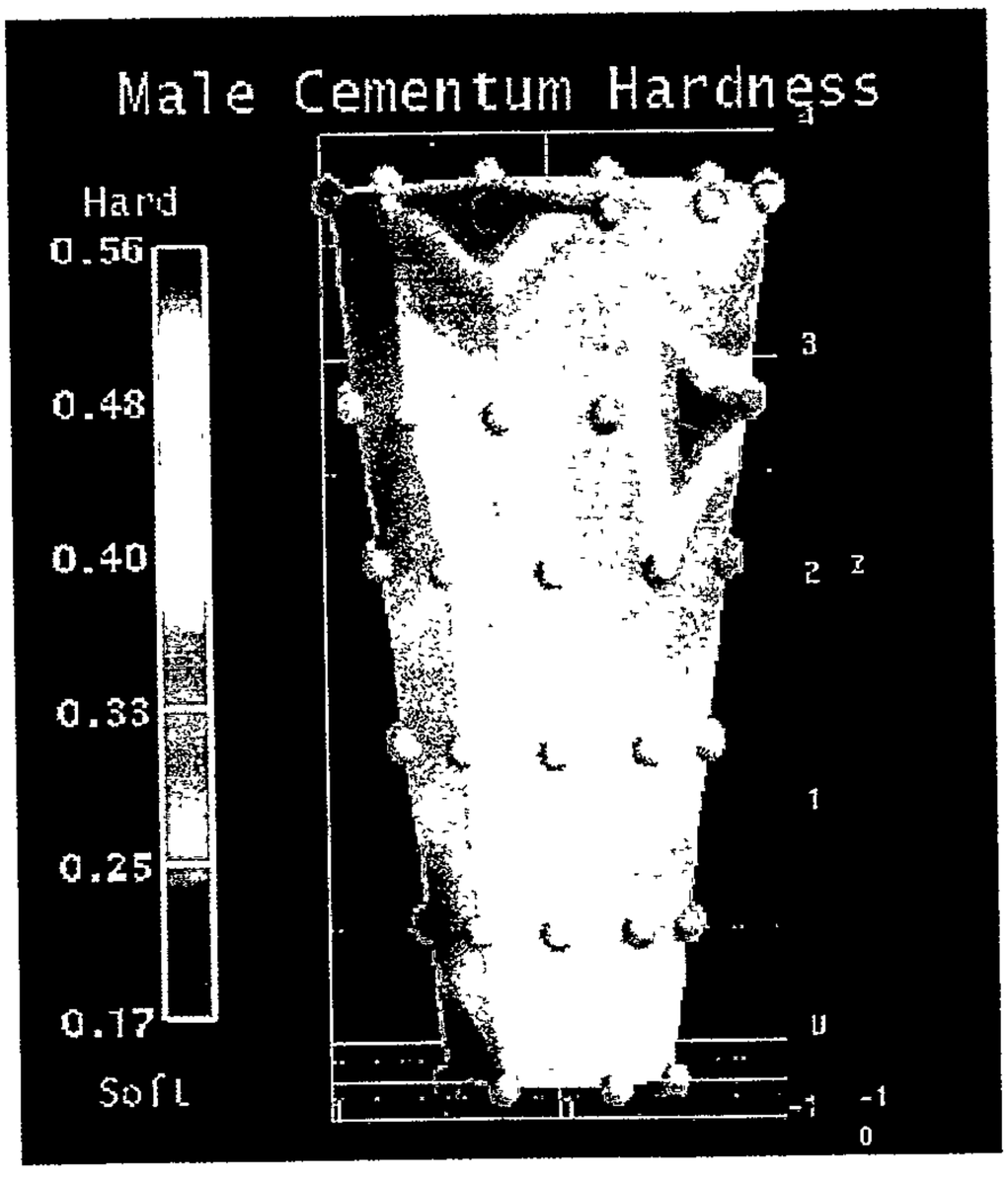

Distal

Figure 5. 22. Average Male Hardness. All surfaces of the first premolar teeth were divided into six layers with calcium content represented in colour. Blue is low and red is hard. The sixty sites tested on this root are depicted by the spheres.

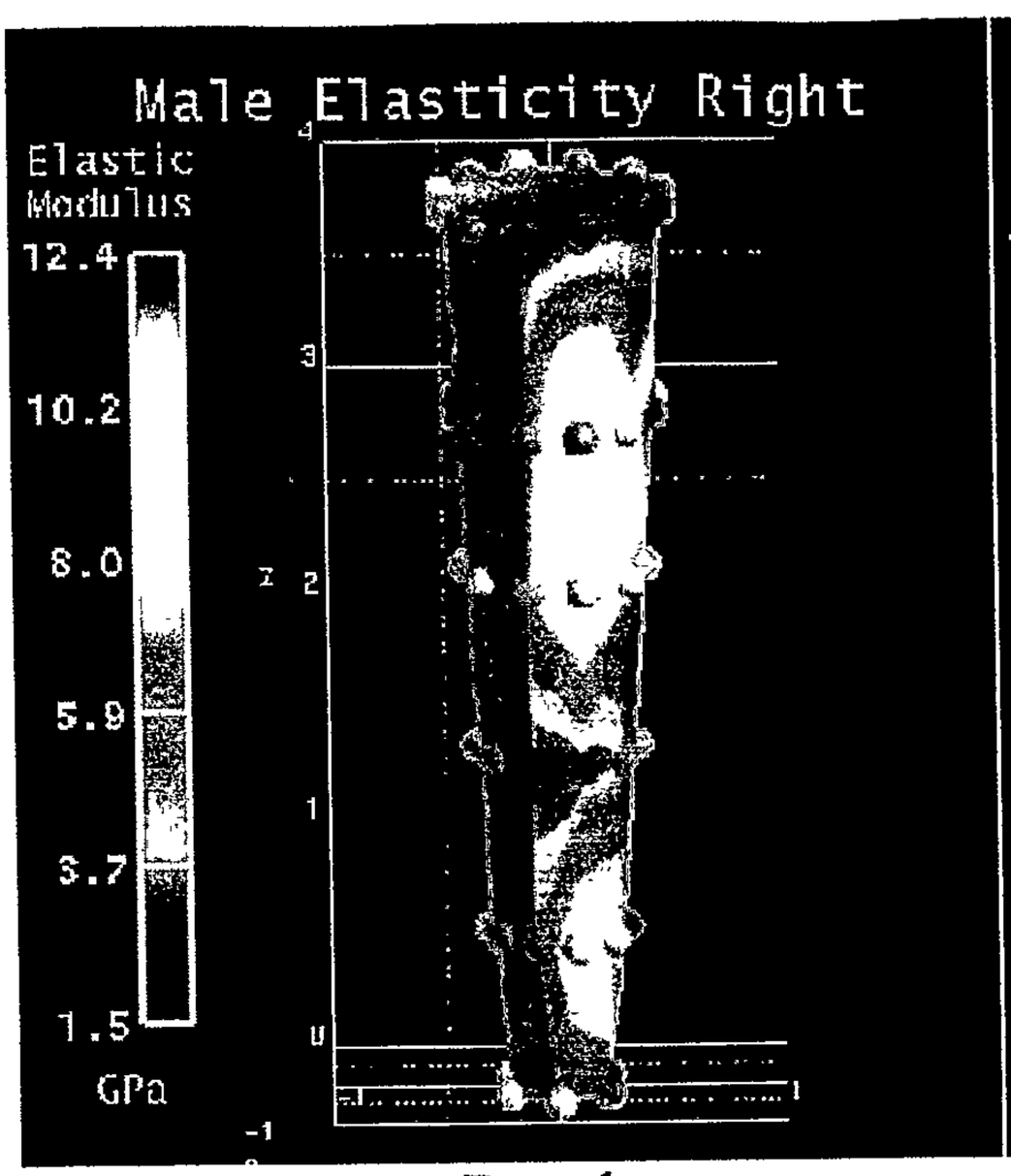

Buccal

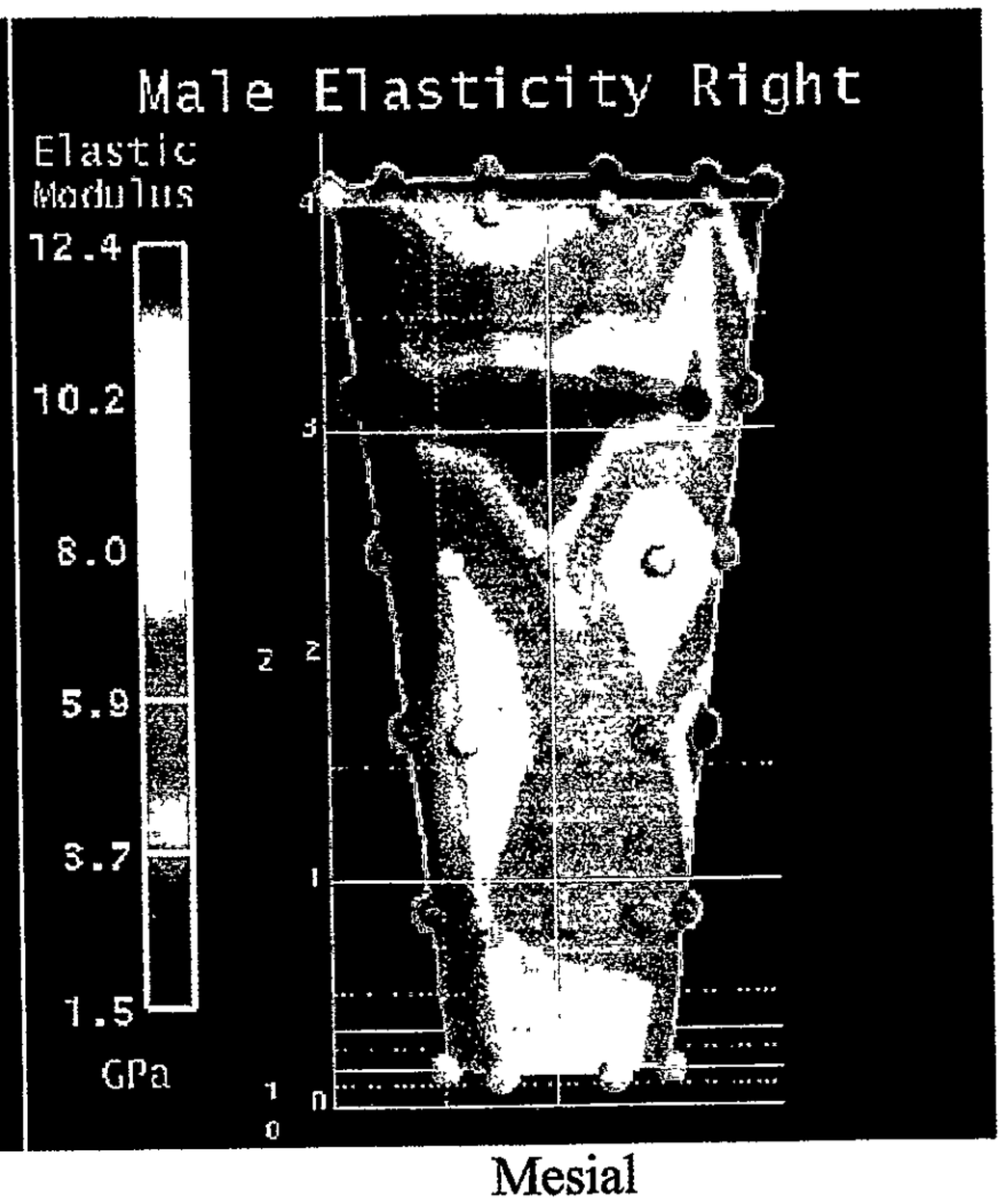

Mesial

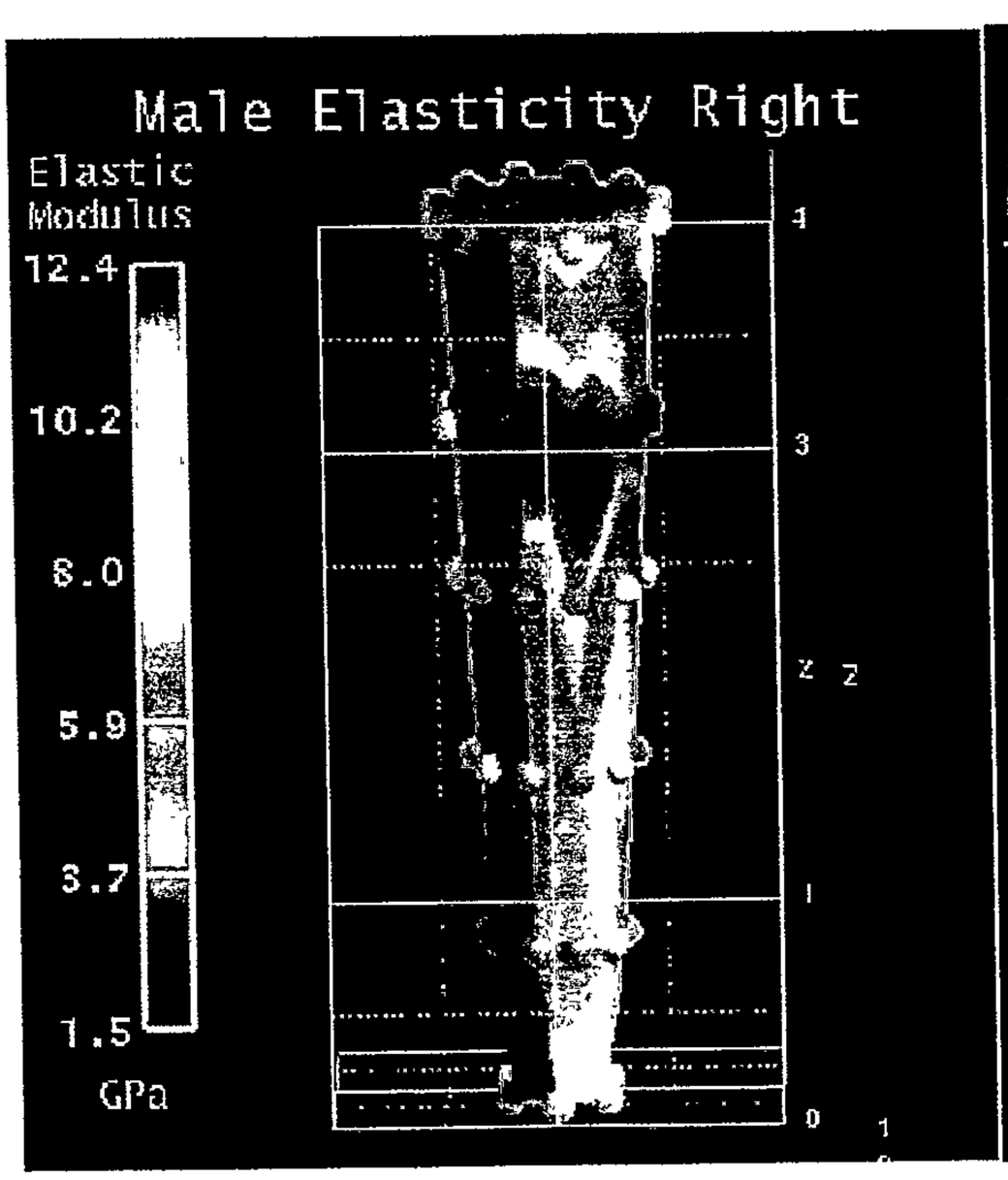

Lingual

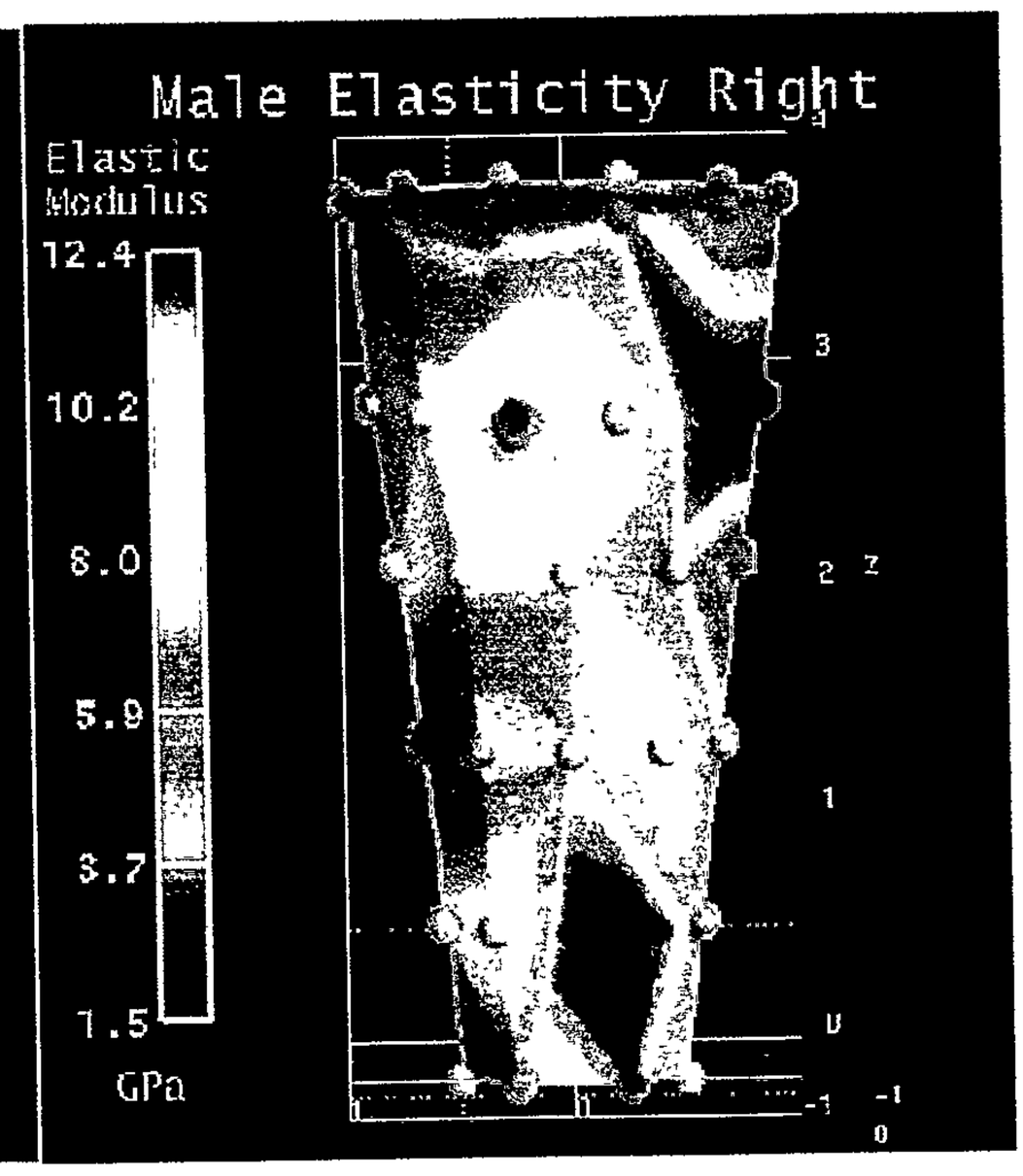

Distal

Figure 5. 23. Composite Summary Male elasticity right.

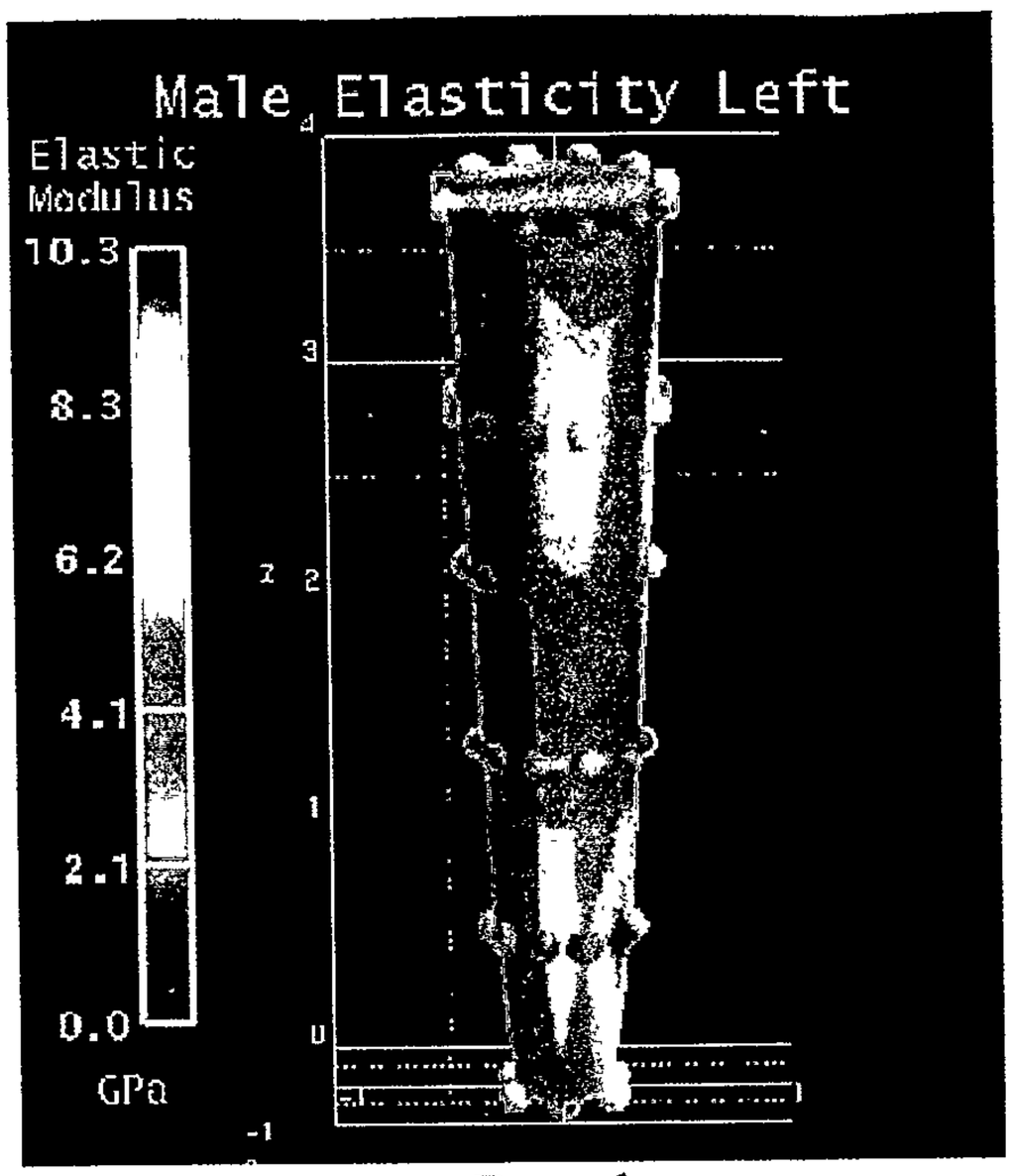

Buccal

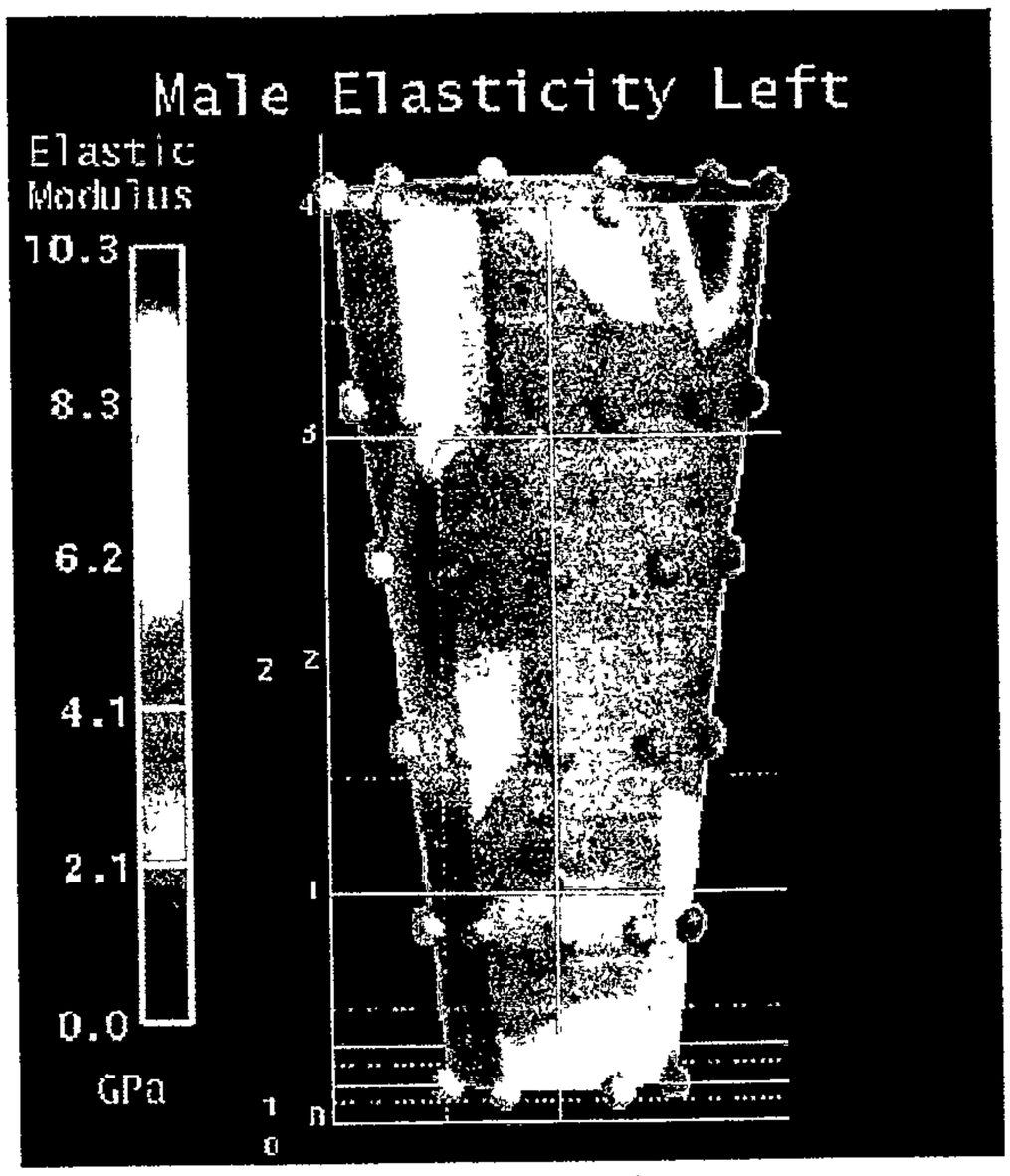

Mesial

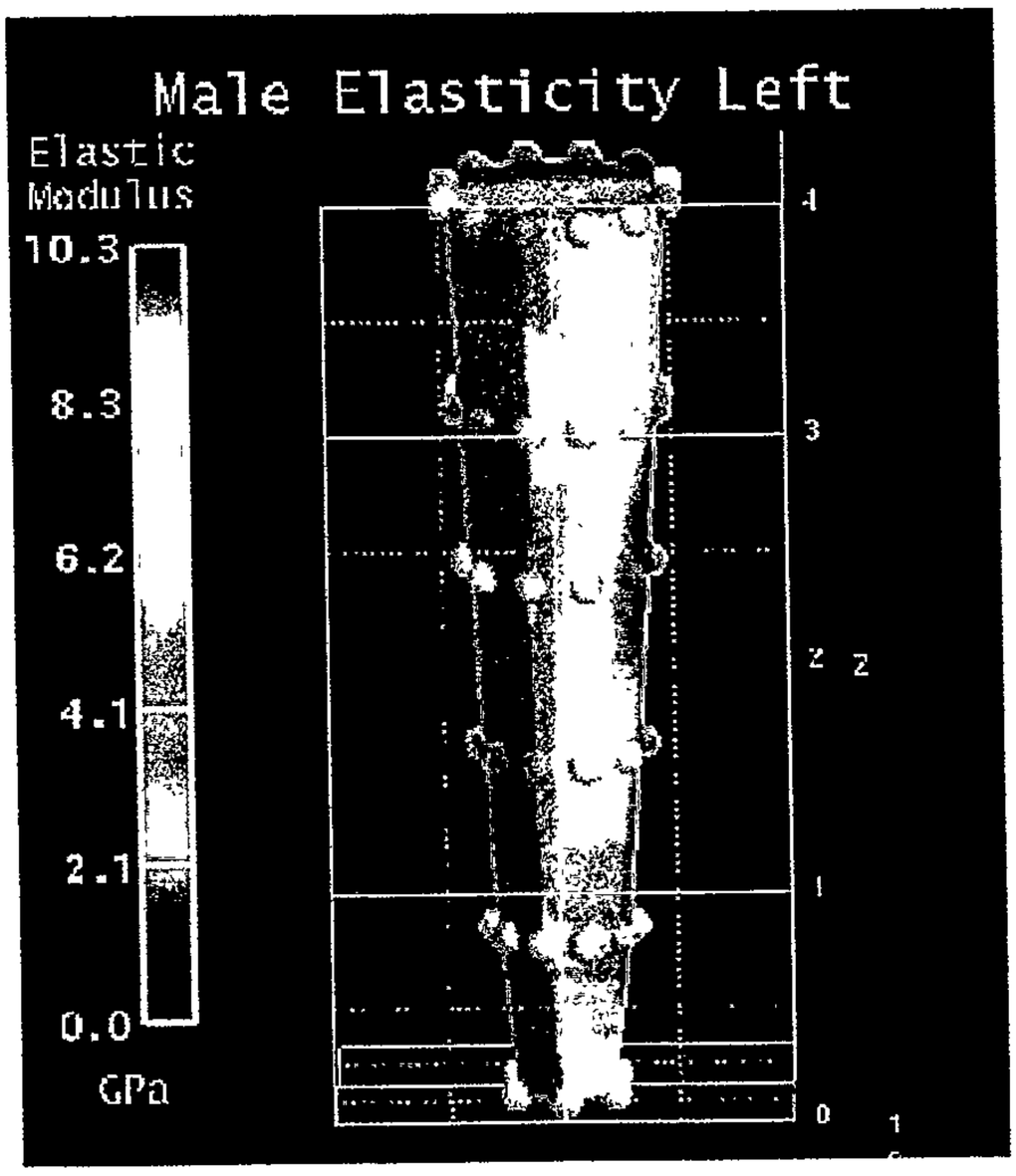

Lingual

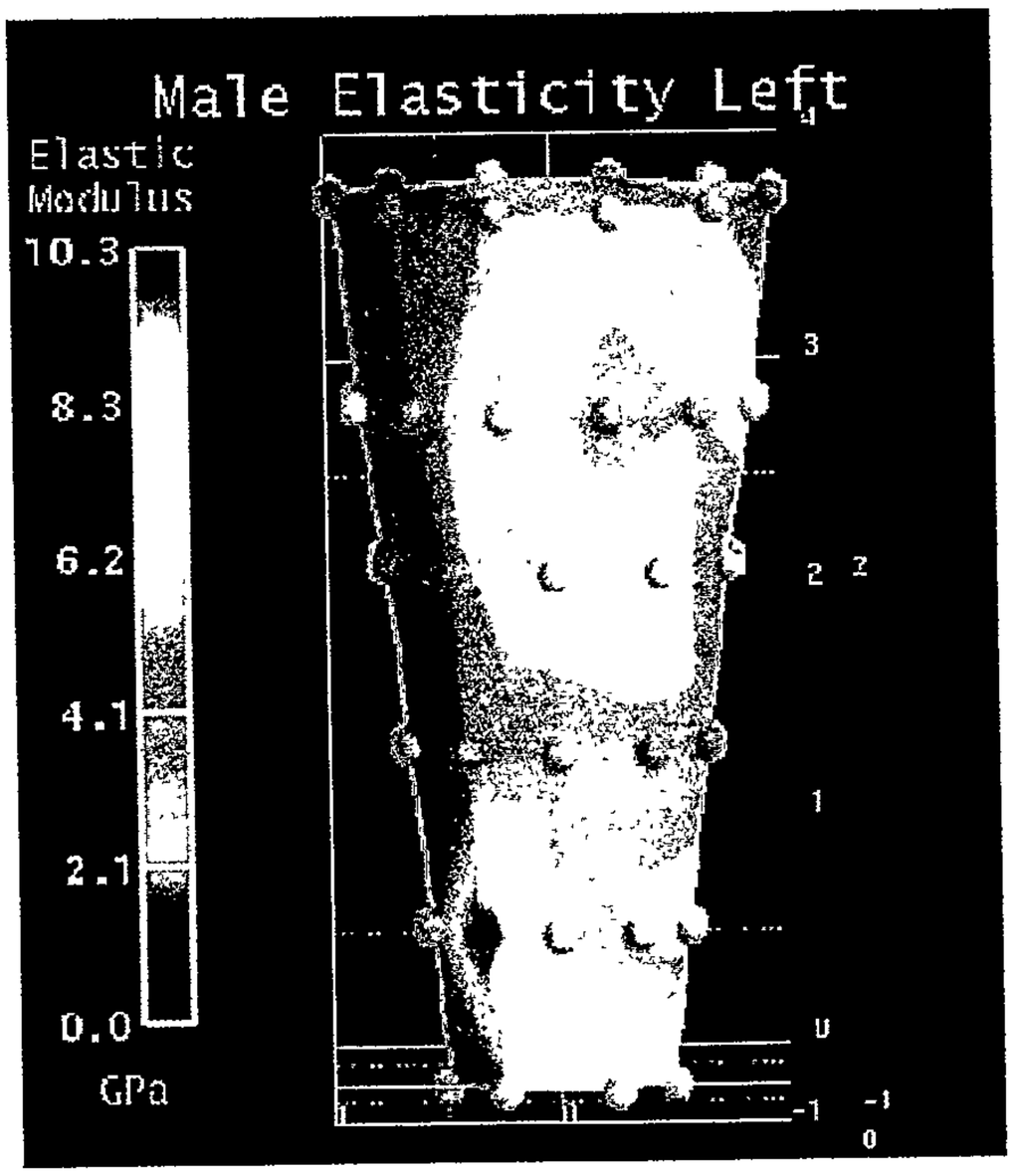

Distal

Figure 5. 24. Composite Summary Male elasticity left.

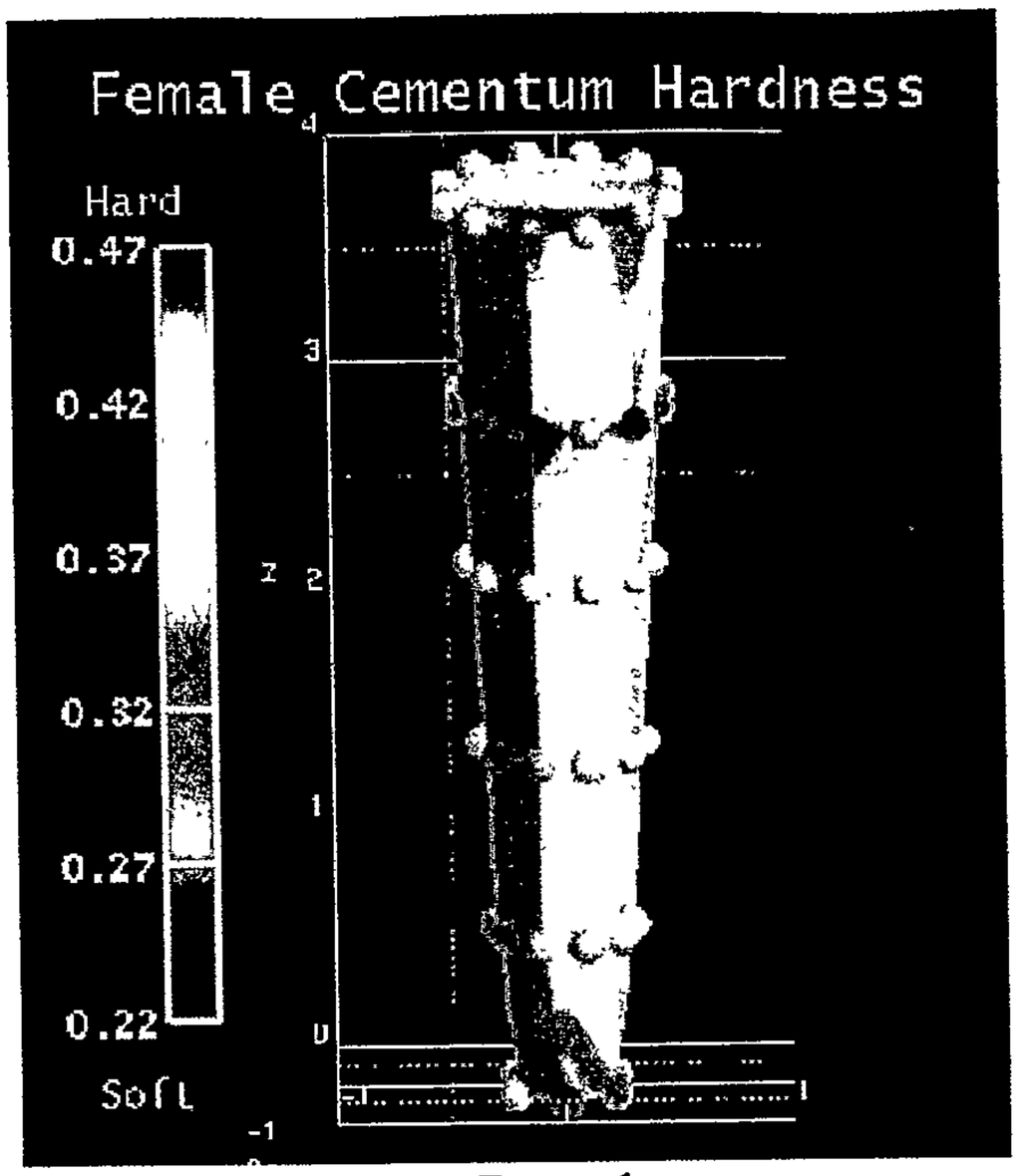

Buccal

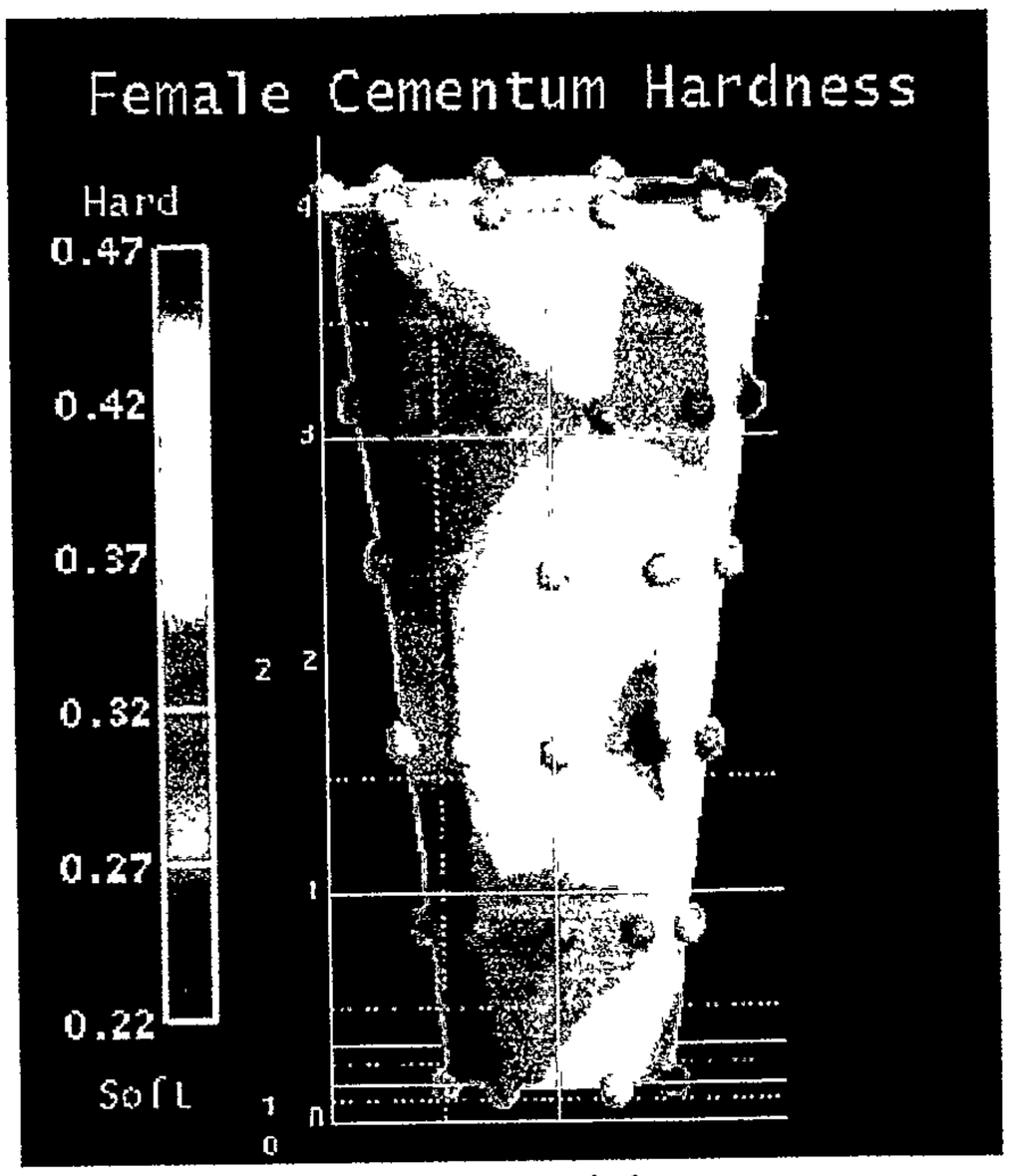

Mesial

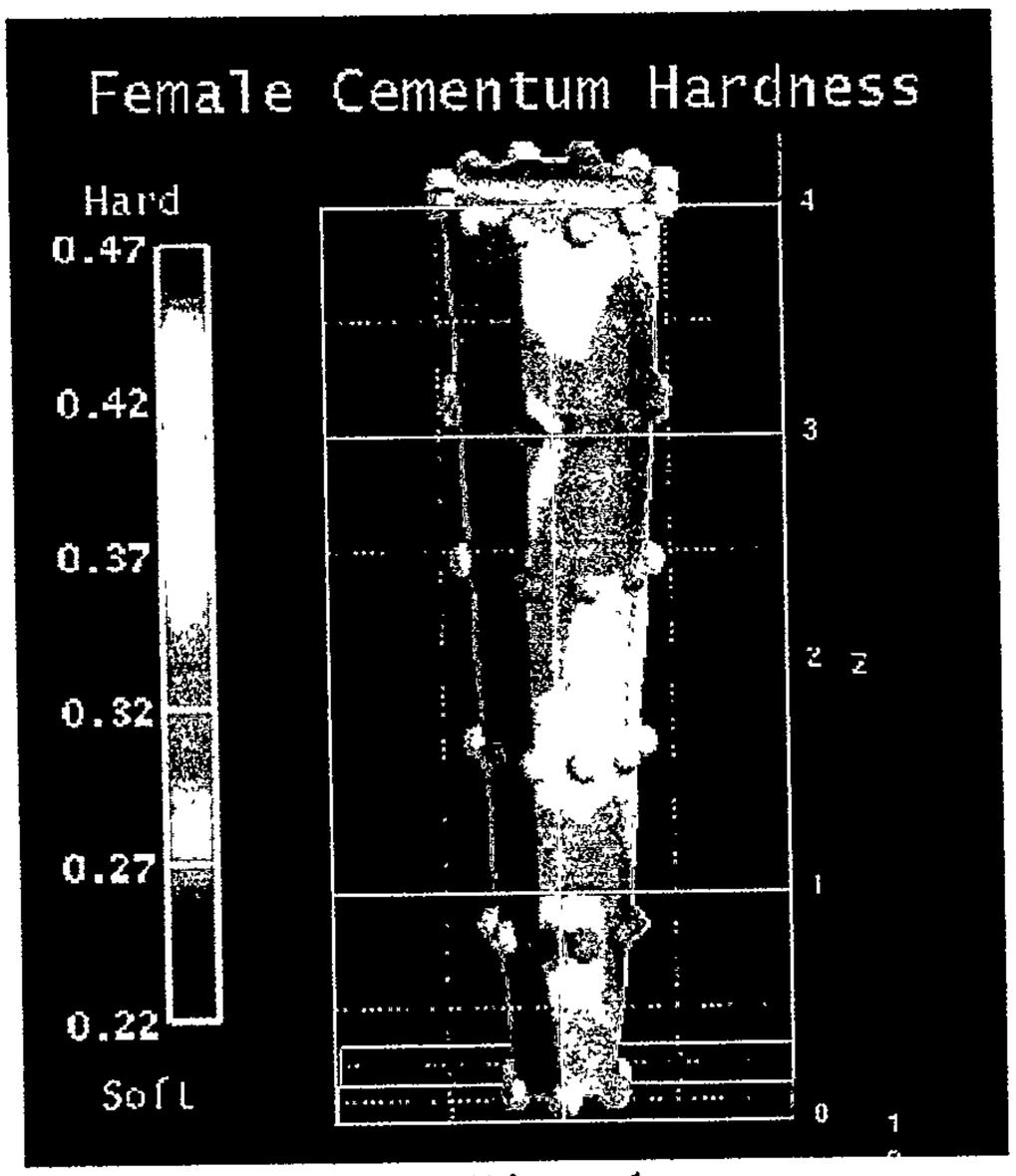

Lingual

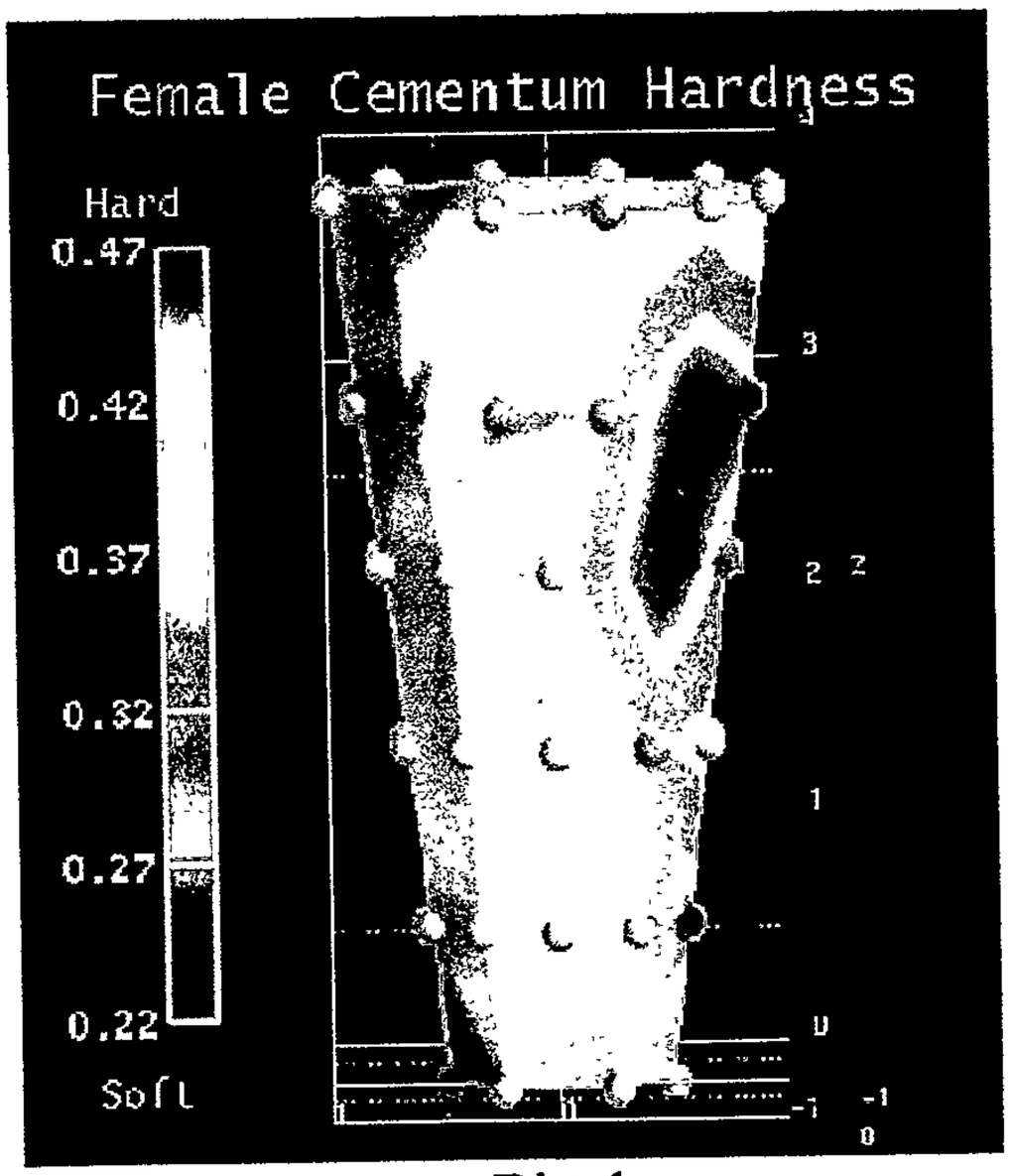

Distal

Figure 5. 25. Average Female Hardness. All surfaces of the first premolar teeth, divided into six layers with calcium content represented in colour. Blue is low and red is hard. The sixty sites tested on this root are depicted by the spheres.

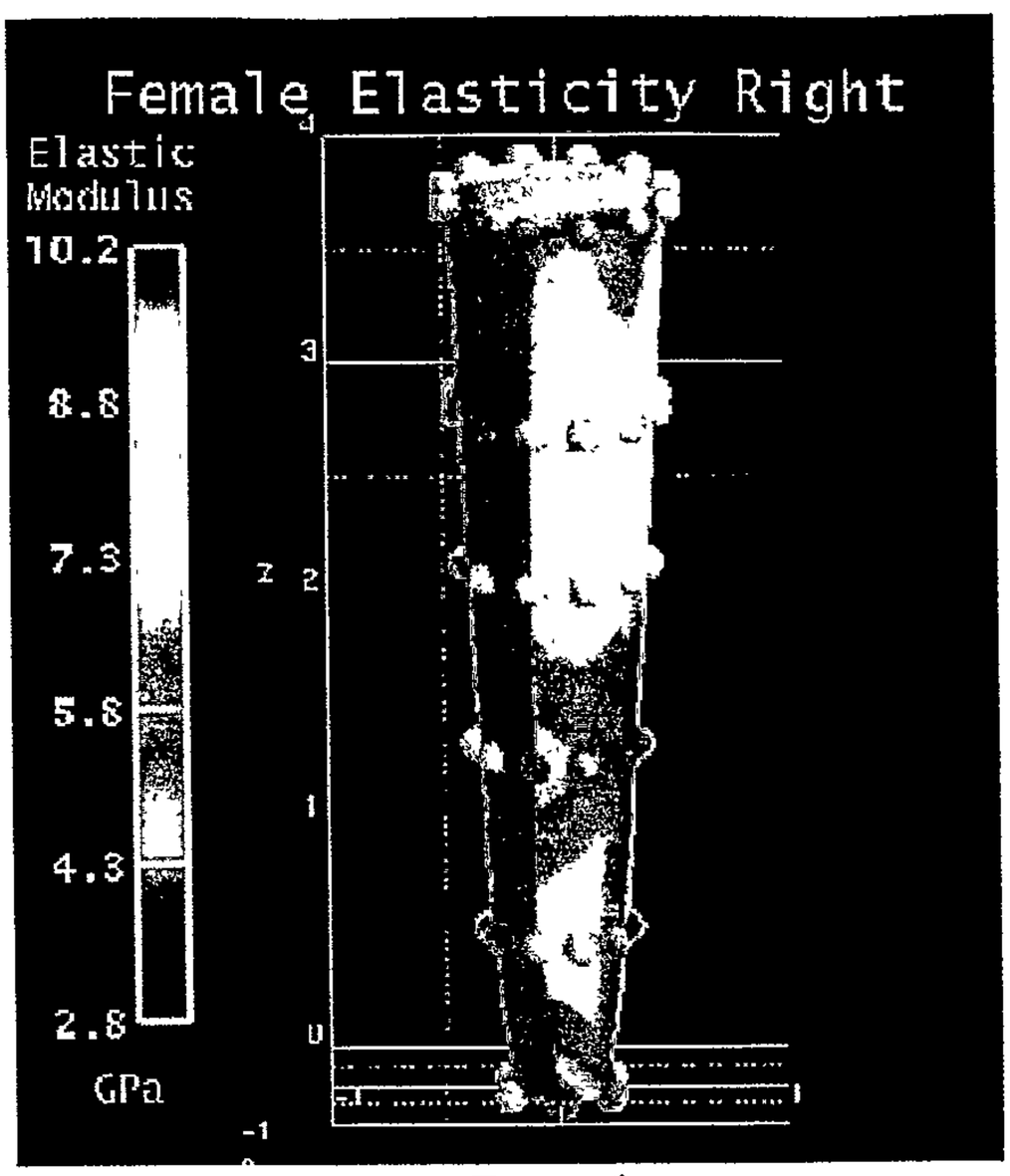

Buccal

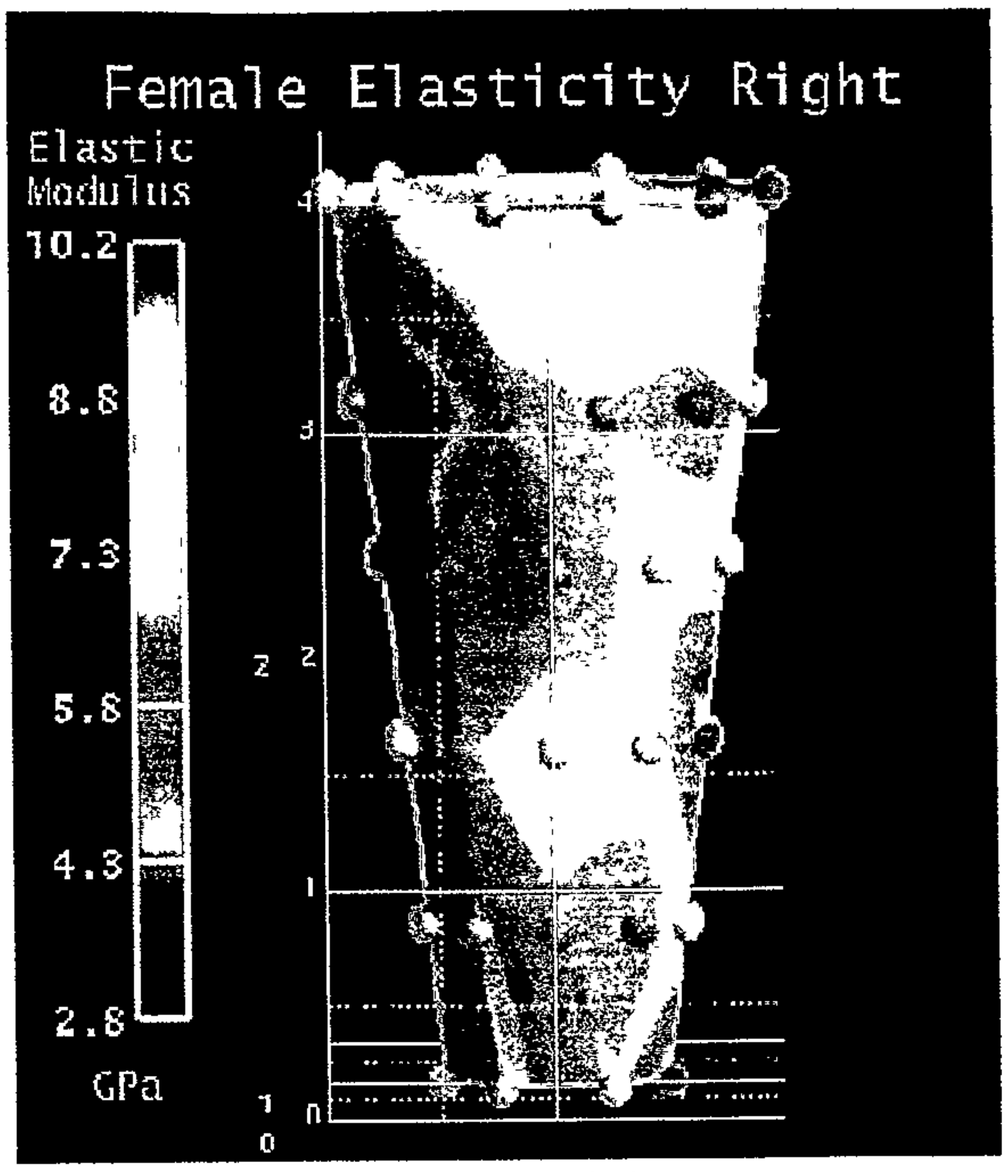

Mesial

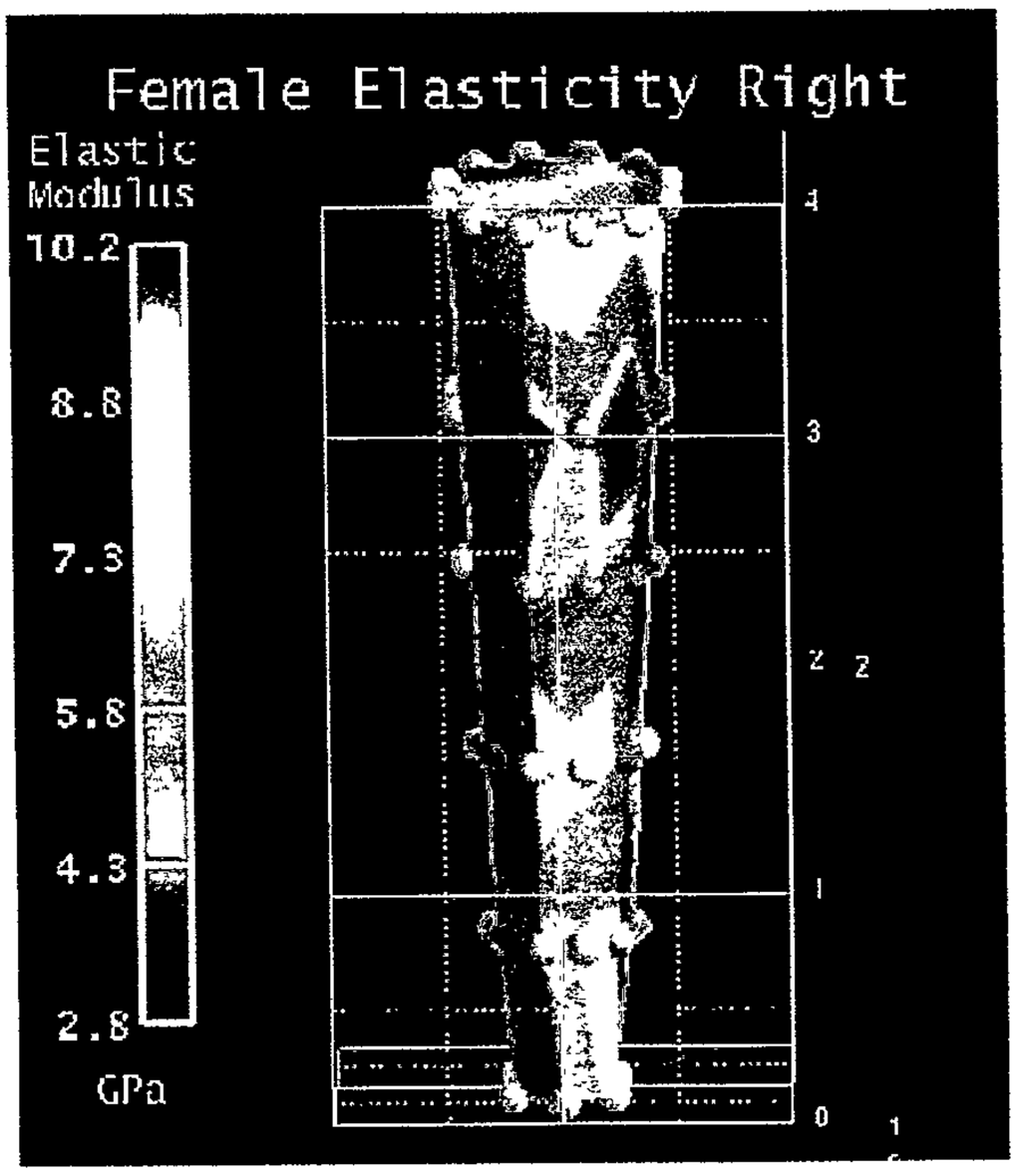

Lingual

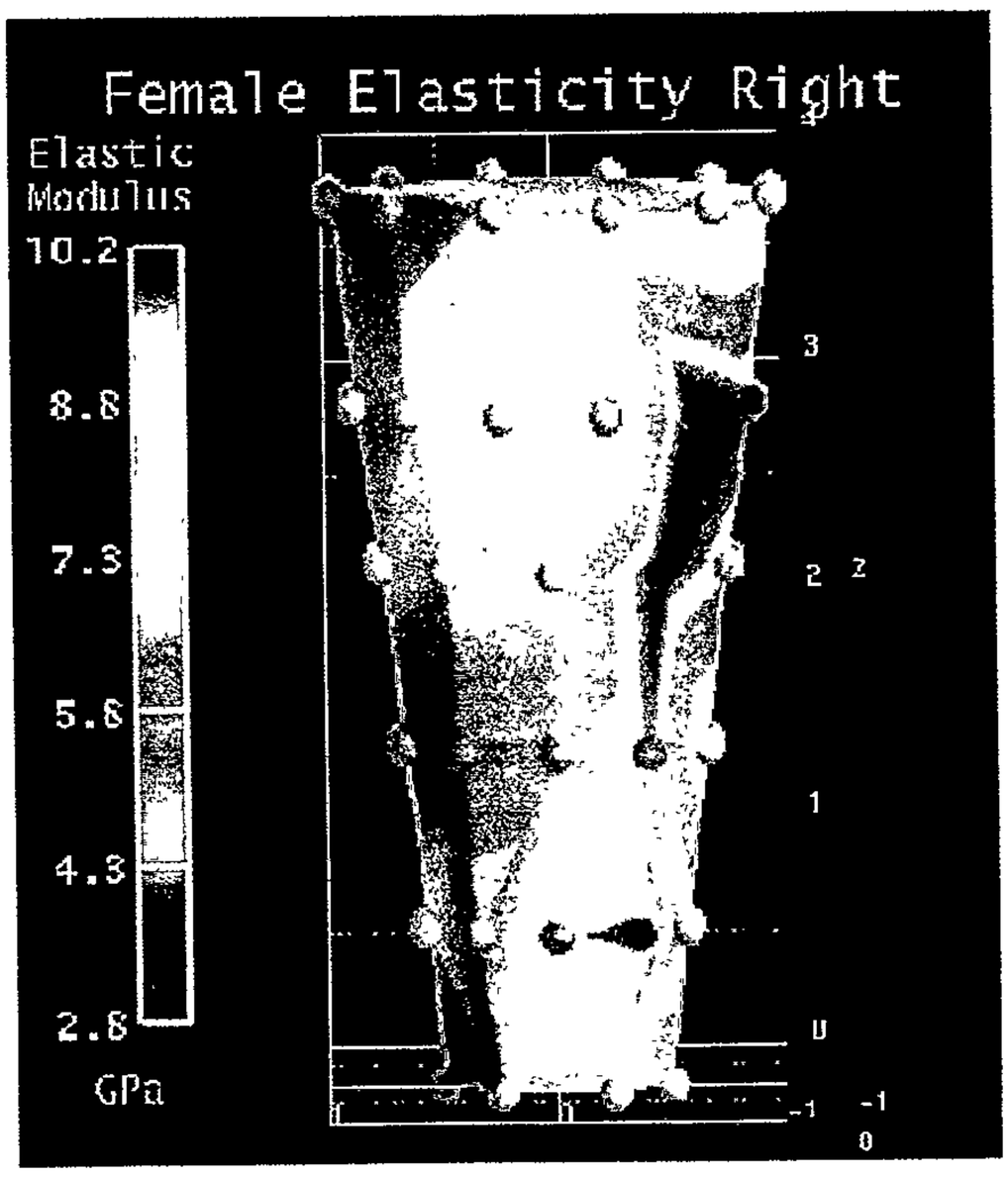

Distal

Figure 5. 26. Composite Summary Female elasticity right.

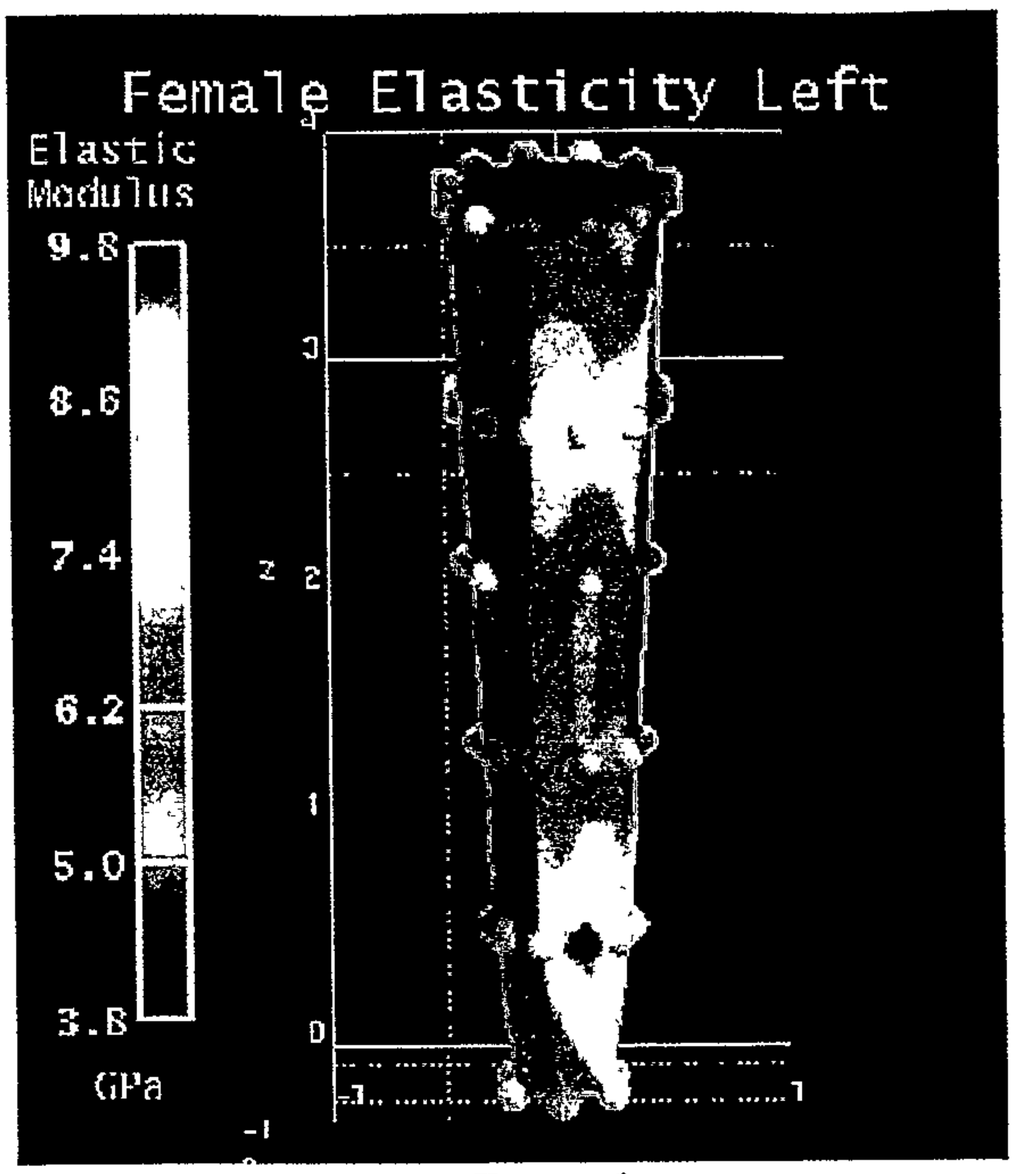

Buccal

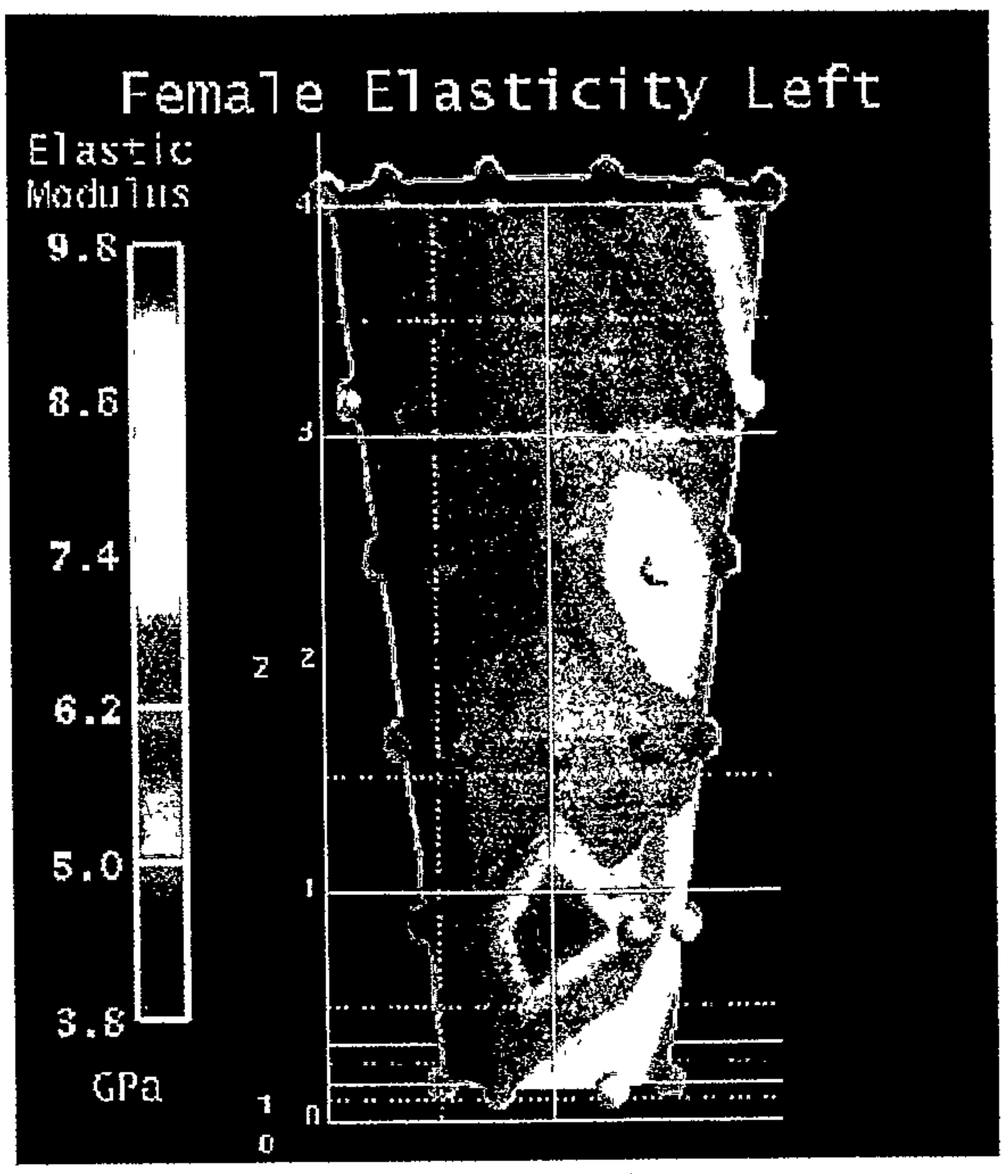

Mesial

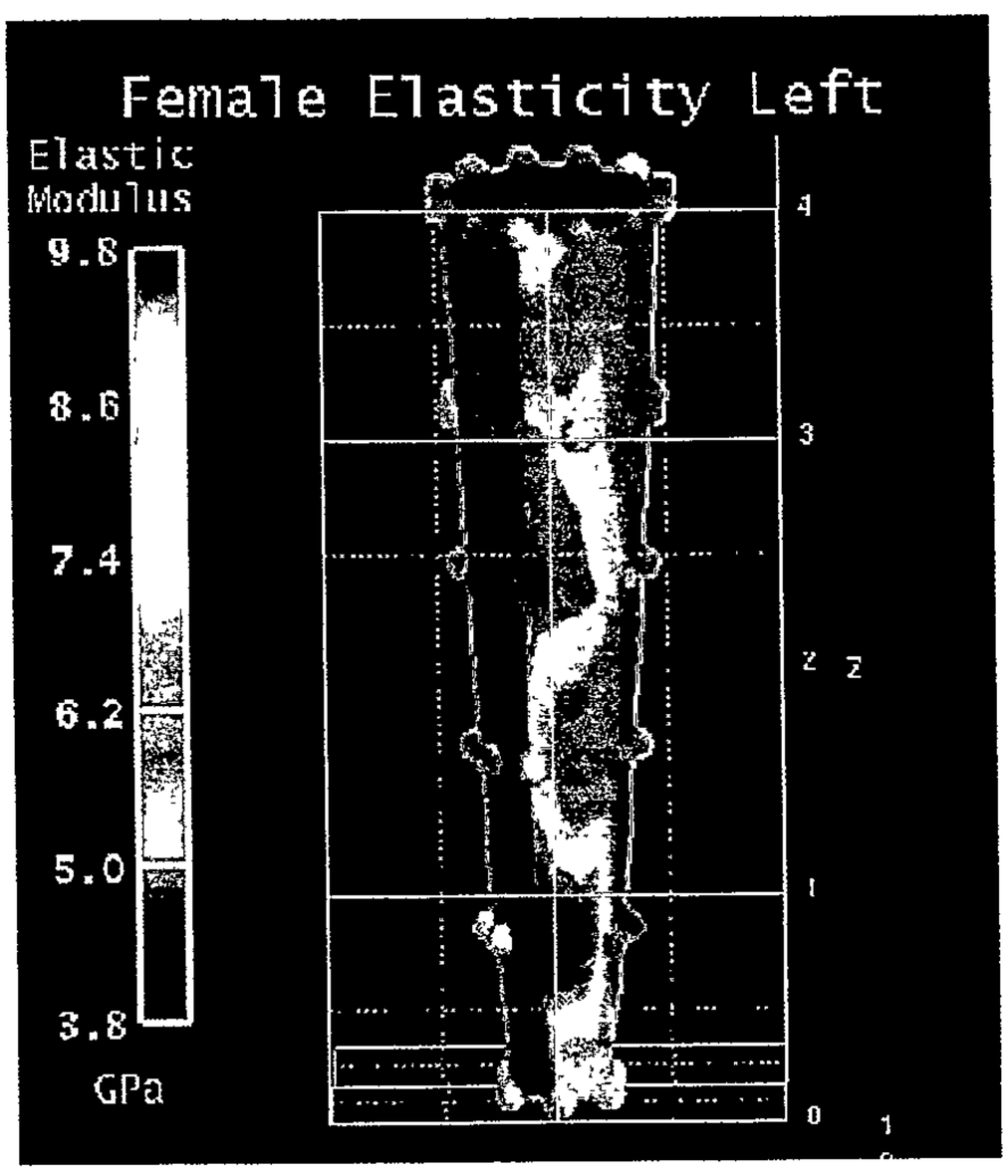

Lingual

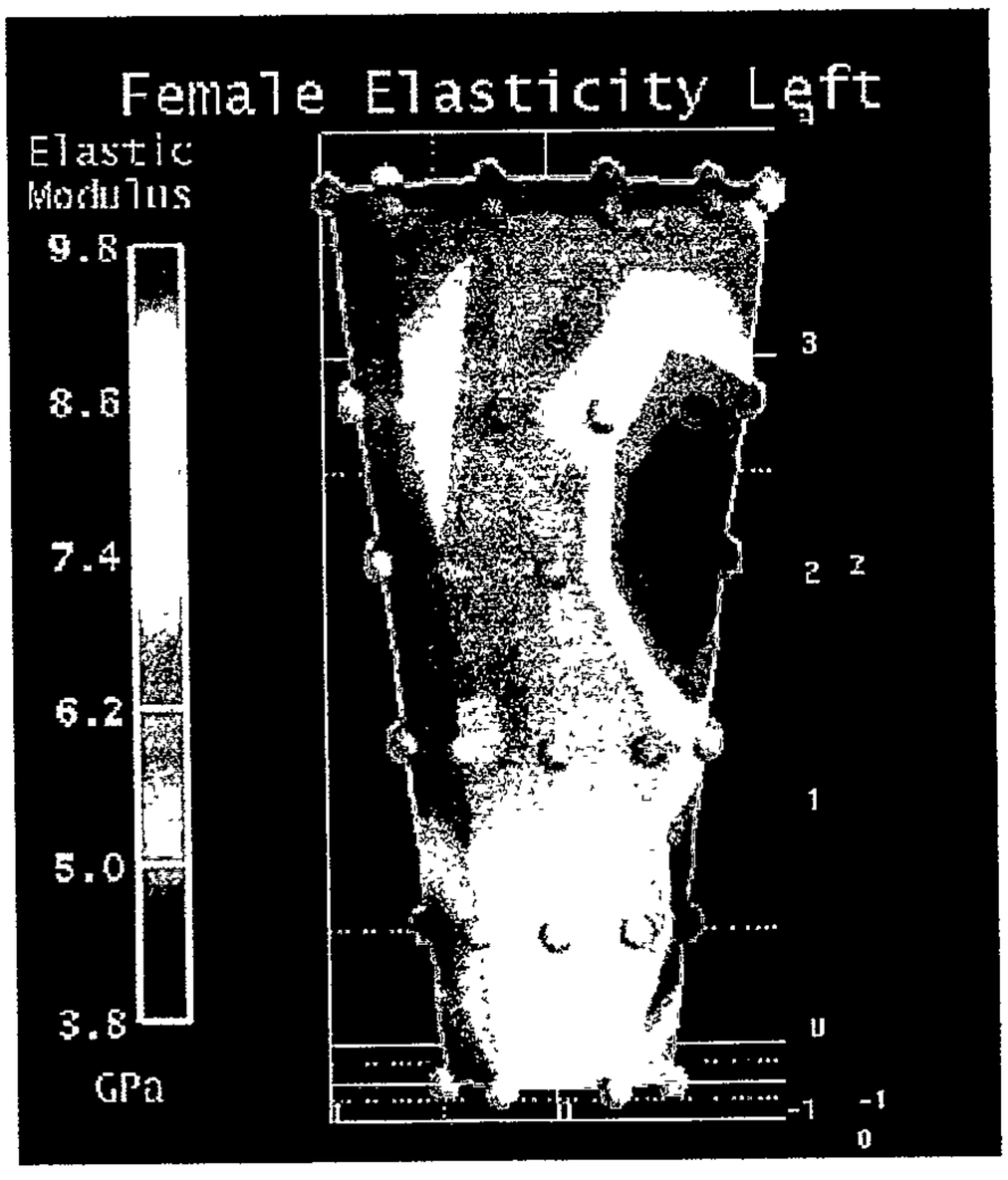

Distal

Figure 5. 27. Composite Summary Female elasticity left.